RIJKSUNIVERSITEIT GRONINGEN

Microbial physiology in relation to the availability of water

Proefschrift

ter verkrijging van het doctoraat in de
Medische Wetenschappen
aan de Rijksuniversiteit Groningen
op gezag van de
Rector Magnificus, dr. F. Zwarts,
in het openbaar te verdedigen op
maandag 10 januari 2011
om 14.45 uur

door

Marcus Christofoor de Goffau
geboren op 23 december 1982
te Colombo, Sri Lanka

Promotores:	Prof. dr. J.M. van Dijl
	Prof. dr. J.E. Degener
Copromoter:	Dr. H.J.M. Harmsen
Beoordelingscommissie:	Prof. dr. S.J. Foster
	Prof. dr. O.P. Kuipers
	Prof. dr. H.C. van der Mei

Contents

Paranimfen: Vivianne J. Goosens
Guido M. Voets

ISBN
978-90-367-4689-2 (printed version)
978-90-367-4687-8 (digital version)

Cover
Phase contrast image of *Bacillus subtilis* cells growing filamentously and in coiled superstructures at a relative humidity of 94.2%.

The studies described in this thesis were performed at the Faculty of Medical Sciences, Department of Medical Microbiology of the University Medical Center Groningen and within the W.J. Kolff institute for Biomedical Engineering and Materials Science. This research was funded by a grant from the User Support Programme Space Research.

WJKI
W.J. KOLFF INSTITUTE
FOR BIOMEDICAL ENGINEERING AND MATERIALS SCIENCE

NWO
Netherlands Organisation for Scientific Research

Chapter 1

General introduction and scope of this thesis

Earth is sometimes called 'the blue planet' due to its abundance of water. Even so, the availability of water remains one of the most important limiting environmental factors for the ability of organisms to thrive within a terrestrial setting. It not only determines whether organisms can grow in a specific environment, but also which organisms will grow where. Cacti for example have a range of specific physiological adaptations, which allow them to survive and thrive in dry places, such as deserts, where many other plants would not stand a chance; they are however likely to be outcompeted by these same plants in more humid environments. The same trends that can be seen on a macroscopic scale, where the availability of water is an important determinant for the vegetation of a region, seem to apply also on a more microscopic scale to the growth capabilities of microorganisms in a variety of microenvironments. Little is yet known about how the availability of water determines which microorganisms can grow where, and even less is known about microbial physiology in general in relation to water limitation.

Whereas the availability of water on a macroscopic scale is often mainly determined by the amount of precipitation, its availability needs to be defined in a different manner when dealing with microorganisms and/or in closed environments. In building sciences concerned with indoor air quality, water

availability is expressed in terms of equilibrium relative humidity (RH_e) values and this parameter is regarded as the most important determinant of indoor bio-aerosol levels; the main cause of building-related illnesses (Green *et al.*, 2003; Hansen, 1999). In the food industry, where the availability of water is of critical importance in predicting the potential for spoilage, its availability is expressed in terms of water activity (a_w) values instead (Baranyi and Tamplin, 2004). There is a direct relationship between these two terms as the a_w of an object in equilibrium with its surroundings is equal to the relative humidity (RH) of its environment divided by 100.

The starting aim of this thesis was to develop a risk assessment model for the growth of surface-attached microorganisms on board of the International Space Station (ISS). Spacecraft hygiene is not only important to prevent the growth of microbes that are potentially pathogenic for the temporarily immunocompromised astronauts (Kaur *et al.*, 2008), but also to prevent the growth of bio-fowling microbes that deteriorate spacecraft, so called technophiles (van Tongeren *et al.*, 2006). Though numerous factors seem relevant in addressing this goal, the only really distinguishing features about the ISS are its microgravity environment and the increased levels of radiation. Based on these considerations, inspiration was first sought by investigating the most important factors here on Earth for the growth of microbes on surface to air interfaces.

Water activity growth limits have been defined in the past for a variety of microbial species by growing them in solutions in which the a_w was modulated by adding variable amounts of salts or other 'humectants' to the medium, such as NaCl or glycerol respectively (Marshall *et al.*, 1971). These experimental setups however suffer from the fact that microbes have to deal with solute-specific effects and, moreover, they do not mimic the way in which the availability of water is reduced on surface to air interfaces.

As documented in this thesis, two novel non-aqueous experimental setups were designed in order to study the availability of water on microbial growth on surface-to-air interfaces within closed environments, such as the ISS. The principle behind the first of these two systems, which is described in *Chapter 2* of this thesis, is to create a RH_e gradient beneath the agar coated lid of a 96-well plate by using a selection of eight saturated salt solutions (Greenspan, 1976; Winston and Bates, 1960). With this setup the growth capabilities of various bacterial and even fungal species (Fig. 1) were studied within a wide range of RH_e values. The RH_e growth limit, an important parameter for predicting the occurrence of microbial growth, was determined for various species. RH_e gradient experiments with multiple species furthermore showed the importance of this parameter on the outcome of interspecies competition. Even more remarkable were the morphological changes that were observed microscopically when microorganisms were grown in a RH_e gradient. The Gram-positive bacterium *Bacillus subtilis*, which showed quite dramatic morphological changes, was subsequently used in a proteomics study to investigate the physiological mechanisms that are used by this microorganism to adapt to a reduced availability of water *(Chapter 3)*.

The second non-aqueous experimental setup involves an environmental control chamber, which provides an unprecedented level of control over the local availability of water *(Chapter 4)*. A RH_e gradient is created inside this system by setting a precisely defined temperature gradient that allows this system to mimic the way in which RH_e gradients exist in natural or man-made environments, such as the cabin of the ISS. The main ecological theory behind this system is that microbial growth does not occur on surfaces which have the most optimal (warm) temperature values, but on surfaces where the temperature is cold enough in comparison to the rest of the environment so that the local availability of water in the form of the local RH_e is high enough for microbial growth. In short, this theory predicts that local cold spots are hotspots for microbial growth (Fig. 2).

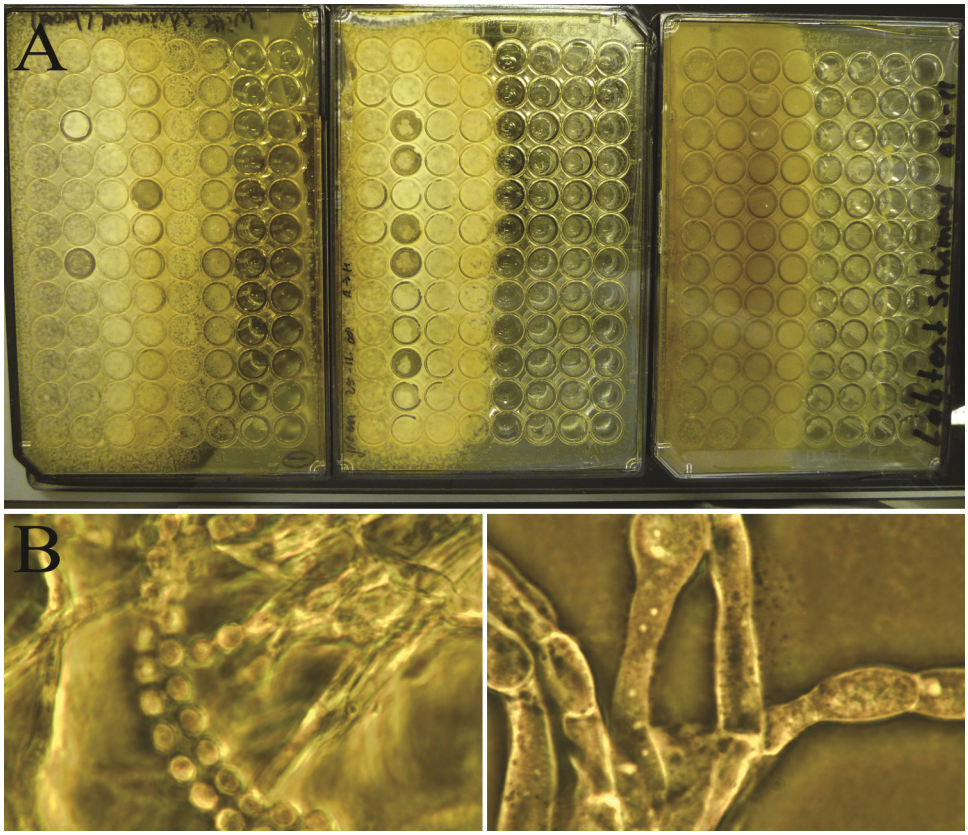

Figure 1. Application of the 96-wells relative humidity gradient setup for studying common bread and lab molds. (**A**) A white and a green mold were isolated from moldy bread (left and middle) and a brownish mold (right) was isolated from dust in a room. The RH_e gradient was created by pipetting H_2O, K_2SO_4, KH_2PO_4, KNO_3, KNa Tartrate, KCL and NaCl in the different rows from left to right (RH = 100, 97, 94, 92.5, 87, 84 and 75% respectively). Molds were grown on top of the Tryptic soy agar-coated lid of the 96-wells plate, which was incubated for 14 days at 29 °C. Differences in RH_e growth limits are visually discernable with the white mold being able to grow at the lowest RH_e values. (**B**) Phase contrast pictures of the green bread mold grown at 100% (left) and approx. 90% RH_e (right). Increased hyphal thickness and the absence of ascus formation were observed in all three fungal species when grown near their respective RH_e growth limits. The white bar represents 10 μm.

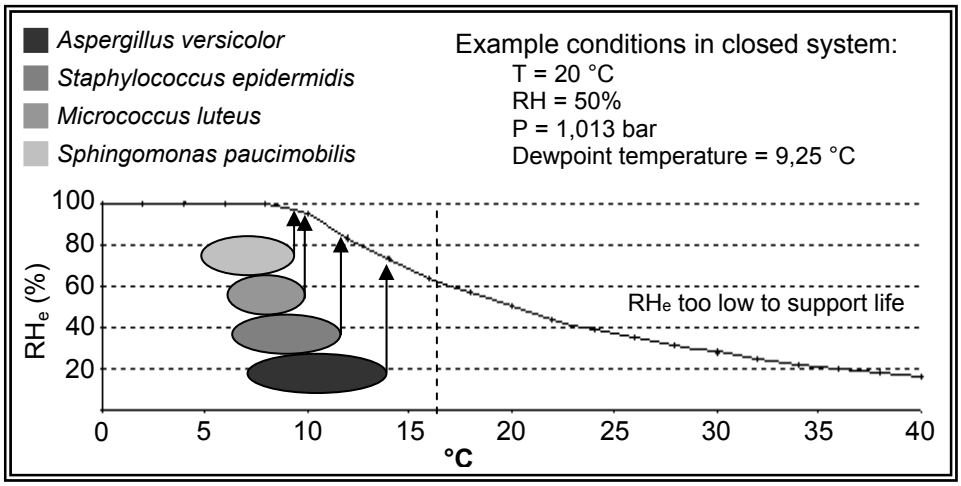

Figure 2. Predicted effects of RH_e on species distribution in a temperature gradient setup. The solid curved line indicates the local RH_e at a particular temperature. The arrows pointing at the curved line indicate the RH_e growth limit of particular species. At temperature above 17 °C (dashed vertical line) the local RH_e is too low for any microbial growth. Growth can also not occur when temperatures are too low. Formulas required to calculate the curved line have been defined previously (Lawrence, 2005).

To ascertain the predictive value of this theory, and to establish a risk assessment model for the occurrence of microbial growth on board of the ISS, a ground-based study was performed in neonatal incubators *(Chapter 5)*. These incubators are precisely controlled environments in which the average air temperature and relative humidity values are kept high in order to provide the neonate with a thermoneutral environment, and to prevent excessive loss of moisture (Antonucci *et al.*, 2009). These properties make incubators ideal candidates for performing controlled environmental studies. The conditions encountered within the neonatal incubators are, unfortunately, also intrinsically ideal for the occurrence of microbial growth. Making matters worse, the warm humidified air that is blown into a neonatal incubator from the hot air vents does not reach all parts of the interior walls equally well, which leads to the occurrence of spots which are relatively cold. An infrared thermometer was used to characterize the interior temperature distribution of a neonatal incubator. In combination with the average

RH and air temperature this makes it possible to calculate local RH_e values and to predict which spots might be more heavily microbially contaminated, according to theory. Swab samples were taken from the warmest (low RH_e) and coldest (high RH_e) spots and these were plated out to determine the number of colony forming units at these locations to test these predictions.

Although the relative humidity on board of spacecraft, such as the ISS, is lower on average than in neonatal incubators (25-75% vs. 50-75% RH), local spots with sufficiently high RH_e values are also still expected to exist due to the relatively large temperature differences on board of the ISS. One of the reasons for this, which is reviewed in *Chapter 6*, is that thermal convection does not occur due to the micro-gravity environment. Micro-gravity is thus expected to increase the number of possible niches suitable for microbial growth on surface to air interfaces. Micro-gravity is furthermore expected to alter the micro-environment represented by the crew. It is furthermore discussed in *Chapter 6* how the elevated levels of radiation on board of spacecraft can possibly select for increased levels of desiccation resistance, which is of great importance as niches are often only temporarily conducive to microbial growth in the case of an environment where surface temperatures are likely to fluctuate in time.

The studies described in *Chapters 2* and *3* have shown that microorganisms adapt to a water-limited environment in specific ways. Many questions regarding the physical and physiological background of these adaptations still remain to be answered. How do microorganisms obtain water from their environment, and why do they change their morphology and growth patterns in the way that they do, and are the answers to these two questions related? The accumulation of water is essential for the growth of organisms, but not all organisms seem to require the presence of liquid water in order to obtain it (Henschel and Seely, 2008). Various organisms in the desert simply obtain water from their food, either in the form of moisture or by generating H_2O (and CO_2) metabolically. Other organisms, such as lichens with green algae (Lange *et al.*, 1994), are capable of taking up water from the air directly as long as the RH is high enough

in a process which is called reverse transpiration (von Willert *et al.*, 1992). Some arthropods can actively take up atmospheric water vapour from unsaturated air (Edney, 1971), but they can only do so above a critical equilibrium activity, the threshold at which water efflux equals vapour influx (Hadley, 1994). For microorganisms it has long been thought that they can accumulate water, and are thus capable of growth, as long as they can lower their internal a_w below that of their external a_w or $RH_e/100$ (Chirife *et al.*, 1981; Csonka, 1989).

In *Chapter 4* it is argued and shown that microorganisms are capable of obtaining water from their environment directly as long as their internal a_w is lower than the external a_w or $RH_e/100$, but that they are also capable of accumulating water by generating it metabolically once the external a_w becomes lower than their internal a_w. As long as microorganisms can generate more water metabolically than they lose to their environment via evaporation, they should be able to grow. The RH_e growth limit of an organism should thus be the point at which the rate of evaporation equals the rate at which water can be generated metabolically. For growth at low RH_e, microorganisms need to accumulate compatible solutes to make their internal a_w as low as it is physiologically possible for them without interfering with essential intracellular processes. They can do so by either synthesizing these solutes biochemically or by importing them, if available, from the external environment (Csonka, 1989).

Once microorganisms can no longer accumulate more compatible solutes for lowering their internal a_w value, they will need to switch gears to start producing water metabolically. This is especially needed once the external a_w becomes lower than their internal a_w. The internal lower limit for the water activity within a cell is thus predicted to be a key turning point in the physiology of a microorganism growing in a RH_e gradient (Fig. 3). A mathematical approach to calculate the internal water activity limit of a microorganism was developed through the studies described in *Chapter 4*, which involved measuring the RH_e growth limit of an organism in a closed environment at different barometric pressure values. Importantly, by being able to control the barometric pressure, it was possible to directly control the rate of evaporation (Smith and Geller, 1979).

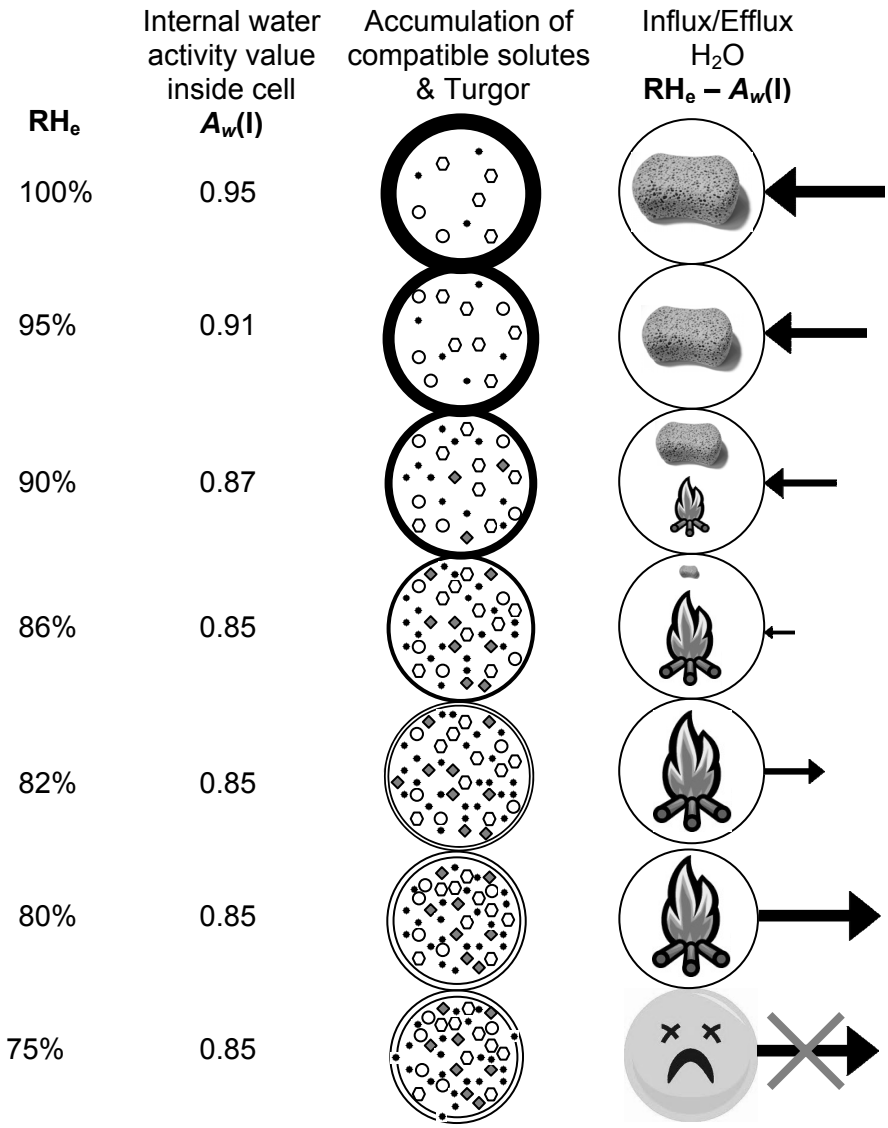

Figure 3. Visualization of the possible mechanism of adaptation of *S. epidermidis* grown in a RH_e gradient. Cells are thought to maintain an osmotic pressure difference between the inside and outside of a cell by maintaining an internal a_w value that is lower than the external $RH_e/100$ by accumulating compatible solutes. This difference can however not be maintained forever in a RH_e gradient, which in turn will likely affect the influx/efflux of water, the need to generate water metabolically (by "burning" carbohydrates, indicated with fire), and cell turgor.

The final factor that is thought to be of importance is the osmotic pressure difference between the inside and outside of a cell when growing in a specific environment (Fig. 3). Not only does it determine the rate at which water can be acquired or lost, but it also determines the amount of physical stress imposed on the cell wall in the form of turgor. As turgor is a necessity for the growth and division of cells (Koch, 2001), this physical stress is thought to place yet an extra set of requirements on the cell wall. The effects that these requirements have on the cell wall composition, morphology, size and growth patterns of *B. subtilis* and *S. epidermidis* have been explored in detail in *Chapter 4*.

Taken together, the studies described in *Chapters 2 to 4* increase our understanding on the relationship between microbial physiology in relation to the availability of water on a fundamental level, studying physiological changes in a RH_e gradient in *Chapters 2 & 4* and using a proteomics approach in *Chapter 3*. The obtained knowledge is applied in a clinical setting in *Chapter 5*, correctly predicting where elevated levels of microbial contamination can be found within neonatal incubators. *Chapter* 6 reviews what these findings mean for the hygienic situation on board of spacecraft in relation to its unique environment. *Chapters 2 to 6* are finally summarized and discussed in *Chapter 7*.

Reference List

Antonucci,R. *et al.* (2009) The infant incubator in the neonatal intensive care unit: unresolved issues and future developments. *J Perinat Med* **37:** 587-598.

Baranyi,J. and Tamplin,M.L. (2004) ComBase: a common database on microbial responses to food environments. *J Food Prot* **67:** 1967-1971.

Chirife,J., Ferro Fontan,C., and Scorzo,O.C. (1981) The intracellular water activity of bacteria in relation to the water activity of the growth medium. Journal of applied microbiology 50[3], 475-479.

Csonka,L.N. (1989) Physiological and genetic responses of bacteria to osmotic stress. *Microbiol Rev* **53:** 121-147.

Edney,E.B. (1971) Some aspects of water balance in tenebrionid beetles and a thysanuran from the Namib Desert of southern Africa. Physiological Zoology 44[2], 61-76.

Green,C.F., Scarpino,P.V., and Gibbs,S.G. (2003) Assessment and modeling of indoor fungal and bacterial bioaerosol concentrations. *Aerobiologia* **19:** 159-169.

Greenspan,L. (1976) Humidity fixed points of binary saturated salt solutions. Journal of Research of the National Bureau of Standards 81A[1], 89-96.

Hadley,N.F. (1994) *Water relations in terrestrial arthropods*. New York: Academic Press.

Hansen,D.L. (1999) Microbial contamination. In *Indoor air quality issues*. London: Taylor & Francis, pp. 45-48.

Henschel,J.R. and Seely,M.K. (2008) Ecophysiology of atmospheric moisture in the Namib Desert. *Atmospheric Research* **87:** 362-368.

Kaur,I., Simons,E.R., Kapadia,A.S., Ott,C.M., and Pierson,D.L. (2008) Effect of spaceflight on ability of monocytes to respond to endotoxins of gram-negative bacteria. *Clin Vaccine Immunol* **15:** 1523-1528.

Koch,A.L. (2001) Turgor pressure of bacterial cells. In *Bacterial growth and form*. Dordrecht, The Netherlands: Kluwer Academic Publishers, pp. 135-160.

Lange,O.L., Meyer,A., Zellner,H., and Heber,U. (1994) Photosynthesis and water relations of lichen soil crusts: field measurements in the coastal fog zone of the Namib Desert. Functional Ecology 8[2], 253-264.

Lawrence,M.G. (2005) The Relationship between Relative Humidity and the Dewpoint Temperature in Moist Air: A Simple Conversion and Applications. *Bulletin of the American Meteorological Society* **86:** 225-233.

Marshall,B.J., Ohye,D.F., and Christian,J.H. (1971) Tolerance of bacteria to high concentrations of NaCL and glycerol in the growth medium. *Appl Microbiol* **21:** 363-364.

Smith,W.K. and Geller,G.N. (1979) Plant transpiration at high elevations: Theory, field measurements, and comparisons with desert plants. *Oecologia* **41:** 109-122.

van Tongeren,S., Raangs,G., Welling,G., Harmsen,H., and Krooneman,J. (2006) Microbial detection and monitoring in advanced life support systems like the international space station. *Microgravity Science and Technology* **18:** 219-222.

von Willert,D.J., Eller,B.M., Werger,M.J.A., Brinckmann,E., and Ihlenfeldt,H.D. (1992) *Life strategies of succulents in deserts*. Cambridge: Cambridge University Press.

Winston,P.W. and Bates,D.H. (1960) Saturated Solutions For the Control of Humidity in Biological Research. *Ecology* **41:** 232-237.

Chapter 2

Bacterial pleomorphism and competition in a relative humidity gradient

Marcus C. de Goffau, Xiaomei Yang,
Jan Maarten van Dijl and Hermie J. M. Harmsen
Environmental Microbiology 11(4), 809-822 (2009)

Abstract

The response of different bacterial species to reduced water availability was studied using a simple relative humidity gradient technique. Interestingly, distinct differences in morphology and growth patterns were observed between populations of the same species growing at different relative humidity. Gram-positive cocci increased in cell size as they approached humidity growth limits and staphylococcal species started growing in tetrad/cubical formations instead of their normal grape-like structures. Gram-negative rods displayed wave-like patterns, forming larger waves as they became increasingly filamentous at low humidity. In contrast, cells of the Gram-positive bacterium *Bacillus subtilis* became shorter, curved, and eventually almost coccoid. Moreover, *B. subtilis* started to sporulate at low humidity.

The altered morphology and/or growth patterns of bacteria growing at low humidity might be more ecologically relevant than their textbook appearance at high humidity since their natural habitats are often dry. Transmission electron microscopic analyses revealed that staphylococci grown at low humidity have significantly thickened cell walls, which may explain why these cells displayed increased resistance to vancomycin.

We conclude that our relative humidity gradient technique is widely applicable for investigating effects of relative humidity on microbial survival, growth and competitive success at solid-air interfaces, making it a versatile tool in microbial ecology.

Introduction

Water availability and the quality of life are strongly linked, as a lack of water eventually causes a cessation of metabolism. In environments like deserts or places with high altitude, freezing temperatures or high salinity a reduced availability of water is not uncommon. Organisms have either adapted their physiology, developed certain survival strategies or they have simply become extinct in such places. Also in less extreme examples water availability remains an important force in shaping the resident composition of life, including the microbial world.

In low-osmotic solutions water is readily available, but in solids or on solid-air interfaces its availability is key in predicting the occurrence of microbial growth. On objects surrounded by air with a relative humidity (RH) of 60% or lower, microbial growth does not occur. RH values need to be approximately 70% or higher to allow for the growth of molds and they need to be even higher to allow for the growth of yeasts (80%), Gram-positive and finally Gram-negative bacteria (85-95%) (Rahman and Labuza, 1999).

The water content of an object when in equilibrium with the relative humidity of its surroundings is given by a material-specific absorption isotherm, but the availability of water to micro-organisms can be better expressed in terms of water potential (Ψ) or water activity (a_w) (Wiebe, 1981). The water activity of an object in equilibrium with its surroundings is namely equal to the RH divided by 100 and is material non-specific. In the food industry a_w is recognized as one of the main environmental factors governing microbial growth together with the temperature and the pH (Baranyi and Tamplin, 2004).

For maintaining indoor air quality it is essential to have a properly designed heating, venting and air conditioning (HVAC) system to keep humidity values below and above certain thresholds. The same is true in museums (Brimblecombe *et al.*, 1999) or in hospitals, where elevated humidity levels might lead to the deterioration of art(ifacts) or cause a decrease in the health conditions of patients.

Another habitat where humidity plays an important role in microbial control is in the interior of spacecraft. In the International Space Station (ISS) the environmental control and life support systems (ECLSS) keep RH values between 25 and 75% (ESA, 2008), which is an improvement over the Mir space station where free floating condensate was not uncommon (Ott *et al.*, 2004). Nonetheless certain molds can grow at 70-75% RH and on a local scale one can expect small niches to occur with humidity values conducive for bacterial growth due to local temperature differences and air circulation.

Prevention of microbial growth on board of spacecraft is doubly important for the health of the crew. Space conditions are thought to increase their immunological vulnerability (Kaur *et al.*, 2004) and the deterioration of spacecraft systems by technophiles (Alekhova *et al.*, 2005) can also cause life-threatening situations.

Water activity growth limits are thus very useful parameters in predicting the occurrence or absence of microbial growth. To mimic such a closed system, a simple assay was established in which a relative humidity gradient was created in a non-aqueous system, avoiding problems such as solute specific effects (Marshall *et al.*, 1971). In the present studies, the specific effects of different a_w values on bacterial survival, growth, cell morphology and competition were tested with a collection of bacterial species that were selected for their relative abundance on board of the ISS (Novikova *et al.*, 2006) and Mir (Novikova, 2004) and/or their clinical relevance.

Results

Method validation for bacterial growth on a a_w gradient

Using a selection of eight pre-warmed saturated salt solutions as listed in Table 1, a RH gradient was created beneath an agar-coated lid of a 96-well plate. This is possible as saturated salt solutions placed within small closed spaces at a certain temperature maintain a specific constant RH (Winston and Bates, 1960).

Table 1. Saturated salt solutions and their corresponding RH values at 28 °C

Saturated salt	**Relative humidity***	**Interpolated from**
Milli-Q	100%	
K_2SO_4	97.1% ± 0.5%	Greenspan (1976)
KH_2PO_4	94.5% ± 1.0%	Winston and Bates (1960)
KNO_3	92.8% ± 0.5%	Greenspan (1976)
Na_2Tartrate	92.0% ± 0.5%	Winston and Bates (1960)
Na_2SO_4	91.0% ± 2.0%	Winston and Bates (1960)
$MgSO_4$	89.4% ± 1.0%	Winston and Bates (1960)
KNaTartrate	87.0% ± 0.5%	Winston and Bates (1960)
KCl	83.9% ± 0.5%	Greenspan (1976)
$(NH_4)_2SO_4$	80.8% ± 0.5%	Greenspan (1976)
NH_4Cl	78.2% ± 0.5%	Greenspan (1976)
NaCl	75.2% ± 0.5%	Greenspan (1976)

*Interpolations are estimated to be correct within the given margins.

The RH gradient translates into an even more "fluid" a_w gradient within the coating of tryptic soy agar on which inoculated bacteria are tested for growth at decreasing water availability. Addition or removal of water from the agar does not affect the RH maintained by saturated salt solutions, because the buffer capacity of these solutions is maintained as long as they consist of a combination of salt crystals and liquid. A detailed protocol can be found in the experimental procedures section. The creation of a RH/a_w gradient and its effects on bacterial growth and competition could be inspected visually (Fig. 1) and were studied in more detail microscopically.

In order to compare and quantify microbial population densities over a broad range, a semi-quantitative scoring system was developed (Table 2). For example images that illustrate the practicability and versatility of this scoring system, see Supplemental Figs. S1 and S2. The scoring system was furthermore extensively validated with the aid of 3 untrained students (Fig. S3). On average interpersonal variance was about 0.7 orders of magnitude and the total variance was approximately one order of magnitude.

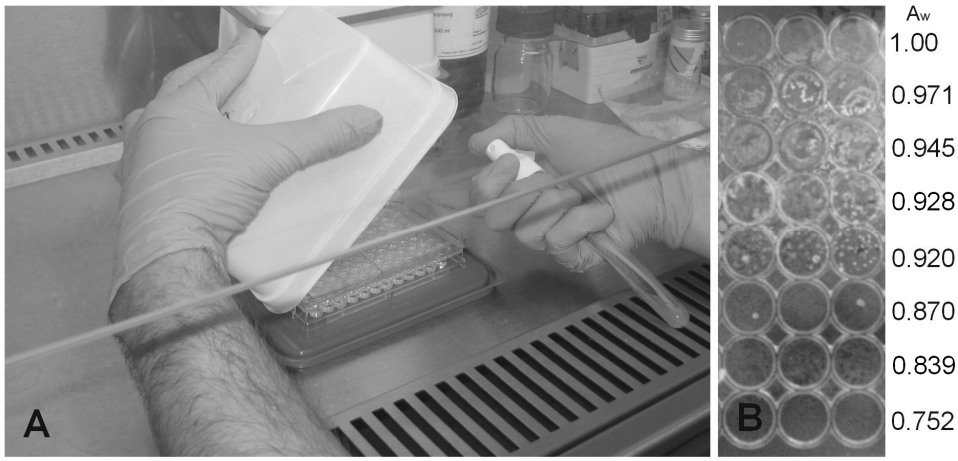

Figure 1. (**A**) Inoculation of the TSA-coated lid of a 96-well plate with bacteria using an aerosol pump. The lid was preincubated above a selection of saturated salt solutions in a 96-well plate. A suspension of bacteria is sprayed into the box. The resulting aerosols and small droplets are allowed to settle onto the TSA coated lid. (**B**) After a 5 day incubation at 28 ^{o}C bacterial growth is visible. The presented lid was inoculated with both *Staphylococcus epidermidis* 12228 and *Sphingomonas paucimobilis*. Microscopic examination showed that *S. paucimobilis* became the dominant species in the first three rows (a_w = 1.0-0.945) and *S. epidermidis* in the next three (a_w = 0.93-0.87). Little to no growth was seen in the last two rows (a_w = 0.841-0.752).

Table 2. Classification system

Order	Descriptor
0	No visible intact cells
1	Inoculation density
2	1-3 cell divisions per cell
3	Small clusters developing
4	Large clusters developing
5	Droplets grown confluent
6	Droplets grown large
7	Surface confluence ~25-75%
8	Surface confluence ~75-100%

The relationship between bacterial growth and a_w was assessed for all bacterial species shown in Table 3. Bacteria of each species or strain were tested at least three times on several different a_w gradients depending upon their suspected a_w growth limits (Fig. 2).

Table 3. Comparison a_w growth limits

Bacterium	**Origin**	**NaCl/ Glycerol**	**A_w gradient**
Pseudomonas fluorescence	ATCC[a] 13525	0.945/0.94[e]	~0.945
Pseudomonas aeruginosa	ATCC 27853	-	~0.945
Escherichia coli	ATCC 25922	0.95/0.935[f]	0.93-0.945
Acinetobacter radioresistens	ISS[b]	-	~0.93
Sphingomonas paucimobilis	MMB[c]	-	~0.93
Micrococcus luteus	ISS	0.83/0.92[g]	0.92-0.93
Bacillus subtilis str. 168	ATCC 23857	0.90/0.93[g]	0.92-0.93
Bacillus subtilis str. 3610	ATCC 6051	-	~0.91
Staphylococcus aureus	NCTC[d] 8325	0.85/0.87[g]	~0.87
Staphylococcus epidermidis	ATCC 12228	-	~0.84
Staphylococcus epidermidis	ATCC 35984	-	~0.81

[a]American Type Culture Collection; [b]Isolate from a surface sample taken inside the Russian segment of the ISS, as part of the SAMPLE experiment; [c]Clinical isolate from the laboratory for Medical Microbiology Groningen; [d]The National Collection of Type Cultures; [e]Li and Torres (1993); [f]Gould *et al.* (1977); [g]Marshall *et al.* (1971).

While assessing the relationship between a_w and bacterial growth several trends were observed in bacterial morphology. As bacterial population densities declined upon approaching their respective a_w growth limits, they also displayed distinct and reproducible changes in morphology and/or growth patterns. These changes are described in the following sections.

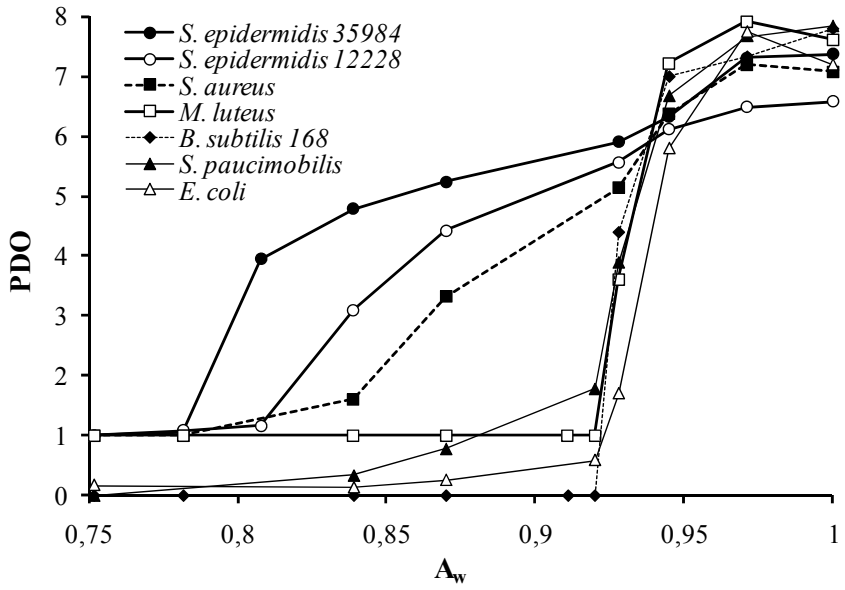

Figure 2. Population density order (PDO) of different bacterial species after an incubation period of 5 days at 28 °C in relation to a a_w gradient. The PDO was scored according to the classification system of Table 2. The curves shown are averages of at least 3 separate experiments. Standard error bars were omitted for purposes of clarity but were on average one order of magnitude.

Gram-negative rods

Filamentous growth of Gram-negative rod-shaped bacteria was an ubiquitously encountered phenomenon when these bacteria approached their respective a_w growth limits. Instead of completing cell division after a doubling in length, these cells seem to forgo complete separation and remain attached to one another. When these filamentous cells are introduced to higher a_w values, like normal water, separation will commence quickly completing the cell division process.

Pseudomonas fluorescence, *Pseudomonas aeruginosa*, *Escherichia coli*, *Acinetobacter radioresistens* and *Sphingomonas paucimobilis* cover the surface of the agar in a chaotic fashion at high a_w values (Fig. 3A). Going down the humidity gradient, short wave-like patterns will become visible (Fig. 3B), which increase in size and structure as the a_w drops further (Fig. 3C) until the edge of a colony is reached (Fig. 3D). Going further down the a_w gradient, strands of

filaments, sometimes escaping from the edges of a large colony, can be observed (Fig. 3E). These filaments tend to grow in straight lines, unless something is blocking their path (Fig. 3F). Filamentous cells also appear to be slightly larger than non-filamentous cells.

In the case of the *P. fluorescence* and *S. paucimobilis* (previously described as a pseudomonad), bundles of filaments were found giving rise to exquisite helical structures in which the filaments are twisted together like the strands of a rope (Fig. 3G). These bundles could consist of one strand, coiled onto itself, or of multiple strands braided together. *A. radioresistens* was found to form filaments of very thick rods past the wave-like growth pattern region (not shown). Beyond their a_w growth limit, Gram-negative rods either lysed, or persisted keeping the appearance they had when they were inoculated onto the agar.

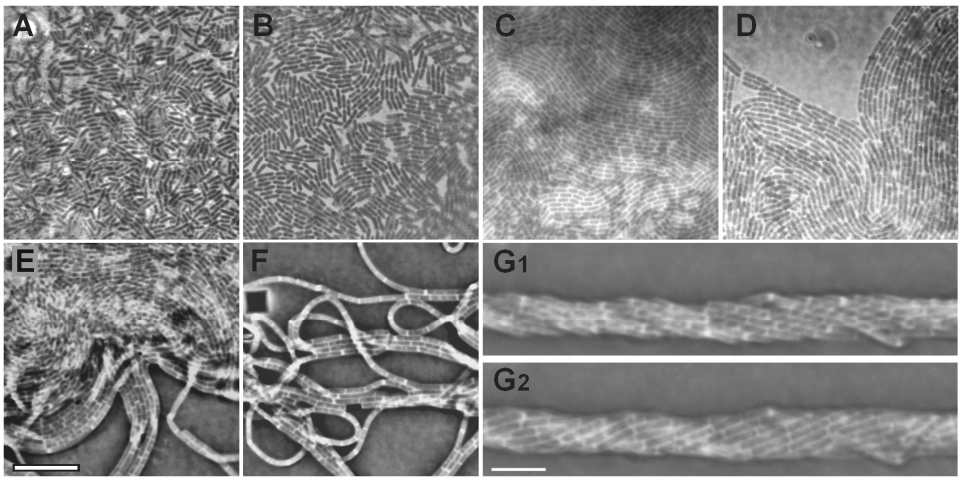

Figure 3. General response in growth patterns and/or morphology of several Gram-negative bacteria to a a_w gradient. Micrographs are shown for: (**A**) *P. fluorescence*, $a_w \approx$ 1-0.97; (**B**) *P. aeruginosa*, $a_w \approx$ 0.97-0.945; (**C**) *E. coli*, $a_w \approx$ 0.97-0.945; and (**D-G**) *S. paucimobilis*, $a_w \approx$ 0.945-0.93. Images (**A-D**) were taken from Gram-stained samples. (**E-G**) were made of unstained samples using only phase contrast microscopy. Samples (**G_1**) and (**G_2**) were taken from the same spot at different planes of focus. The black bordered bar indicates 10 µm (**A-F**). The white bar indicates 5 µm (**G**).

Bacillus subtilis

In the literature, *B. subtilis* is normally depicted as a conglomeration of straight rods and/or spores. At high a_w values *B. subtilis* indeed either covers the agar surface in the form of typical straight rods (strain 168; Fig. 4A) or with a spore-forming biofilm (strain 3610; not shown). However, when approaching the a_w limit of *B. subtilis*, cells at first enter a filamentous phase as described for the Gram-negative rods (Fig. 4B) and after that they become shorter, thicker and curved (Fig. 4C-E).

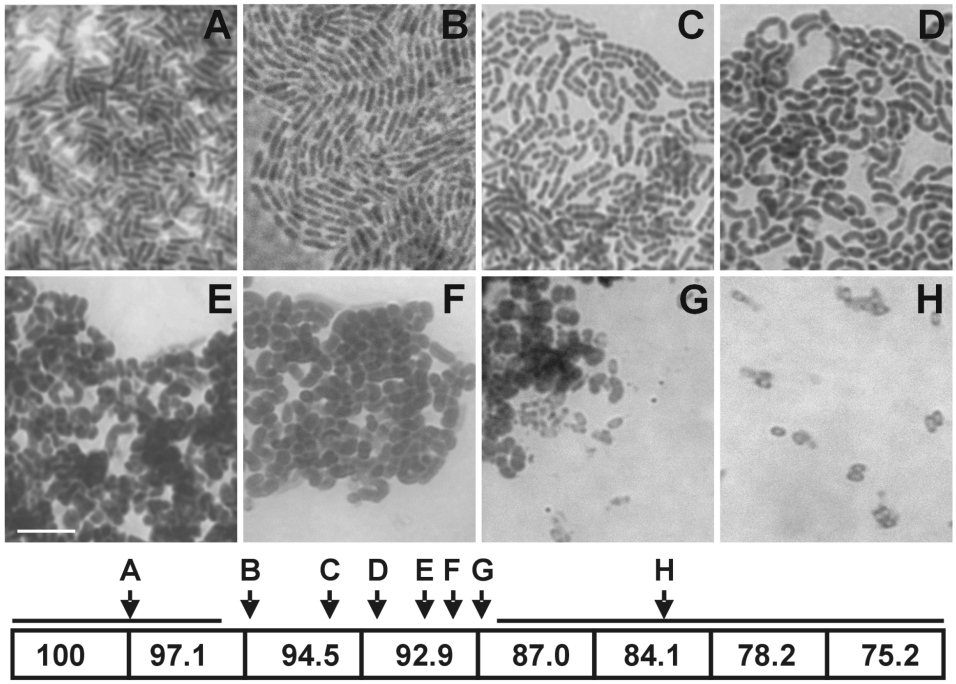

Figure 4. Micrograph of Gram-stained cells of *Bacillus subtilis* strain 168 grown in a relative humidity gradient. The pictures show a gradual change in morphology as *B. subtilis* approaches its a_w growth limit (**A**-**G**). Panel (**H**) shows cells that have sporulated. The RH gradient used in this experiment is depicted at the bottom of the figure. The arrows indicate the position in the RH gradient where each picture was taken (**A**-**H**). The horizontal bars left and right indicate those parts of the gradient where the cells shown in (**A**) and the spores shown in (**H**) can be found. The white bar indicates 5 μm (**A**-**H**).

Eventually, the *B. subtilis* cells become almost coccoid-like (Fig. 4F-G). At their a_w growth limit, there is a fine line where cells are seen growing either very slowly or sporulating. Past this threshold cells do not take on different shapes, but only tend to persist in the way they were applied to the agar or sporulate (Fig. 4H). Interestingly strain 3610 seemed to be able to grow at slightly lower humidities (91%) than its non-biofilm forming counterpart (92-93%; Table 3).

Gram-positive cocci

S. epidermidis and *S. aureus* are known to form grape-like structures of cocci. For a large part of the a_w gradient this is true (Fig. 5A), but once a_w values in the gradient are reached where growth retardation occurs, tetrads start to appear (Fig. 5B-C) and concomitantly the cell size starts to increase. Eventually cubical packets of eight cells are observed (Fig. 5D), which is consistent with the view that cell division of staphylococcal species occurs in three perpendicular planes. In Fig. 5E, the a_w growth limit is nearly reached. Past this limit staphylococcal cells maintain the same morphology that they had when they were inoculated onto the agar (Fig. 5F).

Similar to both *Staphylococcus* species, cells of *Micrococcus luteus* increase in size as their a_w growth limit is reached. Unlike staphylococci, *M. luteus* remains in its irregularly clustered or tetrad arrangements as divisions in this species only occur in two dimensions. Notably, of all species and strains tested (Table 3), the biofilm-forming *S. epidermidis* strain 35984 was able to grow at the lowest relative humidity (81% RH).

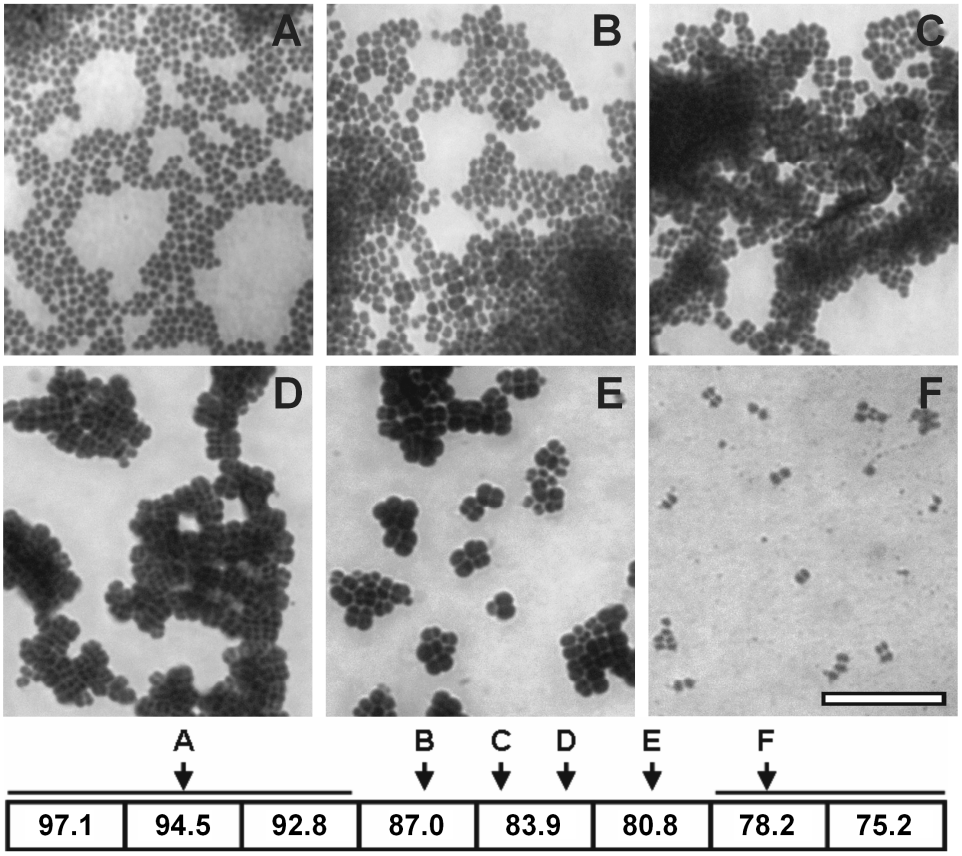

Figure 5. Micrograph of Gram-stained cells of *S. epidermidis* 35984 grown in a relative humidity gradient. The pictures show a gradual change in morphology as *S. epidermidis* approaches its a_w growth limit (**A**-**E**). Panel (**F**) shows cells that do not grow. The RH gradient used in this experiment is depicted at the bottom of the figure. The arrows indicate the position in the RH gradient where each picture was taken (**A**-**F**). The horizontal bars left and right indicate those parts of the gradient where cells with the morphologies shown in (**A**) and (**F**) can be found. The black bordered bar indicates 10 μm (**A**-**F**).

Staphylococcal adaptations to low a_w result in increased vancomycin resistance

To further characterize the phenomenon of enlarged staphylococcal cells in response to low a_w values, transmission electron microscopy (TEM) was performed. For this purpose *S. epidermidis* strain 35984 was used as it has the widest a_w growth range. Additionally, due to its biofilm forming nature, it has the technical advantage of not being washed off very easily during sample preparation from the surface on which it was grown.

A comparison of the TEM results obtained for the high and the low humidity samples showed that cell separation after division was retarded and even more obvious was the significantly increased cell wall thickness of cells grown at low humidity (Fig. 6A-B). Cell wall thickness measurements using TEM were performed with cells grown over the whole range of the RH gradient (Fig. 6C). The highest cell wall thickness was measured when cells were approaching their a_w growth limit, being more than two-fold thicker than the cell wall of cells grown at high RH values (>93%).

It is known from literature that a thickened cell wall and an increased resistance against certain antibiotics, such as vancomycin, are often associated (Cui *et al.*, 2003). To investigate whether growth at low a_w would impact on vancomyin resistance of *S. epidermidis*, vancomycin MIC determinations were done by growing and harvesting staphylococcal cells at various distinct relative humidity values and then inoculating those cells onto ISO-agar plates. E-test strips were placed on top of these plates, and the plates were subsequently incubated at 37 ^{o}C. It should be noted that this course of action mimics a possible infection of the human body with staphylococci that reside in the dry environment of the skin and invade the more humid subcutaneous tissues.

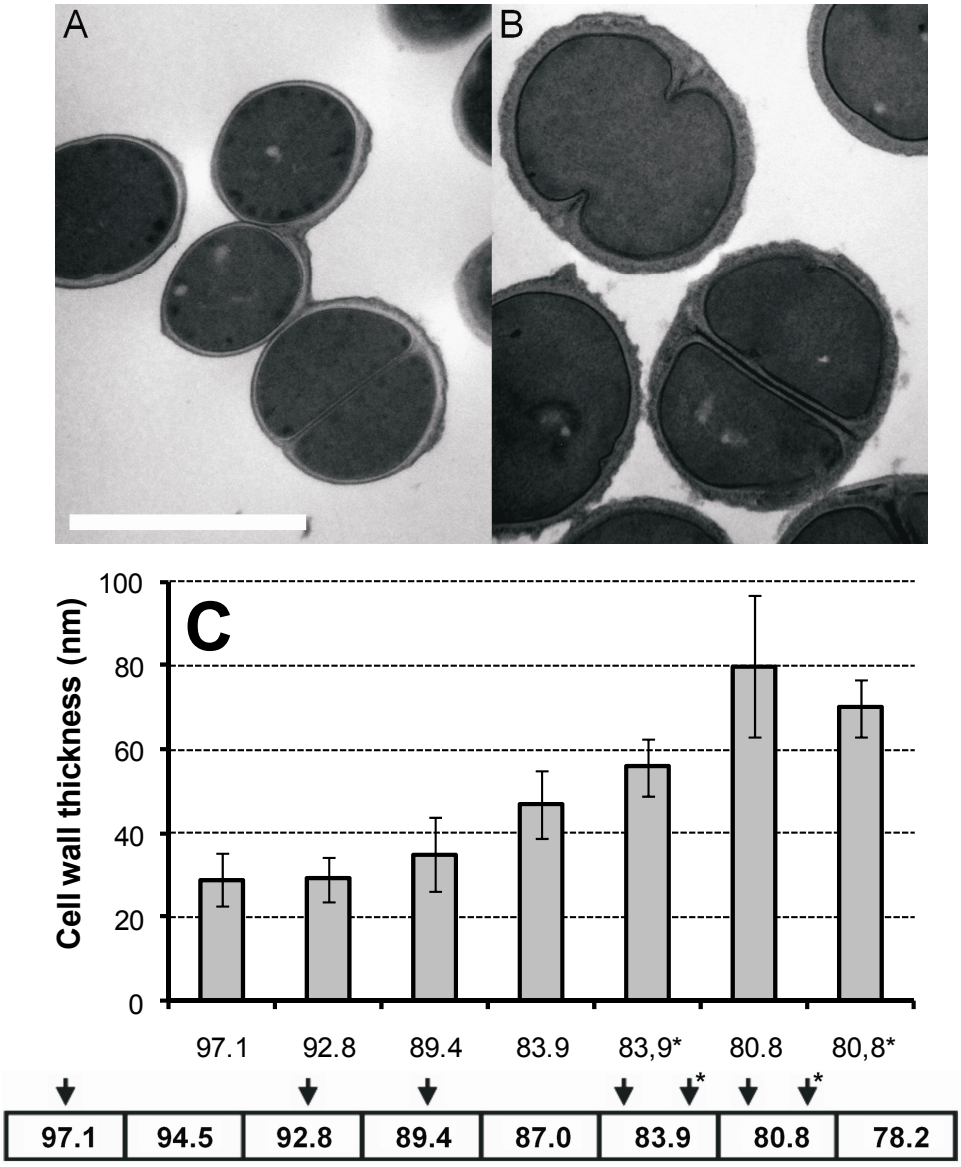

Figure 6. TEM results of *S. epidermidis* 35984 grown in a RH gradient. TEM pictures of *S. epidermidis* 35984 grown at 97% RH (**A**) and 81% RH (**B**) show clear differences in the thickness of cell walls and septa. The white bar indicates 1 µm (**A**-**B**). The RH gradient used in this experiment is depicted at the bottom of the panel (**C**). The cell wall thickness of 20-40 sections divided over several cells were measured for each point in the gradient to calculate averages and standard error bars.

The MIC values of both *S. epidermidis* strains, when grown near their a_w growth limit, increased more than two-fold compared to their MIC values when grown at 100% RH or in broth (Fig. 7). Similarly, the MIC values for *S. aureus* were increased about 1.5-fold. The vancomycin MIC values of *S. epidermidis* and *S. aureus* cells that had been exposed to low a_w values beyond their growth limits were similar to those observed for cells that were grown at high a_w values. Taken together, these findings imply that the staphylococcal adaptations for growth at low a_w make the cells of these organisms more resistant to clinically relevant antibiotics, such as vancomycin.

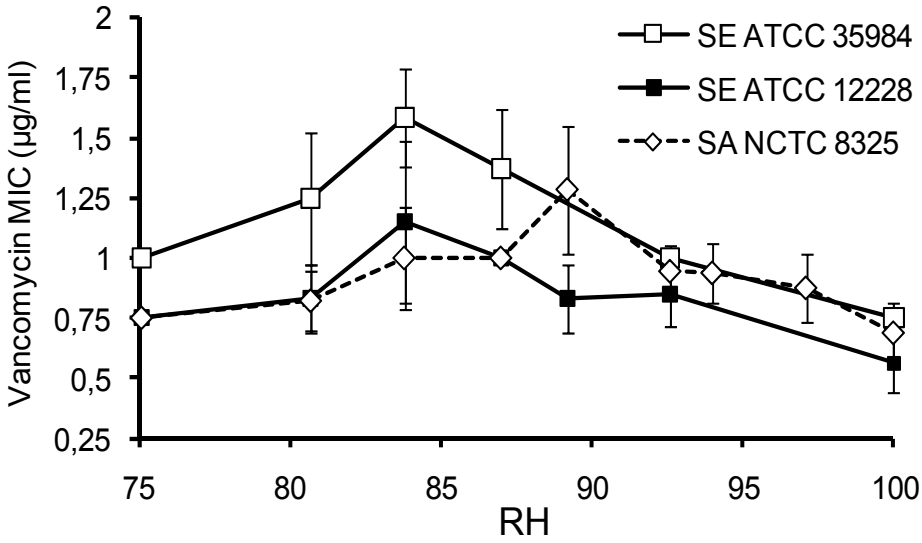

Figure 7. Vancomycin resistance of staphylococcal cells grown at a fixed RH. Averages and standard error bars were calculated from at least 3 independent measurements.

Bacterial competition on a a_w gradient

The developed a_w gradient system does not only facilitate the evaluation of survival and growth of single bacterial species at different relative humidity levels, but it also allows for competition experiments between different microbes. This is an interesting possibility in view of the above findings that different bacterial species behaved very differently under conditions of decreasing water availability.

As a first approach, competition experiments were performed on a_w gradients using *S. epidermidis* and *S. paucimobilis*, two species that are relatively frequently detected in the ISS (Castro *et al.*, 2004). For this purpose, *S. epidermidis* and *S. paucimobilis* were applied to the a_w gradients either independently or in competition with each other. The survival of either species was evaluated after 5 or 10 days of incubation, using Gram-staining and the population density scoring system described above (Table 2).

After 5 days of incubation, *S. paucimobilis* reached maximal population densities (population density order of ~8) at high a_w values. Little difference was seen after 10 days. In contrast, *S. epidermidis* had not yet reached maximal population densities after 5 days of incubation, even at the highest a_w values. In general, *S. paucimobilis* was found to cover the agar surface more rapidly than *S. epidermidis*, provided that its growth was not inhibited due to low a_w. This may relate to a higher growth rate of *S. paucimobilis*, to different surface growth patterns, or both. In this respect, it is important to note that dividing cells of *S. epidermidis* tend to stay together in aggregates, while *S. paucimobilis* cells separate after division (Gottenbos *et al.*, 2000).

At lower a_w values (~0.84-0.92), *S. epidermidis* displayed a clear advantage over *S. paucimobilis*, which is consistent with its lower a_w growth limit. Also at intermediate a_w values (~0.92-0.93), where *S. paucimobilis* had problems growing, *S. epidermidis* reached the highest population densities (Figs. 8A and S4). In contrast, *S. paucimobilis* reached much higher population densities than *S. epidermidis* at high a_w values ($a_w > 0.93$): while the population density of *S. paucimobilis* remained unaffected by the presence of *S. epidermidis* at high a_w values, the *S. epidermidis* population density was much lower under

these conditions than when this organism was grown in the absence of *S. paucimobilis*.

While our population density scoring system works well to monitor the competition between cells with clearly distinct shapes and Gram-staining properties, it cannot be applied to analyze the competitive success of species of similar shapes and Gram-staining properties. Furthermore, this simple scoring system will only allow the detection of major differences, while more subtle changes will be overlooked.

Therefore, a quantitative approach was developed to monitor bacterial growth in a_w gradients that is based on quantitative real-time polymerase chain reactions (qPCR). This approach was tested and validated for competition between the clinically relevant species *S. aureus* and *P. aeruginosa*, because optimised qPCR protocols for the quantification of these species were readily available (De Vos *et al.*, 1997; Ludwig and Schleifer, 2000).

To avoid a possible sampling bias, the general methodology for growth in the a_w gradient had to be slightly adapted. The bacteria were grown on a dialysis membrane that was deposited on top of the agar-coated lid of the a_w gradient. Samples were cut from the membrane after 5 days of incubation and DNA was extracted from these samples (including the dialysis membrane) by bead-beating. This approach has two major advantages: (1) all bacteria attached to the membrane will be released, and (2) the mechanical cell disruption is effective for all micro-organisms, irrespective of particular species properties such as cell wall thickness. Thus, the amounts of bacterial DNA subsequently detected for each species by qPCR will closely reflect their relative abundance.

In the experiment shown in Fig. 8B, overnight cultures of *P. aeruginosa* and 100-fold diluted overnight cultures of *S. aureus* were used to inoculate the plates. The high fidelity of the method used is reflected by the qPCR results obtained from samples that were taken at or below the a_w growth limits of *S. aureus* (~0.87) and *P. aeruginosa* (~0.945). The amounts of DNA detected for *S. aureus* were about two orders of magnitude lower than those for *P. aeruginosa*, closely reflecting the 100-fold dilution of the overnight culture of *S. aureus*.

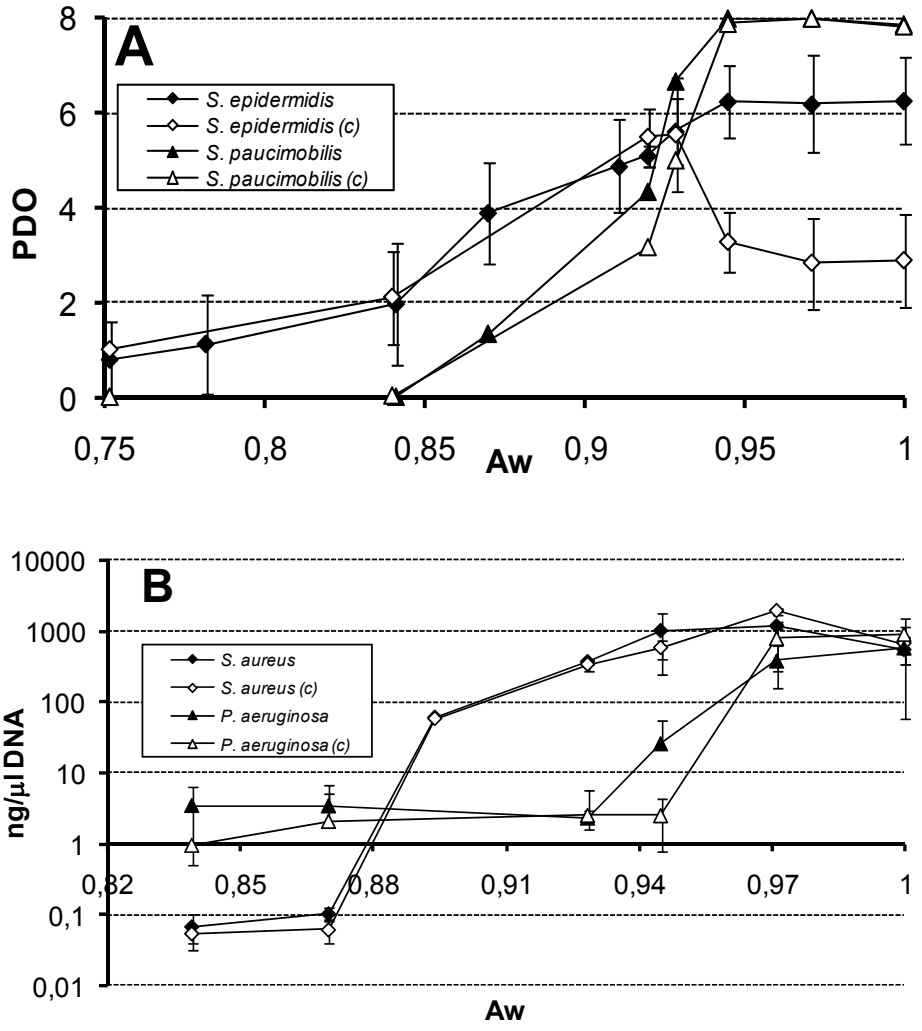

Figure 8. Bacterial competition on a_w gradients. (**A**) *S. epidermidis* and *S. paucimobilis* grown independently and in competition (*c*) with each other for 5 days at 28 °C. Standard error bars were omitted for *S. paucimobilis* as competition induced no significant changes in its population density order (PDO). (**B**) DNA content of *S. aureus* and *P. aeruginosa* in samples derived from mono- and co-cultivations (*c*) of these strains. DNA content was measured by qPCR. Averages and standard error bars were calculated from at least 3 independent measurements.

Remarkably, no major changes were observed when *S. aureus* and *P. aeruginosa* populations were grown alone or together over the largest part of the a_w gradient. However, when co-cultivated both strains reached higher population densities at a_w values between 0.97 and 1 than the respective strains in mono culture. Furthermore, at a a_w of 0.97 the *S. aureus* population was reproducibly about two-fold larger than the *P. aeruginosa* population with no overlaps in the standard deviations of the repeated measurements. Taken together, these results show that quantitative data on the competitive behavior of micro-organisms in relation to the (limited) availability of water can be obtained using the developed a_w gradient technology.

Discussion

The influence of humidity on bacterial growth and morphology has attracted major interest for many years. Early studies in this area were, for example, focused on the effect of moisture content of the medium on colony morphology (Buck and Kelly, 1981). Nevertheless, this is to our knowledge the first time that microbial growth was studied in response to a water activity gradient on an agar surface making use of a relative humidity gradient. The creation of a water activity gradient on a solid surface with the help of saturated salt solutions and a 96-well plate allows for the study of changes in growth patterns, cell morphology, microbial competition and various other microbial processes in response to reduced water availability on a solid-air interface. This method has several advantages over other experimental setups in which the RH is controlled, but where cells come in contact with the chemicals that are used to adjust the RH.

The experiments described in the present studies are easy to set up due to their low-tech and low-cost nature. Perhaps even more important is the fact that a RH gradient can be tested instead of just one RH value at a time. On the other hand, even for testing the effects of just one RH value at a time, the use of a plate placed on top of the saturated solution of a single salt is very convenient and effective. This turned out especially useful for growing sufficient cells at a

specific interesting RH value, as was done to determine the vancomycin MIC values of cells grown at distinct a_w values. The accuracy with which a_w growth limits can be determined using this method depends on the number of well characterized saturated salt solutions available with RH values that lie within the a_w growth range of the selected bacteria.

Importantly, the a_w growth limits found in this study were comparable with those found in previous studies using aqueous systems (Table 3). They mostly seemed to resemble the results of studies that used glycerol as the water activity depressant. As discussed below, several changes seen in cellular morphology have been reported before in different systems and setups, but these studies did not show these changes in such a gradual manner.

Filamentation has been observed in many Gram-positive and negative rod-like bacteria and can be induced by a long list of various stressors. This indicates that the induction of filamentation is part of a general SOS stress response, presumably achieved through a down regulation of autolysin activity (Cirz *et al.*, 2007; Höltje, 1995). In this study and in many others, filamentation is found to be correlated with a reduced growth rate, which is not surprising since a reduced growth rate is often correlated with elevated levels of stress. The changes in growth patterns as the a_w decreases (Fig. 3A-D) are most likely due to a decrease of autolysin activity and as a result rods become more and more filamentous.

Bacterial helical structures have also been found before in some Gram-positive bacilli and notably in mutants of *B. subtilis* strain 168 under conditions that lead to a reduction in autolytic enzyme activity (Mendelson, 1982), but also in cyanobacteria (Hernandez-Muniz and Stevens, Jr., 1988), *Thermus* sp. (Janssen *et al.*, 1991) and in *Zymomonas mobilis* under the influence of salts (Fein *et al.*, 1984). The present finding that *P. fluorescence* and *S. paucimobilis* also display this distinct growth pattern at certain low a_w values adds credence to the notion of helical growth being more widespread in the bacterial world than might have been previously thought. By forming these rope-like structures these bacteria decrease their (exposed) surface to volume ratio.

In fact, all changes observed in bacterial cells grown at low a_w values cause a decrease in surface to volume ratio, suggesting that this is part of the bacterial response to limited availability of water. At the single cell level cells become bigger and/or rounder, while at a multicellular level bacteria tend to stick more together (Figs. S1 and S2). Especially this latter aspect seems to indicate a role of subaerial biofilm formation in the observed adaptational process.

Some of the changes seen in *B. subtilis* have been reported previously. The bent cells seen in Fig. 4D also appeared in response to sub-lytic concentrations of glycerol and sucrose esters of fatty acids (Tsuchido *et al.*, 1987). The sphere-like clumps as seen in Figs. 4F-G have been observed in mutants lacking in autolysin activity (Shiflett *et al.*, 1977). In the present studies, the more natural stress of reduced water availability revealed a series of morphological changes that are indicative of a controlled adaptive response of wild-type *B. subtilis* allowing this organism to grow slowly under sub-optimal conditions instead of just achieving survival by means of sporulation.

Increased cell size and decreased cell separation have been observed for wild-type staphylococci exposed to stressors such as penicillin, or grown under conditions of high ionic stress. Both types of stress resulted in the formation of tetrads and ultimately cubical cell packets (Tzagoloff and Novick, 1977; Vijaranakul *et al.*, 1995). Such changes have also been observed for mutants deficient in autolytic enzyme activity (Koyama *et al.*, 1977), or cells grown in the presence of autolysin inhibitors such as polyanethole sulfonate (Wecke *et al.*, 1986).

Decreased autolysin activity often is associated with a thickening of the peptidoglycan layer, *i.e.* an increased cell wall thickness (Shiflett *et al.*, 1977; Sieradzki and Tomasz, 2006). These changes in metabolism and cell morphology are not just indirect results of stress, but appear to be a response of these cells to become more stress resistant. Decreased autolytic activity and/or increased cell wall thickness has been reported to decrease adsorption of bacteriophages (Shiflett *et al.*, 1977) and release of phages from infected cells (Ronda-Lain *et al.*, 1977).

More importantly there is strong evidence that these adaptations make bacteria more resistant against various antibiotics (Horne and Tomasz, 1980; Maisnier-Patin and Richard, 1996). In particular, cell wall thickening has been proposed as a mechanism for vancomycin resistance in *S. aureus* (VRSA) (Cui *et al.*, 2003; Renzoni *et al.*, 2006).

Thickened peptidoglycan layers can be brought about by two mechanisms, namely overproduction of peptidoglycan or reduced peptidoglycan turnover (Hiramatsu, 2001). In the present studies, all bacterial species tested showed reduced levels of cell separation after division in response to lower a_w values. This seems to suggest that the mechanism of cell wall thickening, as shown in Fig. 7, is caused by a reduced cell wall turnover rate which in turn is most likely due to reduced autolytic activity.

Consistent with the thickened cell walls, staphylocci adapted to growth at low humidity levels showed a significant increase in vancomycin resistance. Though the vancomycin MIC increase was relatively small its effect might still be relevant in a clinical setting as a stepping stone for bacteria towards higher resistance, for example via biofilm formation, or for pharmacokinetic reasons where a poor tissue penetration of certain antibiotics might be an issue (Goldstein, 2007). The altered morphology or growth patterns of some bacteria grown at low humidity could thus be more relevant than their much better known morphology or growth patterns at high humidity. For example, the normal habitat of *S. epidermidis* is the human skin, which can be a relatively dry place depending on the depth in the skin and the surrounding humidity (Blank *et al.*, 1984). It therefore seems no coincidence that these staphylococci have adapted to growth at such low a_w values and are the dominant group found on human skin (Bibel *et al.*, 1976). If water activity values become higher staphylococci will probably lose the competition with other bacteria (Marsh and Selwyn, 1977).

Indeed, it has been reported that Gram-negative bacteria can become more prevalent on human skin under conditions of elevated RH (Aly *et al.*, 1978; McBride *et al.*, 1975). Thus, species like *S. epidermidis* will dominate probably only at the low a_w values where other species have problems growing.

In (closed) systems where the RH is maintained at a certain level, usually between 40 to 60%, like in hospitals or spacecraft, the actual RH will have deviations on a local scale due to local temperature differences and air convection. The cause of this is that the RH of air becomes higher if it is cooled down, or lowered when the air is warmed up. It can thus be expected that the larger a deviation is from the average RH the more uncommon it is. This means that if niches capable of supporting microbial growth exist at all, there will be more niches available with low a_w rather than high a_w values. It is therefore very well conceivable that, for example, susceptible staphylococci could thus become more resistant against various antibiotics and other stressors in the water challenged habitats where they are actually growing.

The a_w gradient technology as described in the present studies is also suitable for studies on bacterial competition, making it an even more relevant tool for ecological research. In its most simple form, this technology can already be applied to study competition of microbes with clearly distinct cell morphologies and/or Gram-staining properties, such as *S. epidermidis* and *S. paucimobilis*, provided that these properties are not influenced by changing a_w conditions.

As shown in co-cultivation experiments with *S. aureus* and *P. aeruginosa*, these limitations can be overcome altogether by bacterial detection through qPCR, which has the additional advantages of increased sensitivity and the provision of quantitative data. Over a wide range of a_w conditions, no significant differences were detectable by qPCR in the co-cultivation of *S. aureus* and *P. aeruginosa* as compared to the results obtained with the respective mono-cultures. The results however did show that both *S. aureus* and *P. aeruginosa* reached higher densities at a_w values where both could still grow well (0.97-1) as compared to the respective mono-cultures. Notably, it has been reported that *S. aureus* and *P. aeruginosa* can suppress each other's growth, but it also appears that these bacteria can form more robust biofilms when grown together (Goldsworthy, 2008), and that co-cultivation makes them more resistant against certain antibiotics (Hoffman *et al.*, 2006). This might partly explain why these two species are often found together in wound infections.

In conclusion, the recognition that the relative humidity is an important natural factor in determining bacterial growth, survival, cell morphology, sporulation, subaerial biofilm formation, antibiotic resistance and competitive success is likely to trigger many new applications for the relative humidity gradient method reported in the present studies. Perhaps most importantly, this novel methodology enables the exploration of relevant water-limited growth conditions at air-surface interfaces that represent major ecological niches.

Experimental Procedures

Organisms

All bacterial species used in this study are listed in Table 3 and were freshly grown overnight in tryptic soy broth (Oxoid, England) at 35 ^{o}C before being used as an inocculant.

Materials and chemicals

96-well plates from Corning Incorporated were used in combination with 76mm x 26mm microscope slides from Menzel Glazer. All salts used (Table 1) were of laboratory grade.

A_w assay

The lid of a 96-well plate (96-WP) was pre-coated with tryptic soy agar (TSA) and allowed to dry for 10 minutes after which 4 microscope slides were deposited onto the lid each covering a surface equivalent to 3 by 8 wells. The lid with the microscope slides inside was then coated with another layer of TSA and was left to dry in a laminar flow cabinet for 16 hours or longer. 100 µl of a pre-warmed (>28 ^{o}C) fully saturated salt solution was then pipetted into each well of a row of a 96-WP. When cooled down to 28 ^{o}C the saturated salt solutions formed crystals at the bottom of the 96-WP. The coated lid was then put on top of the 96-WP and pre-incubated at 28 ^{o}C for 6 hours.

A humidity gradient is created by choosing the appropriate saturated salt solutions per row from Table 1. After pre-incubation the lid of the 96-WP was inoculated with the desired microorganism(s) by spraying 2 ml or less of an overnight culture using an aerosol pump into a box held above the TSA coated inside of the 96-WP lid (Fig. 1). After having dispersed 1 ml into the box the lid was turned 180^{o} horizontally before dispersing the remaining ml. Using this technique only aerosols and very small droplets reached the agar surface causing only minimal disruption of the a_w gradient.

After the bacteria were dispersed the box was closed and the aerosols were allowed to settle for 15 minutes after which the box was opened to put the inoculated lid back on top of the 96-WP. The box containing the 96-WP was then closed again for an incubation period of 5 days at 28 ^{o}C. After the incubation period the lid of the 96-WP was removed again and microscope slides inside the lid were cut out. The microscope slides were first air-dried for approximately 5 minutes before direct inspection using contrast microscopy or before being Gram-stained in their entirety. After the Gram staining procedure microscope slides were again air-dried before being put under an oil immersion microscope for inspection. Images were captured using a digital camera and software from SPOT, Diagnostic Instruments (Puchheim, Germany), coupled to an Olympus-BH2 fluorescence microscope (Zoeterwoude, the Netherlands).

The inoculating density in a_w gradient assays was determined by studying the cells in a droplet at a RH value below the growth limit of the respective strain used for analysis. Lack of growth was easily recognizable as non-growing cells showed no changes in morphology compared to the morphology of the cells that were sprayed on the agar. By making this comparison, the number of divisions that slow growing cells had undergone upon incubation under conditions of severe water limitation could be estimated.

Transmission electron microscopy

S. epidermidis 35984 was grown as is described in the a_w assay. After the incubation period glass slides were cut out and the cells on these slides were fixed with 2% glutaraldehyde (pH 7.4, using a 0.1 M Cacodylate buffer). After fixation the glass slides were removed leaving just the TSA agar layer for further treatment. Postfixation of the samples was performed with 1% osmium tetroxide and 1.5% potassium ferrocyanide (pH 7.4, using a 0.1 M Sodium Cacodylate buffer). The postfixed samples were washed 4 times in MQ and then dehydrated using an ascending series of ethyl-ethanol. After dehydration, sub-samples corresponding to various positions within the RH gradient were cut out of the TSA agar layer. These sub-samples were then routinely embedded in Epon 812. Ultrathin sections were cut on a microtome and were placed on copper grids. Images taken on a Philips CM100 (FEI, Eindhoven, the Netherlands) electron microscope operated at 80 kV were digitized.

Vancomycin resistance assay

After an incubation period of 5 days at distinct RH values, set by equilibrating plates with a single saturated saturated salt solution (Table 1), staphylococcal cells were harvested in PBS buffer. The bacterial suspensions in PBS buffer were subsequently diluted to reach optical density levels equivalent to 0.5 McFarland. 25 µl of these solutions was then spread out over large ISO agar plates (Oxoid, England). Up to three vancomycin strips were placed on top of these plates (S-Dimecon, the Netherlands). The ISO agar plates were then incubated at 37 ^{o}C and vancomycin resistance levels were determined after at least 24 hours.

DNA extraction and (qPCR)

Samples were grown as described for the a_w assay with the exceptions that a Nadir dialysis membrane (Roth, Karlsruhe, Germany) was deposited onto the agar-coated lid and that two rows of the 96-WP were used for each saturated salt instead of one. After 5 days of incubation, dialysis membrane samples with a surface equal to 3 wells were cut from the middle of these two rows. These samples were immediately transferred to 2 ml screw-cap tubes. 900 µl TE buffer

(10 mM Tris-HCl pH 8.0, 1 mM EDTA), 500 µl phenol and approximately 200 µl 0.1 mm glass beads were added to each sample. Samples were vortexed for 15 s and then homogenized for 60 s at 3450 oscillations/min in a Mini-Beadbeater-16 (Biospec Products). After bead-beating the samples were cooled on ice for 1 min. These bead-beating/cooling steps were repeated three times. After bead-beating Tris-buffered (pH 8.0) phenol:chloroform:isoamyl 25:24:1 extraction was perfomed using a standard protocol (Sambrook *et al.*, 1989) with some modifications to ensure quantitative extraction. With each transfer of the aqueous phase, 150 µl ml of the sample was left at the phenol-sample interphase for accuracy and purity reasons. A 15 minute RNAse treatment at 37 ^{o}C was included in the procedure as well in between PCI extractions using 1 µl of a 20 mg/ml RNAse solution (Sigma). After isopropanol precipitation and subsequent washing with 70% ethanol, the DNA pellet was dissolved in 50 µl of TE buffer. DNA purity and approximate DNA content was checked using a spectrofotometer (Thermo Scientific Nanodrop 1000).

To compare population densities of both the mixed culture biofilm and the mono-cultures of *S. aureus* and *P. aeruginosa*, quantitative real-time PCR (qPCR) was performed using the Smart^{TM} Kit (Eurogentec, Seraing, Belgium) containing dUracil nucleotides and duraciliase. For 1 ml of *S. aureus* reaction mixture, 500 µl 2x PCR Master Mix solution was used, 1 µl forward primer (150 µM), 1 µl reverse primer (150 µM), 6 µl reverse primer (20 µM) and 392 µl nuclease-free water (AccuGENE). For 1 ml of *P. aeruginosa* reaction mixture 500 µl 2x PCR Master Mix solution was used, 1.5 µl forward primer (100 µM), 1.5 µl reverse primer (100 µM), 3 µl reverse primer (100 µM) and 394 µl nuclease-free water (AccuGENE). 3 µl of sample DNA was mixed with 27 µl reaction mixture in the final reaction volume. Both the 16s primers and the probe had been previously designed (De Vos *et al.*, 1997; Ludwig and Schleifer, 2000). The *S. aureus* primers are: forward 5'-GCT GTG ATG GGG AGA AGA CAT-3', reverse 5'-CGG TAC GGG CAC CTA TTT TC-3', probe: 5'-AGA GGC TTT TCT CGG CAG TGT GAA ATC AAC GA-3', labels: FAM + DabCyl. The *P. aeruginosa* primers are: forward 5'-CAA CGT TCT GAA ATT CTC TGC T-3', reverse 5'-

CTT GCG GCT GGC TTT TTC-3', probe: 5'-AAA GAA ACC GAA GCW CGT CTG AC-3' (W is T or A), labels: FAM + Darquencher. Reaction conditions were optimized previously for both strains (S. van Tongeren, personal communication). The DNA was amplified real-time on a Cepheid Smart Cycler, version 2.0d (Lucron Bioproducts B.V., Gennep, the Netherlands) using the following cycle protocol: *S. aureus*, 1 cycle for 120 s at 50 °C and 600 s at 95 °C followed by 45 cycles for 15 s at 95 °C and 60 s at 60 °C. *P. aeruginosa*: 1 cycle for 120 s at 50 °C and 600 s at 95 °C followed by 45 cycles for 10 s at 95 °C, 60 s at 62 °C and 15 s at 72 °C. The amplified DNA was quantified using a calibration curve made with purified DNA of either species (isolated as described above) and the Cepheid software.

Acknowledgments

M.C.d.G and H.J.M.H were supported by the Netherlands Institute for Space Research (SRON) grants MG-064 and MG-068. J.M.v.D. was supported in part by European Union Grants LSHG-CT-2004-503468 and LSHM-CT-2006-019064. We wish to thank Sandra van Tongeren for her help starting up the qPCR experiments and for providing strains isolated from ISS samples of the SAMPLE experiments that are supported by ESA.

Supplementary Figures

Figure S1.

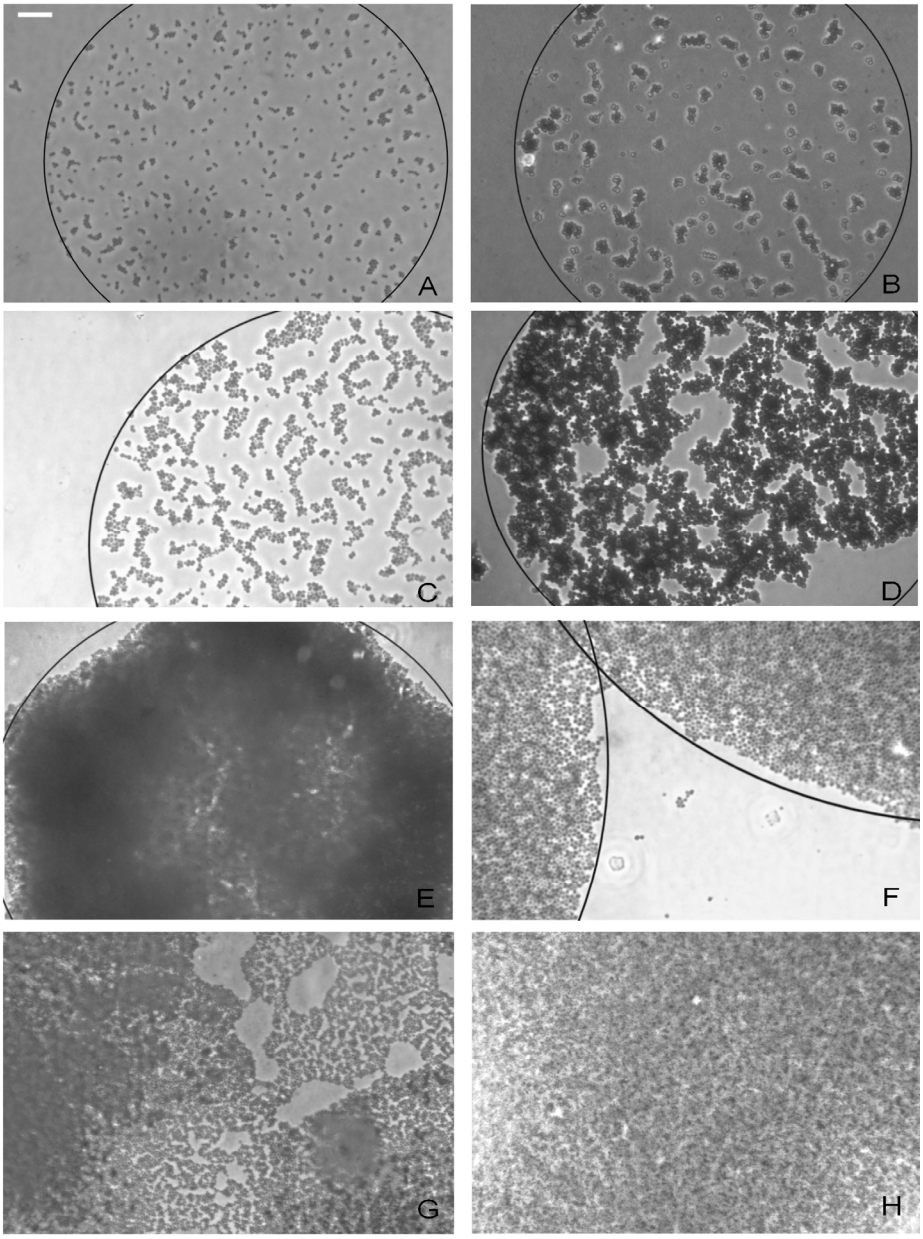

Figure S2.

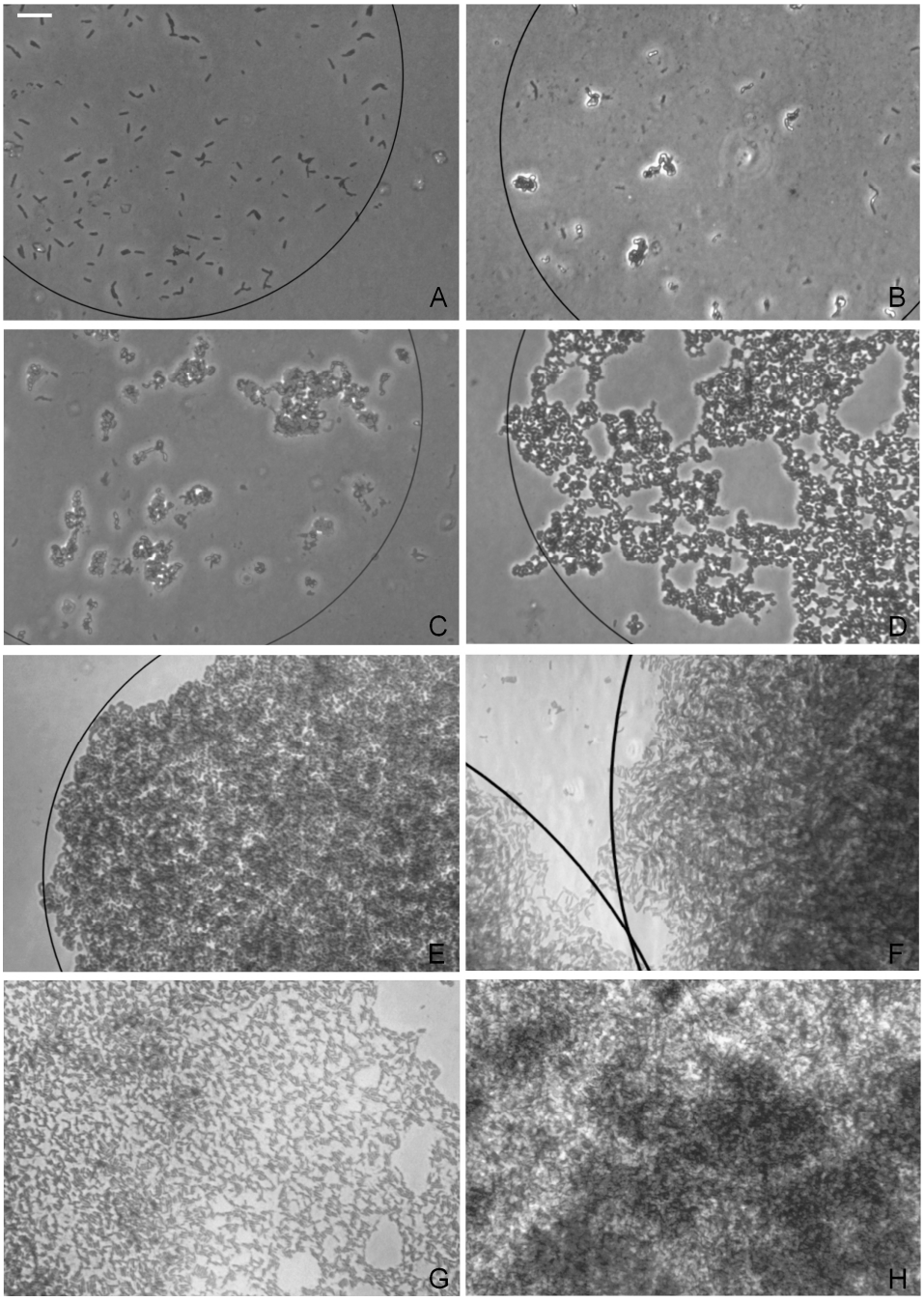

Figure S1. *Staphylococcus epidermidis* population density order (PDO) examples for the scoring system shown in Table 2. Samples (**A**-**H**) represent PDO values going from 1 to 8. (**A**) shows a droplet inoculated onto the agar of which the cells have not been able to grow. (**B**) shows a droplet in which most cells have divided a few times. Small clusters of cells are shown in (**C**) leading to larger clusters in (**D**). At (**E**) an inoculated droplet has grown to confluence. Once a droplet has grown to confluence it will start increasing in size (**F**) until a point is reached where individual droplets are no longer recognizable (**G**). Thick layers of bacteria will eventually cover most of the agar surface (**H**). Circles are drawn to show the edges of inoculated droplets or colonies grown to confluence.

Figure S2. *Bacillus subtilis* population density order (PDO) examples for the scoring system shown in Table 2. The description of (**A**-**H**) as given for Fig. S1 also applies to (**A**-**H**) of this figure.

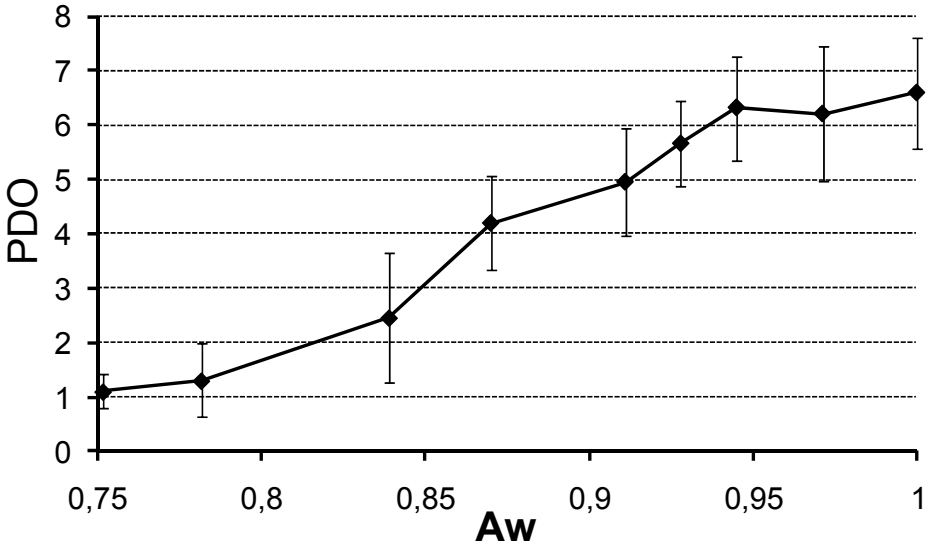

Figure S3. *Staphylococcus epidermidis* 12228 population density order (PDO) scores after an incubation period of 5 days at 28°C. The PDOs were scored using the classification system of Table 2. The given averages and standard error bars are the result from three separate experiments performed on different days, each scored by four observers.

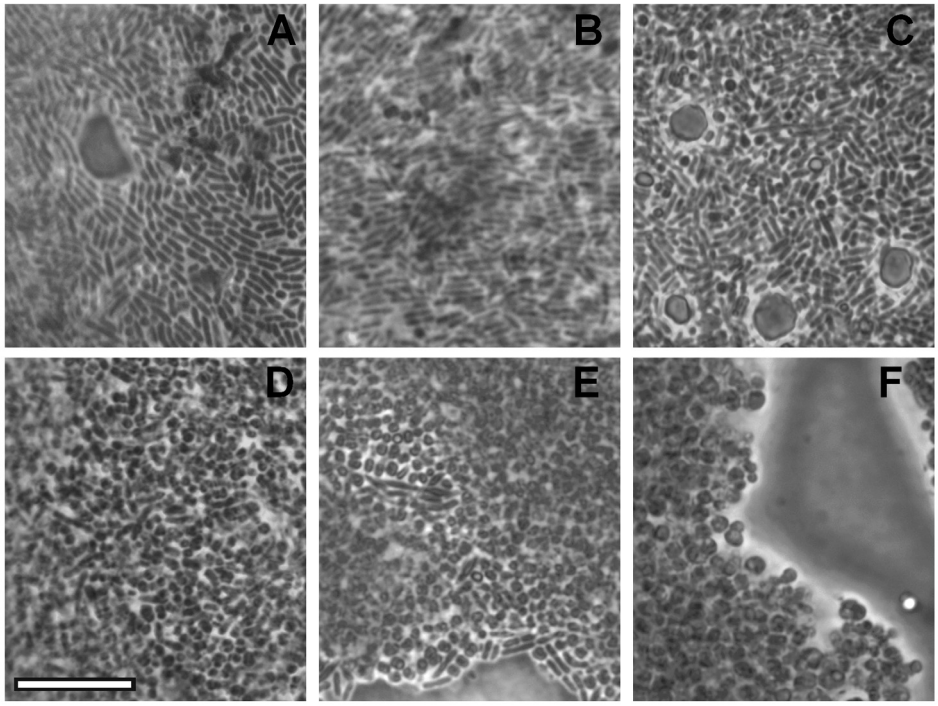

Figure S4. Micrograph of *S. epidermidis* and *S. paucimobilis* grown in competition with each other for 5 days at 28°C. (**A-F**) were taken at a_w values of 1.0, 0.97, 0.945, 0.93, 0.92 and 0.87 respectively. *Staphylococcus epidermidis* can be recognized by its round shape and *S. paucimobilis* by its rod-like shape. The black bordered bar indicates 10 μm (**A-F**).

Reference List

Alekhova,T.A., Aleksandrova,A.A., Novozhilova,T.I., Lysak,L.V., Zagustina,N.A., and Bezborodov,A.M. (2005) [Monitoring of microbial degraders in manned space stations]. *Prikl Biokhim Mikrobiol* **41:** 435-443.

Aly,R., Shirley,C., Cunico,B., and Maibach,H. (1978) Effect of Prolonged Occlusion on the Microbial Flora, pH, Carbon Dioxide and Transepidermal Water Loss on Human Skin. *J Investig Dermatol* **71:** 378-381.

Baranyi,J. and Tamplin,M.L. (2004) ComBase: a common database on microbial responses to food environments. *J Food Prot* **67:** 1967-1971.

Bibel,D.A.V.I., Lovell,D.A.V.I., and Smiljanic,R.O.K.O. (1976) Effects of occlusion upon population dynamics of skin bacteria. *British Journal of Dermatology* **95:** 607-612.

Blank,I.H., Moloney,J., III, Emslie,A.G., Simon,I., and Apt,C. (1984) The diffusion of water across the stratum corneum as a function of its water content. *J Invest Dermatol* **82:** 188-194.

Brimblecombe,P., Blades,N., Camuffo,D., Sturaro,G., Valentino,A., Gysels,K. *et al.* (1999) The indoor environment of a modern museum building, the Sainsbury Centre for Visual Arts, Norwich, UK. *Indoor Air* **9:** 146-164.

Buck,G.E. and Kelly,M.T. (1981) Effect of moisture content of the medium on colony morphology of Campylobacter fetus subsp. jejuni. *J Clin Microbiol* **14:** 585-586.

Castro,V.A., Thrasher,A.N., Healy,M., Ott,C.M., and Pierson,D.L. (2004) Microbial characterization during the early habitation of the International Space Station. *Microb Ecol* **47:** 119-126.

Cirz,R., Jones,M., Gingles,N., Minogue,T., Jarrahi,B., Peterson,S., and Romesberg,F. (2007) Complete and SOS-Mediated Response of Staphylococcus aureus to the Antibiotic Ciprofloxacin. *J Bacteriol* **189:** 531-539.

Cui,L., Ma,X., Sato,K., Okuma,K., Tenover,F.C., Mamizuka,E.M. *et al.* (2003) Cell wall thickening is a common feature of vancomycin resistance in Staphylococcus aureus. *J Clin Microbiol* **41:** 5-14.

De Vos,D., Lim,A., Jr., Pirnay,J.P., Struelens,M., Vandenvelde,C., Duinslaeger,L. *et al.* (1997) Direct detection and identification of Pseudomonas aeruginosa in clinical samples such as skin biopsy specimens and expectorations by multiplex PCR based on two outer membrane lipoprotein genes, oprI and oprL. *J Clin Microbiol* **35:** 1295-1299.

ESA (2008). European users guide to low gravity platforms [WWW document]. URL http://www.spaceflight.esa.int/users/downloads/userguides/chapter_7_iss.pdf

Fein,J., Barber,D., Charley,R., Beveridge,T., and Lawford,H. (1984) Effect of commercial feedstocks on growth and morphology of Zymomonas mobilis. *Biotechnology Letters* **6:** 123-128.

Goldstein,F. (2007) The potential clinical impact of low-level antibiotic resistance in Staphylococcus aureus. *J Antimicrob Chemother* **59:** 1-4.

Goldsworthy,M.J.H. (2008) Gene expression of Pseudomonas aeruginosa and MRSA within a catheter-associated urinary tract infection biofilm model. *Bioscience Horizons* **1:** 28-37.

Gottenbos,B., van der Mei,H.C., and Busscher,H.J. (2000) Initial adhesion and surface growth of Staphylococcus epidermidis and Pseudomonas aeruginosa on biomedical polymers. *J Biomed Mater Res* **50:** 208-214.

Hernandez-Muniz,W. and Stevens,S.E., Jr. (1988) Significance of braided trichomes in the cyanobacterium Mastigocladus laminosus. *J Bacteriol* **170:** 1519-1522.

Hiramatsu,K. (2001) Vancomycin-resistant Staphylococcus aureus: a new model of antibiotic resistance. *Lancet Infect Dis* **1:** 147-155.

Hoffman,L.R., Deziel,E., D'Argenio,D.A., Lepine,F., Emerson,J., McNamara,S. *et al.* (2006) Selection for Staphylococcus aureus small-colony variants due to growth in the presence of Pseudomonas aeruginosa. *Proc Natl Acad Sci U S A* **103:** 19890-19895.

Höltje,J.V. (1995) From growth to autolysis: the murein hydrolases inEscherichia coli. *Archives of Microbiology* **164:** 243-254.

Horne,D. and Tomasz,A. (1980) Lethal effect of a heterologous murein hydrolase on penicillin-treated Streptococcus sanguis. *Antimicrob Agents Chemother* **17:** 235-246.

Janssen,P., Parker,L., and Morgan,H. (1991) Filament formation inThermus species in the presence of some D-amino acids or glycine. *Antonie van Leeuwenhoek* **59:** 147-154.

Kaur,I., Simons,E.R., Castro,V.A., Mark Ott,C., and Pierson,D.L. (2004) Changes in neutrophil functions in astronauts. *Brain Behav Immun* **18:** 443-450.

Koyama,T., Yamada,M., and Matsuhashi,M. (1977) Formation of regular packets of Staphylococcus aureus cells. *J Bacteriol* **129:** 1518-1523.

Ludwig,W. and Schleifer,K.H. (2000) How quantitative is quantitative PCR with respect to cell counts? *Syst Appl Microbiol* **23:** 556-562.

Maisnier-Patin,S. and Richard,J. (1996) Cell wall changes in nisin-resistant variants of Listeria innocua grown in the presence of high nisin concentrations. *FEMS Microbiology Letters* **140:** 29-35.

Marsh,P.D. and Selwyn,S. (1977) Studies on antagonism between human skin bacteria. *J Med Micro* **10:** 161-169.

Marshall,B.J., Ohye,D.F., and Christian,J.H. (1971) Tolerance of bacteria to high concentrations of NaCL and glycerol in the growth medium. *Appl Microbiol* **21:** 363-364.

McBride,M.E., Duncan,W.C., and Knox,J.M. (1975) Physiological and environmental control of Gram negative bacteria on skin. *Br J Dermatol* **93:** 191-199.

Mendelson,N.H. (1982) Dynamics of Bacillus subtilis helical macrofiber morphogenesis: writhing, folding, close packing, and contraction. *J Bacteriol* **151:** 438-449.

Novikova,N., De Boever,P., Poddubko,S., Deshevaya,E., Polikarpov,N., Rakova,N. *et al.* (2006) Survey of environmental biocontamination on board the International Space Station. *Res Microbiol* **157:** 5-12.

Novikova,N.D. (2004) Review of the knowledge of microbial contamination of the Russian manned spacecraft. *Microb Ecol* **47:** 127-132.

Ott,C.M., Bruce,R.J., and Pierson,D.L. (2004) Microbial characterization of free floating condensate aboard the Mir space station. *Microb Ecol* **47:** 133-136.

Rahman,M.S. and Labuza,T.P. (1999) Water activity and food preservation. In *Handbook of food preservation*. Rahman,M.S. (ed). New York: Marcel Dekker Inc., pp. 339-382.

Renzoni,A., Barras,C., Francois,P., Charbonnier,Y., Huggler,E., Garzoni,C. *et al.* (2006) Transcriptomic and functional analysis of an autolysis-deficient, teicoplanin-resistant derivative of methicillin-resistant Staphylococcus aureus. *Antimicrob Agents Chemother* **50:** 3048-3061.

Ronda-Lain,C., Lopez,R., Tapia,A., and Tomasz,A. (1977) Role of the pneumococcal autolysin (murein hydrolase) in the release of progeny bacteriophage and in the bacteriophage-induced lysis of the host cells. *J Virol* **21:** 366-374.

Sambrook,J., Fritsch,E.F., and Maniatis,T. (1989) *Molecular cloning : a laboratory manual*. New York: Cold Spring Harbor Laboratory Press.

Shiflett,M.A., Brooks,D., and Young,F.E. (1977) Cell wall and morphological changes induced by temperature shift in Bacillus subtilis cell wall mutants. *J Bacteriol* **132:** 681-690.

Sieradzki,K. and Tomasz,A. (2006) Inhibition of the autolytic system by vancomycin causes mimicry of vancomycin-intermediate Staphylococcus aureus-type resistance, cell concentration dependence of the MIC, and antibiotic tolerance in vancomycin-susceptible S. aureus. *Antimicrob Agents Chemother* **50:** 527-533.

Tsuchido,T., Ahn,Y.H., and Takano,M. (1987) Lysis of Bacillus subtilis Cells by Glycerol and Sucrose Esters of Fatty Acids. *Appl Environ Microbiol* **53:** 505-508.

Tzagoloff,H. and Novick,R. (1977) Geometry of cell division in Staphylococcus aureus. *J Bacteriol* **129:** 343-350.

Vijaranakul,U., Nadakavukaren,M.J., de Jonge,B.L., Wilkinson,B.J., and Jayaswal,R.K. (1995) Increased cell size and shortened peptidoglycan interpeptide bridge of NaCl-stressed Staphylococcus aureus and their reversal by glycine betaine. *J Bacteriol* **177:** 5116-5121.

Wecke,J., Lahav,M., Ginsburg,I., Kwa,E., and Giesbrecht,P. (1986) Inhibition of wall autolysis of staphylococci by sodium polyanethole sulfonate liquoid. *Archives of Microbiology* **144:** 110-115.

Wiebe,H.H. (1981) Measuring Water Potential (Activity) from Free Water to Oven Dryness. *Plant Physiol* **68:** 1218-1221.

Winston,P. and Bates,D. (1960) Saturated Solutions For the Control of Humidity in Biological Research. *Ecology* **41:** 232-237.

Chapter 3

Adaptation of *Bacillus subtilis* to low humidity requires the general sigma B response for protection against self-inflicted oxidative stress

Marcus C. de Goffau[†], Xiao-Mei Yang[†], Emma L. Denham, Sjouke Piersma, Haike Antelmann, Michael Hecker, Hermie J. M. Harmsen and Jan Maarten van Dijl

[†] These authors contributed equally to this work

Submitted for publication

Abstract

Bacillus subtilis displays massive morphological changes in response to reduced water availability as it becomes filamentous, shorter, curved and eventually almost coccoid at low relative humidity (RH) values. These changes turned out to be completely reversible in the presence of water as rod-like cells grew out of coccoid cells in a germination-like process. To obtain a better understanding of the underlying adaptive mechanisms, a proteomics analysis was performed. This revealed three main cellular responses to water limitation.

Firstly, the proteomics data were indicative of the adjustment of intracellular osmotic values, and changes in cell wall composition. Alterations in the cell wall were subsequently confirmed using transmission electron microscopy. Importantly, the proteomic signatures of water-limited cells indicated a strong Sigma B (σ^B)-dependent oxidative stress response. The σ^B-dependent gene expression was shown to be essential for the survival of *B. subtilis* cells under conditions of limited water availability since deletion mutants lacking the *sigB* gene, or the σ^B-regulated catalase *katE* gene were unable to adapt to low RH values.

Taken together, our findings show that *B. subtilis* needs to protect itself against self-inflicted oxidative stress under water-limited growth conditions.

Introduction

Desiccation is one of the most critical environmental hazards that organisms need to deal with in terrestrial environments and, as such, it has played a major role in the evolution of prokaryotes (Battistuzzi and Hedges, 2009). The Gram-positive bacterium *Bacillus subtilis* is often found in the upper soil layer, where the organism is exposed to a wide variety of environmental insults, including a severely limited availability of water. To describe the relationship between the available water content and bacterial growth, W.J. Scott first established the term water activity (a_w) in 1953 (Scott, 1953). Since then, this term has been widely applied, especially in the food industry in relation to the prevention of spoilage by microorganisms.

The effects of water limitation on bacterial growth have traditionally been investigated by adding variable amounts of solute to either nutrient broths or agar plates. Apart from causing a reduction in growth rate, water limitation is also known to influence colony color and/or texture. On a microscopic scale, we have recently reported various morphological changes of bacteria in response to reduced water availability in a relative humidity gradient system (de Goffau *et al.*, 2009). Using a selection of eight saturated salt solutions, a relative humidity (RH) gradient can be created beneath the agar-coated lid of a 96-well plate. This translates into a a_w gradient within the agar-coated lid since the a_w of the agar will be equal to RH/100 under equilibrium conditions. The relative humidity gradient system is comparable to traditional aqueous systems with the additional advantage of not having any direct solute-specific effects on the growth of bacteria (Marshall *et al.*, 1971). Moreover, it allows monitoring the growth and survival of bacteria at surface-air interfaces under varying conditions of water availability, which is highly relevant from an ecological perspective.

With decreasing a_w values, it was observed that *B. subtilis* becomes filamentous at first, but then also becomes shorter, curved, and thicker, eventually transforming into an almost coccoid state before finally starting to sporulate at high frequency (de Goffau *et al.*, 2009). The changes in cell morphology of *B. subtilis* grown at low a_w values have been interpreted as

physiological adaptations that protect this bacterium against the stress of low water availability. It is known that *B. subtilis* has several sophisticated mechanisms to sense and adapt to environmental changes and insults, using highly integrated regulatory networks. Thus, the expression of many genes of this organism is dependent on the recognition of their promoters by different sigma subunits of the DNA-dependent RNA polymerase (Haldenwang, 1995). The vegetative sigma factor B (σ^B) is activated when *B. subtilis* enters the stationary growth phase. However, environmental insults such as freezing and thawing, alkaline shock, ethanol shock and many others can also induce σ^B-dependent stress responses. This would suggest that σ^B might also have a role in modulating cellular responses for growth and survival at low a_w values, but this had so far not been investigated.

The first goal of the present studies was to determine whether the morphological transition of *B. subtilis* cells from the rod to the coccoid state are completely reversible, or whether this transition results in a non-culturable state. Secondly, a proteomics analysis was performed to elucidate the poorly understood molecular mechanisms of cellular adaptation to water deprivation.

Our findings show that many of the observed changes in the *B. subtilis* cells upon water deprivation relate to a strong σ^B-dependent stress response, which seems to be triggered to a large extent by self-inflicted oxidative stress. This stress response is required to thrive and survive at low a_w values. Additional changes in the proteome seem to relate to an adaptation of the internal osmotic value and adjustments of the cell wall.

Material and Methods

Bacterial strains, media, and chemicals

All bacterial species used in this study are listed in Table 1. Bacteria were grown overnight in Luria Bertani broth or Tryptic soy broth (LB, TSB, Oxoid, England) at 37 ^{o}C before being used as an inoculant. 24- and 96-wells plates from Corning Incorporated were used for creating a_w gradients, sometimes in combination with 76mm x 26mm microscope slides from Menzel Glazer. All salts used (Table 2) were of laboratory grade.

Table 1. Bacteria

***B. subtilis* strain**	**Relevant genotype**	**Reference**
168	*trpC2*	(Brigulla *et al.*, 2003)
BSM 29	*trpC2*, *sigB*Δ2::Sp, Sp^R	(Brigulla *et al.*, 2003)
MAY1	*trpC2*, *katA*::Sp, Sp^R	This study
MAY2	*trpC2*, *katE*::Sp, Sp^R	This study
gsiB-gfp	*trpC2*, P*gsiB-gfp*, Sp^R	This study
ydaP-gfp	*trpC2*, P*ydaP-gfp*, Sp^R	This study

Table 2. Saturated salt solutions and their corresponding RH values

Salt	**RH at 29 ^{o}C**	**RH at 32 ^{o}C**	**Reference**
H_2O	100%	100%	-
K_2SO_4	97.1% ± 0.5%	96.9% ± 0.5%	(Greenspan, 1976)
KH_2PO_4	94.0% ± 1.0%	93.3% ± 1.0%	(Winston and Bates, 1960)
$NH_4H_2PO_3$	92.9% ± 0.5%	-	(O'Brien, 1948)
KNO_3	92.6% ± 0.5%	91.7% ± 0.5%	(Greenspan, 1976)
KNaTartrate	87.0% ± 1.0%	86.6% ± 1.0%	(Winston and Bates, 1960)
KCl	84.1% ± 0.5%	83.3% ± 0.5%	(Greenspan, 1976)
$NH_4H_2SO_4$	80.7% ± 0.5%	80.5% ± 0.5%	(Greenspan, 1976)
NaCl	75.1% ± 0.5%	75.0% ± 0.5%	(Greenspan, 1976)

Analysis of bacterial growth on a_w gradients

A_w gradients were created beneath the lid of 24- or 96-wells plates using saturated salts, according to the method described previously (de Goffau *et al.*, 2009). Overnight grown bacteria (2 ml) were used to inoculate the a_w gradient with the help of an aerosol pump. The a_w gradients were subsequently incubated for 5 days at 29°C or 32°C. After 5 days of incubation the lid of the 24- or 96-wells plate was removed again and, if applicable, the microscope slides inside the lid were cut out. These microscope slides were then directly inspected using fluorescence or phase contrast microscopy. Images were recorded using a digital camera (SPOT Diagnostic Instruments, Puchheim, Germany), coupled to an Olympus-BH2 fluorescence microscope (Zoeterwoude, the Netherlands). Agar-coated lids without glass slides were photographed using a G:box (Syngene, Leusden, The Netherlands).

Time-lapse microscopy

Time-lapse microscopy was performed essentially as described by Botella *et al.* (2010). *B. subtilis* cells grown on LB agar at a_w 0.926 RH were used to inoculate a gene frame with LB agar. Growth of cells at 37 °C was monitored for 17 h and phase contrast images were recorded every 10 min.

Electron microscopy

B. subtilis 168 was grown in a a_w gradient as described earlier. For the transmission electron microscopy (TEM) experiments, glass slides were cut out after the incubation period and the cells on these slides were fixed with 2% glutaraldehyde in a 0.1 M Cacodylate buffer (pH 7.4). After fixation, the glass slides were removed leaving just the TSA agar layer for further treatment. Post-fixation of the samples was performed with 1% osmium tetroxide and 1.5% potassium ferrocyanide in a 0.1 M Sodium Cacodylate buffer (pH 7.4). The resulting samples were washed 4 times in Milli-Q and then dehydrated using an ascending series of ethyl-ethanol. After dehydration, sub-samples corresponding to various positions within the a_w gradient were cut out of the TSA agar layer. These sub-samples were then routinely embedded in Epon 812. Ultrathin sections

were cut on a microtome and placed on copper grids. Images recorded with a Philips CM100 (FEI, Eindhoven, the Netherlands) electron microscope operated at 80 kV were digitized. For the scanning electron microscopy (SEM) experiments, glass slides were cut out after the incubation period and the cells on these slides were fixed with glutaraldehyde followed by osmium tetroxide, dehydrated in a graded series of acetone, and critical-point dried with liquid CO_2. The cells were coated and examined in a Cambridge model 240 SEM operating at 15 kV.

Proteomics analyses

B. subtilis 168 cells were cultured at a_w 1 or 0.926 on top of an agar-coated lid on which a dialysis membrane had been deposited. The dialysis membrane does not interfere with the uptake of nutrients and facilitates the collection of cells at the end of the experiment as it would be difficult otherwise to separate the cells from the agar. Samples were collected after an incubation period of 1 day for the a_w 1 samples and 5 days for a_w 0.926 samples after which the cell densities on the plates were comparable. Cells were collected by pipetting killing buffer (10 mM Tris, 1 mM EDTA, 1 mM PMSF, 2 mM NaN_3) on top of the dialysis membrane and subsequently scraping them off the membrane. Bacteria were then disrupted by sonication and, after the removal of cell debris by centrifugation (20000 g for 30 min at 4^{o}C), the protein concentration of the crude protein extracts was determined according to the method of Bradford. Two-dimensional poly-acrylamide gel electrophoresis (2-D PAGE), image comparison and protein identification were performed as described previously (Brigulla *et al.*, 2003). Each experiment was performed at least three times.

Construction of promoter-GFP fusions in *B. subtilis*

The promoter regions of *ydaP* (primers ydaP Fwd 5'-CCGCGGGCTTTCCC-AGCgtgatcgtattgaacgaaagtc and ydaP Rev 5'-GTTCCTCCTTCCCACCcctttttt-caataccacaggag) and *gsiB* (primers gsiB Fwd 5'-CCGCGGGCTTTCCCAGC-ctgatgttgtcggcaaaagatcgattttg and gsiB Rev 5'-GTTCCTCCTTCCCACC-attggtgttggttgttgtattcccgctc) were amplified by PCR. Bases in capital letters

define regions for ligation-independent cloning (LIC). PCR products were purified and cloned by LIC into the BaSysBioII plasmid as described by Botella *et al.* (2010) to create the P*ydaP*-GFP and P*gsiB*-GFP fusions. *B. subtilis* cells were transformed with the resulting plasmids, and transformants were selected with spectinomycin (Sp).

Construction of catalase mutants

To delete the *katA* gene of *B. subtilis*, DNA fragments of ~1 kb corresponding to the upstream region of *katA* (positions -1000 to -1 relative to the *katA* start codon) and the downstream region of *katA* (positions +1443 to 2451) were PCR-amplified with the primer pairs katA-D1 and katA-D2 (5'-CATTTCCTAAATA-AACAGATTCAT and 5'-CGAAAATCGCCATTCGCCAGACCTCTTGGAAT-TTATAAGAACAT, respectively), and katA-D3 and katA-D4 (5'- AACCCTTG-CATAGGGGGATCGATTAAAAAAGATTCTTAATGGAG and 5'- ATTTGA-ACAGCTGACTGTAATC, respectively). A Sp resistance gene was PCR-amplified with primers sp1- (5'-CT GGCGAATGGCGATTTTCG) and sp2 (5'-GATCCCCCTATGCAAGGGTT) from pGDL1726, using the high-fidelity Pwo polymerase (Roche). Equal amounts of PCR products of the up- and down-stream regions of *katA* and the Sp resistance gene were used for a fusion PCR, which generated a 2689bp DNA fragment. Transformation of *B. subtilis* 168 with this fragment resulted in the deletion of the *katA* gene through homologous recombination. A *katE* mutant was constructed by the same procedure using the primer pairs katE-D1 and katED2 (5'- CATTTGGATAGTTAACCATCAA and 5'- CGAAAATCGCCATTCGCCAGGTCTGCTCCCCCTTTTTAAAA), and katE-D3 and katE-D4 (5'-AACCCTTGCATAGGGGGATCTGATCGG-CTCCTGTATCTTTAAG and 5'-AACAGCACATCGTGTTTTTTGAT).

Results and Discussion

Real-time microscopy shows that morphological changes due to growth at low a_w are fully reversible

To investigate whether the morphological changes from a rod- into a coccoid shape are fully reversible, *B. subtilis* cells were grown in a 96-wells plate a_w gradient as previously described (Fig. 1) (de Goffau *et al.*, 2009).

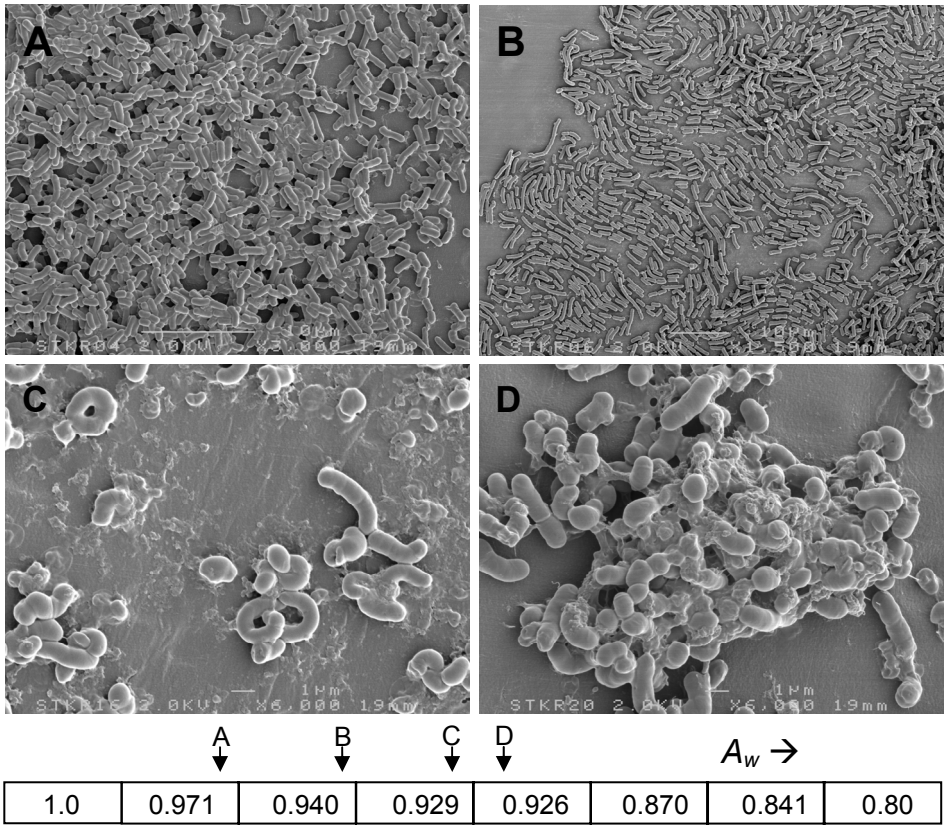

Figure 1. Scanning electron micrographs of *B. subtilis* 168 grown in a a_w gradient. The pictures show a gradual change in morphology as *B. subtilis* approaches its a_w growth limit (**A**-**D**). The a_w gradient used in this experiment is depicted at the bottom of the figure. The black arrows indicate the position in the a_w gradient where each picture was taken (**A**-**D**). The white bars indicate 10µm in (**A**) and (**B**), and 1 µm in (**C**) and (**D**).

Coccoid cells were harvested from a gradient position with a a_w value of 0.926, and these cells were subsequently used to inoculate a microscope slide with LB (a_w > 0.99) for time-lapse microscopy. After a short lag phase, rod-shaped cells emerged from the coccoid cells, which were morphologically indistinguishable from cells growing at high a_w levels (Fig. 2).

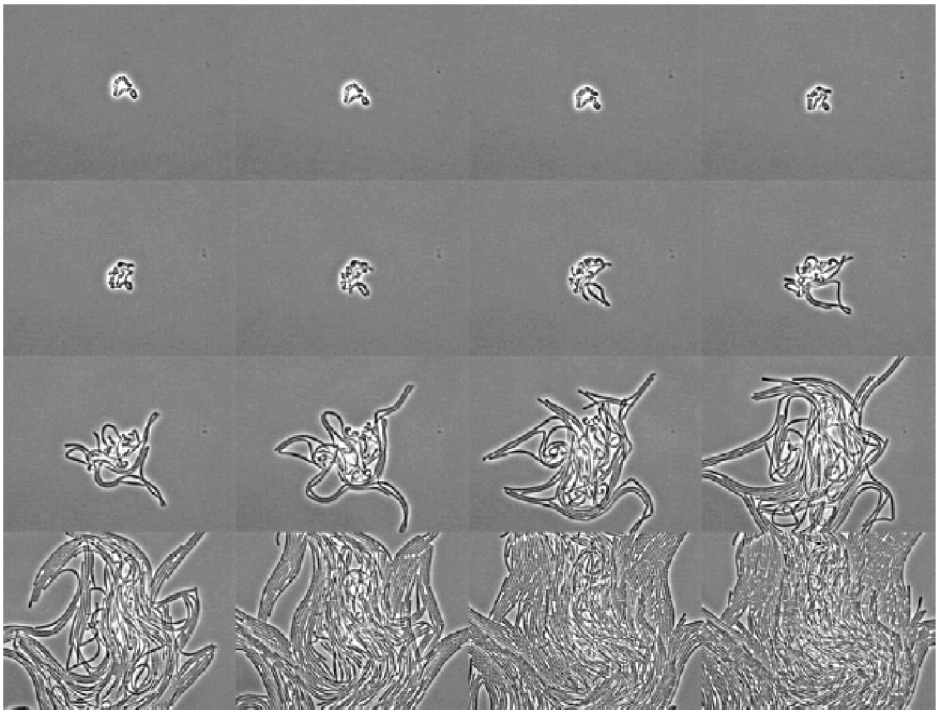

Figure 2. Time-lapse microscopy of *B. subtilis* 168. Cells were initially grown at a_w 0.926 a_w and then transferred to a a_w > 0.99 environment under the microscope. The images shown were recorded at 30 min intervals.

Interestingly, the transition from the coccoid- to the rod-like shape involved a process that is reminiscent of spore germination, as the rod-like cells grew out of the coccoid cells, apparently leaving the 'old' cell wall behind. Careful analysis of the time-lapse microscopy data suggests that the old walls of cells grown at low a_w were shed as new cell walls were formed, which apparently have a more suitable composition for growing at high a_w values.

The real-time microscopy data thus show that the changes in morphology, which occur when *B. subtilis* is grown at sub-optimal a_w values, are fully reversible and that they have no bearing on cell culturability. The phenotypic changes are thus the result of adaptations that will most likely contribute to the growth and survival of *B. subtilis* in water-limited environments.

Proteomics analysis of *B. subtilis* cells grown at low a_w

To obtain insights in the physiological adaptations of *B. subtilis* in response to reduced water availability, a proteomics analysis was performed on *B. subtilis* cells that were grown either at a_w 1 or at a_w 0.926. Total soluble protein extracts of these cells were used for 2-D PAGE. A false-color overlay of two representative 2-D gels is shown in Fig. 3.

The proteomics data are indicative of three main responses (Tables 3, S1 and S2). Two groups of proteins present in different amounts are involved in determining the cell wall composition (Group 1) and in regulating the intracellular osmotic value (Group 2). Notably, the largest group of proteins present in different amounts (Group 3) has functions in the cellular response to oxidative stress (e.g. catalases and hydroperoxide resistance proteins), or they have the potential to generate oxidative stress (e.g. dehydrogenases).

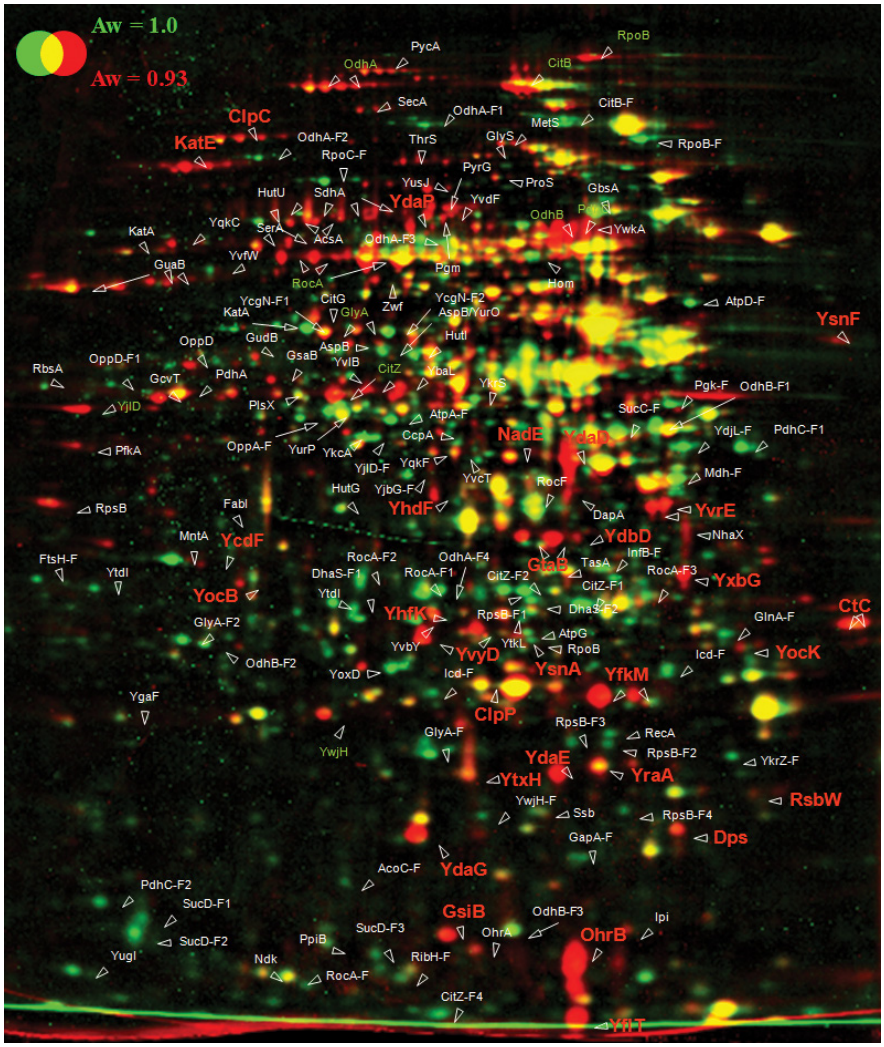

Figure 3. The proteomes of *B. subtilis* cells grown at a_w 1 or a_w 0.93. Proteins of *B. subtilis* cells grown at a_w 1 or a_w 0.93 were separated on 2-D gels and stained with Sypro Ruby. The presented picture was obtained by dual channel imaging of two representative warped images. The names of proteins identified by MALDI-TOF mass spectrometry are indicated. Green protein spots are predominantly present in the image of proteins of *B. subtilis* 168 cells grown at a_w 1; red protein spots are predominantly present in the image of proteins of *B. subtilis* 168 grown at a_w 0.93; and yellow protein spots are present at similar amounts in both images. Some green spots for proteins of low molecular mass correspond to degradation products of the respective proteins (Tables S1 and S2).

Table 3. Ratio between the levels of proteins involved in determining cell wall composition, regulating intracellular osmotic values, and responses to oxidative stress from cells grown at a a_w 0.926 or 1 that were found to be significantly altered. Positive and negative values denote that a protein was present at a higher concentration at a a_w value of 0.926 or 1 respectively.

Protein	Ratio	Function/Similarity
Group 1 - ***Cell wall composition***[1]		
FtsH	-27.0	Cell division protease
RecA	- 4.4	Recombinase A, induces a repressor of an inhibitor of FtsH
DapA	4.7	Dihydrodipicolinate synthase
GtaB[B]	2.7	UDP-glucose pyrophosphorylase
Pgm	4.3	Phosphoglucomutase
Group 2 - ***Compatible solutes & plant dessication protein***[2] ***homologs***[3]		
RocA	20.1	1-pyrroline-5-carboxylate dehydrogenase
AspB	4.2	Aspartate aminotransferase
GsiB[B]	5.0	Homologue of a late embryogeneis abundant (LEA) protein
YtxH[B]	1.9	Homologue of a late embryogeneis abundant (LEA) protein
GtaB[B]	2.7	UDP-glucose pyrophosphorylase
Pgm	4.3	Phosphoglucomutase
Group 3a - ***Catalases & hydroperoxide resistance proteins***[3]		
OhrB[B]	17.8	Hydroperoxide-resistance protein; conversion of hydroperoxides into alcohols and water
KatE[B]	12.4	Catalase 2, conversion of hydrogenperoxide to water
YdbD[B]	6.2	Unknown, similar to manganese-containing catalase
YkcA	3.5	hydroquinone-specific dioxygenase
OhrA	3.3	Hydroperoxide-resistance protein; conversion of hydroperoxides into alcohols and water
KatA	1.6	Catalase 1, conversion of hydrogenperoxide to water and molecular oxygen
Group 3b - ***Bypass of the electron transport chain complex I***[3]		
YusJ	55.8	Acyl-CoA dehydrogenase
SdhA	2.6	Succinate dehydrogenase
YjlD	10.7	NADH dehydrogenase, respiration (Menaquinone)

Table 3 continued

Group 3c - ***Up/Down regulation of NADPH/NADH***[3]		
YcdF[B]	6.6	Glucose 1-dehydrogenase
YhdF[B]	8.2	Short chain dehydrogenase, with similarities to YcdF
YdaD	6.4	Short chain dehydrogenase, similar to alcohol dehydrogenase
Zwf	4.4	Glucose-6-phosphate 1-dehydrogenase
Yxbg	3.8	YcdF paralogue (glucose-1-dehydrogenase)
YoxD	4.2	Putative oxidoreductase
YvcT	3.0	Putative 2-ketogluconate reductase
YqkF	3.0	Aldo/keto reductase
PycA	9.4	Pyruvate carboxlyase
YwkA	7.1	Malate dehydrogenase
FabI	-18.2	Enoyl-Acyl carrier protein reductase III
YdjL	-10.4	Acetoin reductase/2,3-butanediol dehydrogenase
DhaS	- 6.4	Aldehyde dehydrogenase
Group 3d - ***Indirect inhibition of Fenton-like reactions***[3]		
Dps[B]	3.3	General stress protein 20M, strong iron chelator
HutI	- 5.1	Imidazolonepropionase
HutU	- .6	Urocanate hydratase
HutG	- 2.8	Formimidoylglutamase
Miscellaneous - ***Other interesting proteins***		
YdaP[B]	11.0	Pyruvate oxidase
AcsA	6.9	Acetyl-coenzyme A synthase
PfkA	10.6	Phosphofructokinase
GsaB	9.8	Glutamate-1-semialdehyde aminotransferase

[1]Cell wall composition
[2]Compatible solutes
[3]Oxidative stress response
[B]σ^B regulated genes

Detailed information about all the proteins that were found to be present in significantly different amounts is presented in Supplemental Tables S1 and S2.

Transmission EM experiments performed with *B. subtilis* cells grown in a a_w gradient provided direct support for the proteomics findings as they indicated that the cell walls are changed when cells are grown at low a_w. Specifically, cells grown at a_w 0.926 displayed thickened cell walls and irregularly formed septa (Fig. 4). This could very well reflect an altered cell wall composition.

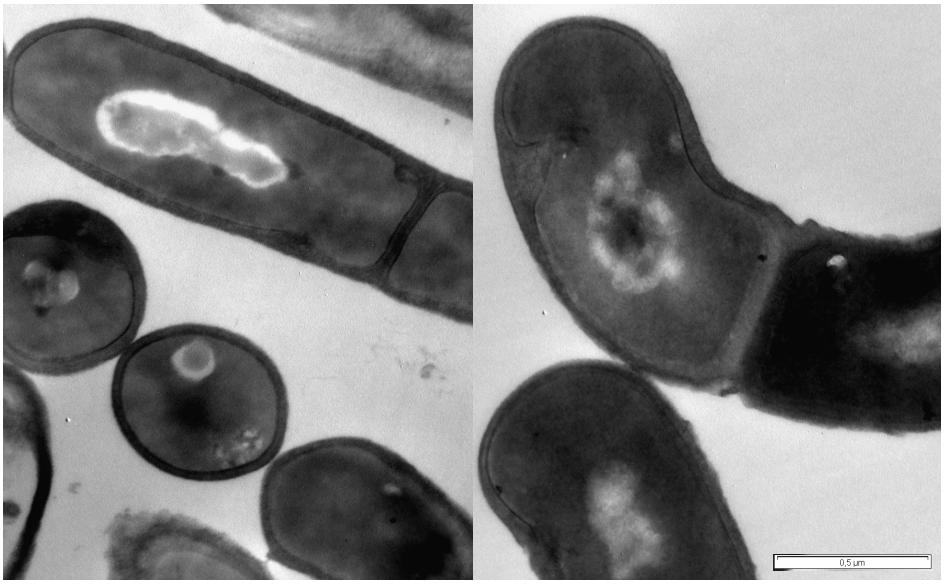

Figure 4. Transmission electron micrographs of *B. subtilis* strain 168. *B. subtilis* was grown at a_w 1 (left) or a_w 0.926 (right). The white bar indicates 0.5µm.

The sigma factor σ^B is required for growth at low a_w values

The expression of many proteins present at different amounts in cells grown at low a_w values is controlled by the general stress response sigma factor σ^B (Table 3). The *gsiB* gene, for example, is transcribed exclusively from a σ^B-dependent promoter, and the GsiB protein is known to be involved in adaptive responses to glucose starvation, heat shock, salt stress and oxidative stress (Volker *et al.*, 1994). Using a reporter strain with a *gsiB* promoter *gfp* fusion, we confirmed that the *gsiB* promoter activity was indeed upregulated when cells were growing at reduced a_w levels (Fig. 5). This is fully consistent with the proteomics data, which indicated that the levels of GsiB are 5-fold higher at a_w 0.926 than at a_w 1.

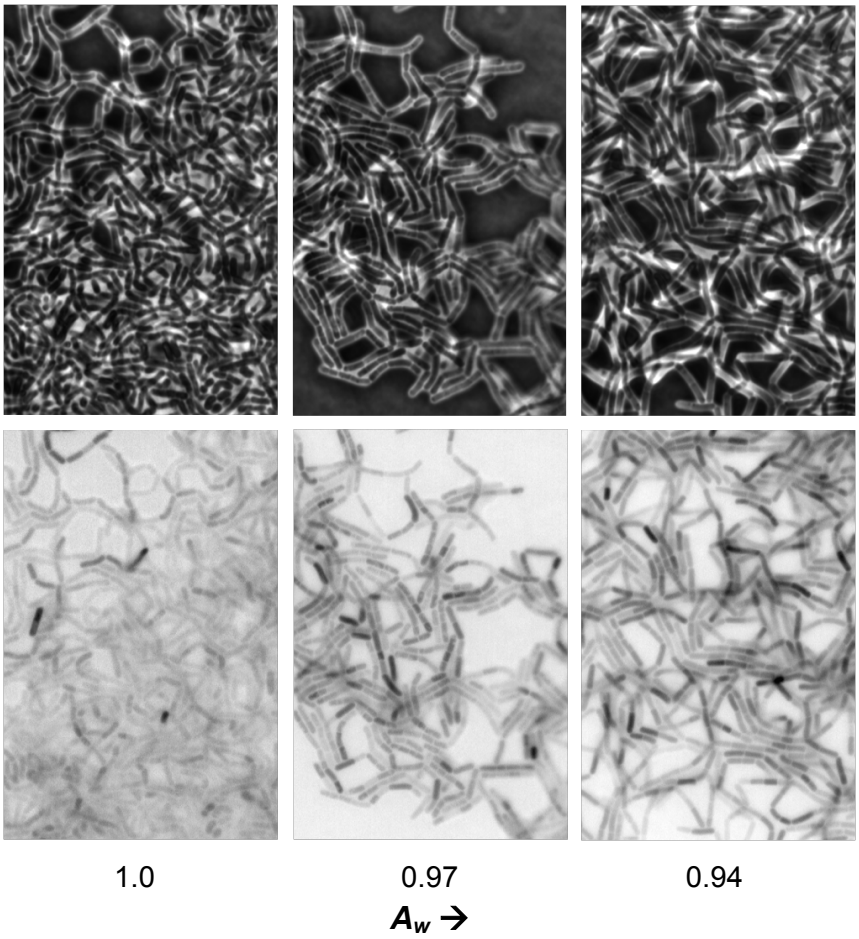

Figure 5. Activity of the *gsiB* promoter in *B. subtilis* 168 cells growing on a a_w gradient using a *gsiB* promoter-GFP fusion. Phase contrast (top) and fluorescent images (bottom) of cells grown at a_w 1, 0.97 or 0.94 are shown. Fluorescence intensities are shown in an inverted grayscale for purposes of clarity.

The importance of σ^B in the cellular response to low water availability was also tested directly. To this end, a *sigB* deletion mutant (BSM29) was grown in various a_w gradients. The results showed that the *sigB* mutant was unable to grow and survive at low a_w values. The *sigB* mutant was barely capable of growth above a saturated salt solution of KH_2PO_4 at 29 ^oC (a_w 0.94), but it did not grow at all under these conditions when the temperature was raised to 32^oC (a_w 0.933).

In contrast, the parental strain 168 was capable of growing at a_w values slightly below 0.92 (Fig. 6A).

Oxidative stress in *B. subtilis* grown at low a_w

The pronounced oxidative stress signature in the proteome of cells grown at low a_w suggested that the cells might be generating an oxidizing compound, such as hydrogen peroxide under these conditions. Consistent with this notion, the cells produced elevated levels of the pyruvate oxidase YdaP, of which the gene is also exclusively regulated by σ^B (Petersohn *et al.*, 1999). The pyruvate oxidase catalyzes the conversion of pyruvate, phosphate and molecular oxygen to acetyl phosphate, carbon dioxide and hydrogen peroxide. Similar to *gsiB*, transcription of the *ydaP* gene was strongly upregulated when cells were growing at decreasing a_w values as was shown with a *ydaP* promoter *gfp* fusion (Fig. 7).

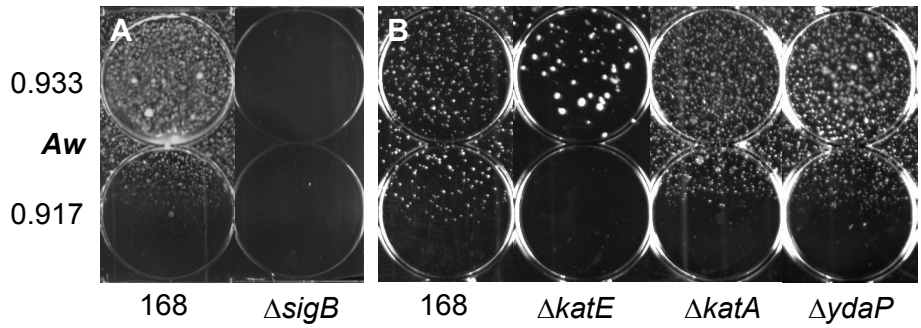

Figure 6. A_w growth limits of *B. subtilis* cells. (**A**) *B. subtilis* 168 and Δ*sigB* cells were inoculated on a 6-well a_w gradient using KH_2PO4 and KNO_3 to set the a_w gradient. An image of the inoculated gradient was recorded after incubation for 5 days at 32 ^oC. (**B**) *B. subtilis* 168 and Δ*katE*, Δ*katA* or Δ*ydaP* cells were inoculated on a 24-well RH-gradient using K_2SO_4, KH_2PO4, KNO_3 and KNaTartrate to set the a_w gradient. An image of the inoculated gradient was recorded after incubation for 5 days at 32 ^oC. Only the KH_2PO4 and the KNO_3 wells are shown.

Consistent with our findings above, *katE* expression is σ^B-regulated and the amount of KatE was 12.4-fold increased near the a_w growth limit of *B. subtilis*, while the amount of KatA increased merely 1.6-fold under these conditions.

Taken together, these findings show that *B. subtilis* suffers from self-inflicted oxidative stress under conditions of water limitation, and that the σ^B-dependent expression of *katE* is needed to survive this stress. This implies that the cells need to protect themselves from metabolically produced hydrogen peroxide and possibly also other oxidizing compounds that they produce when water availability is low. A *ydaP* deletion mutant was however not detectably enhanced in its ability to grow at low a_w values (Fig. 6B) nor was a *ydap katE* double mutant (not shown). This implies that YdaP cannot be the sole source of oxidative stress during growth at low a_w.

Judged by the results of the proteomics analyses, the electron transport chain (ETC) seems to be the main causative agent of self-inflicted oxidative stress. This would be consistent with other studies where the ETC was found to account for more than 85% of the total cellular hydrogen peroxide production (Gonzalez-Flecha and Demple, 1995). The majority of the reactive oxygen species (ROS) generated by electron transport through the ETC is formed at complexes I, III and IV, but not at complex II (Yankovskaya et al., 2003). A shift from the use of complex I to complex II for electron transport might thus alleviate some of the oxidative stress. Complex II uses succinate or $FADH_2$ as electron donors while complex I uses NADH.

In the present proteomics studies, it was indeed observed that the acyl-CoA dehydrogenase YusJ, implicated in the production of $FADH_2$, is 55.8-fold upregulated in cells growing at low a_w. Furthermore, the amounts of the succinate dehydrogenase SdhA, which is part of Complex II were significantly increased (Table 3, group 3b). Although complex II is seemingly less energy efficient than complex I, because it does not contribute to the generation of a proton-motive force, its redox centers are positioned in such a way that it keeps electrons more within the plane of the plasma membrane than on the cytosolic side of the membrane, thereby limiting electron leakage and the subsequent formation of ROS (Yankovskaya *et al.*, 2003). Apparently, the usage of the less effective complex II for electron transport helps the cells to minimize the levels of self-inflicted oxidative stress at low a_w.

In addition, the proteomics study suggests an alternative bypass of the ETC complex I as the NADH dehydrogenase YjlD (Ndh) was increased more than 10-fold. Ndh does also not contribute to the proton-motive force, but this alternative NADH-quinone reductase is thought to oxidise excess NADH in order to regulate the $NADH/NAD^+$ ratio in cells (Gyan *et al.*, 2006).

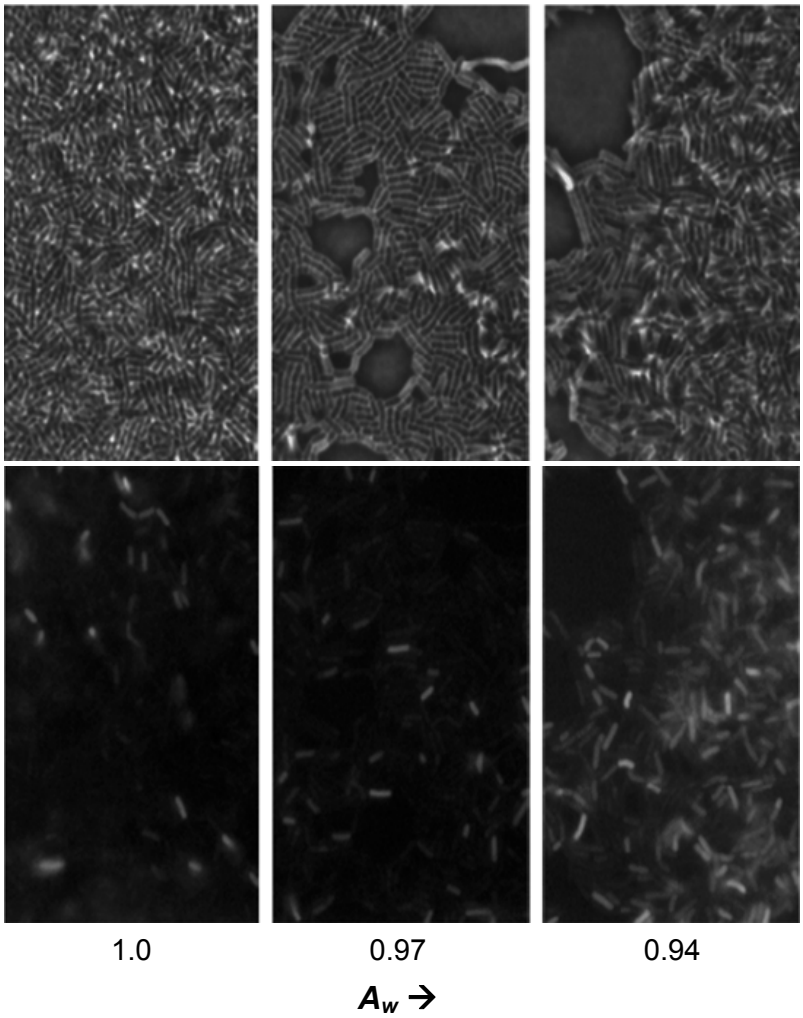

Figure 7. Activity of the *ydaP* promoter in *B. subtilis* 168 cells growing on a a_w gradient using a *ydaP* promoter-GFP fusion. Phase contrast (top) and fluorescent images (bottom) of cells grown at a_w 1, 0.97 and 0.94 are shown.

Previous research has shown that oxidative stress induces a metabolic adaptation that favors increased NADPH synthesis and decreased NADH production (Singh *et al.*, 2007). This seems to have two advantages. First, the produced NADPH will serve in maintaining a reductive environment that enables cells to eliminate the ROS generated as a consequence of oxidative phosphorylation. Secondly, decreased levels of NADH might help facilitating the shift from complex I to complex II, thereby minimizing the generation of ROS.

Many proteins involved in the synthesis of NADPH or NADH were indeed found to be up- or downregulated, respectively (Table 2, group 3c). Proteins from the pentose phosphate pathway, which is known for its importance in the synthesis of NADPH, are well represented in this group. Examples include Zwf (4.4), YcdF (6.6), YhdF (8.2), YxbG (3.8) and YvcT (3.0). An enhanced direct conversion of NADH into NADPH is furthermore suggested by the upregulation of YwkA (7.1) and PycA (9.4) (Singh *et al.*, 2007). Even though the malic enzyme YwkA has a 10-fold higher affinity for NAD than for NADP *in vitro*, Doan *et al*. reported that it does not contribute to cell growth, perhaps because YwkA has a higher affinity for NADP than for NAD *in vivo* (Doan *et al.*, 2003).

The last set of differentially produced proteins that may serve to minimize oxidative stress upon growth at low a_w is involved in the indirect inhibition of Fenton-like reactions (Table 2, group 3d). Frederickson *et al.* (2008) reported previously that desiccation resistant bacteria contained higher intracellular levels of manganese and lower iron concentrations than less desiccation resistant bacteria. This would serve to minimize Fenton reactions. As the manganese-containing catalase YdbD was up-regulated at low a_w it is conceivable that *B. subtilis* might have an increased intracellular manganese level when growing at low a_w values.

Furthermore, several proteins in the histidine utilization pathway (HutG, HutU and HutI) are downregulated at low a_w. Histidine is a well known chelator of iron and copper, which are both renowned catalysts of Fenton reactions. Increased intracellular concentrations of histidine might lead to lower intracellular concentrations of free iron, which would in turn minimize the

occurrence of Fenton reactions (Xu *et al.*, 2003). The observed upregulation of the general stress protein Dps (3.3) would have a similar effect, as it is also a strong chelator of iron (Ishikawa *et al.*, 2003).

Overall, the high level of oxidative stress at low a_w can probably be attributed also to an imbalance between anabolism and catabolism. The amounts of damaged (oxidized) proteins and other cellular components will increase during growth at low a_w due to the fact that the anabolic rate of slowly growing cells is much reduced, while their catabolic rate and especially their respiratory activity does not seem to drop under these conditions (Ballesteros *et al.*, 2001). This view is underscored by the finding that the phosphofructokinase PfkA, which is rate-limiting for glycolysis, was upregulated more than 10-fold in cells growing at low a_w values. Thus, the ability to dilute oxidized cellular components by sufficient levels of their *de novo* synthesis and by cell division is severely hampered by the slow growth at low a_w. Additionally, the increased levels of oxidative stress might also relate to an increased cellular concentration of organic osmolytes that can be oxidized, which is due to the fact that the cells will increase their internal a_w values by taking up compatible solutes or by generating them metabolically (Table 3, group 2). While this will allow the cells to grow in low a_w environments, it will also make them more vulnerable to self-inflicted oxidative damage.

As argued above, the σ^B induced pyruvate oxidase YdaP has probably only a minor role in the self-inflicted oxidative stress. This raises the question whether there is a meaning in the upregulation of this protein upon growth at low a_w. An explanation can perhaps be derived from the observed upregulation of the acetyl coenzyme A synthetase AcsA (6.9) during growth at low a_w. Combined with an as yet hypothetical acetate kinase, AcsA could turn the process of converting acetyl phosphate into acetyl coenzyme A via acetate into an ATP neutral process. Combined, these three proteins would form a bypass of the pyruvate dehydrogenase complex (PDHC) for converting pyruvate into acetyl coenzyme A, despite that the PDHC is theoretically more energy efficient.

The upregulation of YdaP and AcsA might thus be part of a greater regulatory mechanism, in which acetyl phosphate could act as a global signalling molecule that is used to phosphorylate certain response regulators, which have yet to be identified (Wolfe, 2005).

Proteomics data related to cell wall composition and the accumulation of compatible solutes

From the group of proteins involved with changes in morphology or an altered cell wall composition (Table 3, group 1) the protease FtsH was identified at about 27-fold reduced levels. Even though very little is known about the specific targets of this protease in *B. subtilis*, the deletion of *ftsH* is known to result in filamentously growing cells. Wehrl *et al.* (2000) reported that the FtsH protein accumulates at the septum of *B. subtilis* during cell division and sporulation. The aberrant septal development observed in our TEM experiments seems to be in line with this finding (Fig. 3). Consistent with the reduced level of FtsH is the observed reduced level of RecA (-4,4) since RecA induces a repressor of an inhibitor of FtsH (Lewis, 2000).

Another candidate protein for affecting the cell wall composition and possibly the cell morphology is the dihydrodipicolinate synthase DapA (4.7), which is involved in the biosynthesis of diaminopimelate. *Escherichia coli* mutants of *dapA* fail to make cell walls and lyse readily (McLennan and Masters, 1998). The ionic form of diaminopimelate, diaminopimelic acid, is a component of the peptidoglycan of bacterial cell walls. Furthermore, the UDP-glucose pyrophosphorylase GtaB (2.7) and the phosphoglucomutase Pgm (4.3) are likely to have a role in the altered morphology of cells grown at low a_w. GtaB is essential for the production of glucosylated glycerol teichoic acid, galactosamine-containing teichoic acid and teichuronic acid. Importantly, *B. subtilis* mutants lacking intact *gtaB* or *pgm* genes have a coccoid shape (Lazarevic *et al.*, 2005), similar to the shape that was observed for wild-type *B. subtilis* cells growing near their a_w growth limit.

Interestingly, coccoid cells are also formed by cells with mutations in the *ypfP* gene, which is required for the formation of lipoteichoic acid (Lazarevic *et al.*, 2005). However, the YpfP protein was not detected in our analyses and it remains to be investigated whether the cellular levels of this protein are altered in cells growing at low a_w.

As was mentioned above, *B. subtilis* responds to reduced water availability by increasing its internal osmotic potential (Table 3, group 2). Accordingly, GtaB may have a second possible function in facilitating growth at low a_w levels, since its product D-glucose 6-phosphate is the direct precursor for trehalose, an important compatible solute. Trehalose is thought to protect biological membranes against desiccation, and the dry weight of organisms capable of surviving complete desiccation consists for as much as 20% of trehalose (Crowe *et al.*, 1984).

Furthermore, the general stress protein GsiB (5.0) (Fig. 5) and, to a lesser extent, the YtxH protein (1.9) are both σ^B regulated and have strong similarities with Late Embryogenesis Abundant (LEA) proteins (Stacy and Aalen, 1998; Varon *et al.*, 1996), which are thought to protect cellular components against desiccation-induced damage in plant seeds. LEA proteins are very hydrophilic proteins with multiple extremely hydrophilic motifs of 20 amino acids. Increased concentrations of GsiB and YtxH are thus likely to serve for increasing the internal osmotic potential of cells growing at low a_w.

Intracellular osmoprotectants could also be generated through the increased conversion of oxoglutarate into glutamate by AspB (4.2) and subsequently from glutamate into proline by RocA (20.1), a pyrroline-5-carboxylate dehydrogenase (Cherian *et al.*, 2006). Pyrroline-5-carboxylate is however in chemical equilibrium with glutamate-1-semialdehyde. Thus, RocA might also provide GsaB (9.8) with the necessary substrate for increased production of 5-aminolevulinate, which is a precursor of the tetrapyrrole compounds that are basic building blocks of catalases, peroxidases and respiratory cytochromes involved in electron transfer.

Concluding Remarks

B. subtilis shows a whole array of morphological and physiological adaptations to survive and thrive within habitats where it experiences transient desiccation. These adaptations are so extreme that, when comparing the morphology and proteome of *B. subtilis* cells grown near their a_w growth limit with the morphology and proteome of cells grown at a a_w value close to 1, one might almost get the impression of comparing two completely different bacterial species. Yet, these adaptations can be rapidly reversed when sufficient amounts of water become available. These observations make the elucidation of the responses of *B. subtilis* to growth at low a_w values a very interesting scientific challenge. Moreover, knowledge of the altered metabolic pathways in cells growing at low a_w could potentially be utilized in novel biotechnological applications of *B. subtilis*. *Streptomyces coelicolor* was for example found to produce up to six times more antibiotics when its production of NADPH was increased (Borodina *et al.*, 2008).

Studies on the adaptive responses of *B. subtilis* to limited water availability can also be used to increase our understanding of similar responses in pathogenic bacteria that thrive and survive in water-limited environments such as surface-to-air interfaces or the human skin. This view is underscored by studies with the opportunistic human pathogen *Staphylococcus aureus*, in which it was shown that the catalase KatA is very important for desiccation resistance. Like the *B. subtilis katE* gene, the *S. aureus katA* gene is known to be σ^B-regulated, which suggests that an adequate σ^B-dependent stress response is also important for desiccation resistance of *S. aureus* (Cosgrove *et al.*, 2007).

Taken together, our present studies have revealed a critical need for combating oxidative stress, adapting the cell wall and accumulating compatible solutes in *B. subtilis* cells growing at low a_w values. However, we have only obtained a first glimpse of the intriguing adaptive responses to water deprivation, and further molecular and physiological studies will be needed to obtain a detailed understanding of the adaptations that allow *B. subtilis* and related bacterial species to survive in dry environments.

Reference List

Ballesteros,M., Fredriksson,A., Henriksson,J., and Nystrom,T. (2001) Bacterial senescence: protein oxidation in non-proliferating cells is dictated by the accuracy of the ribosomes. *EMBO J* **20:** 5280-5289.

Battistuzzi,F.U. and Hedges,S.B. (2009) A major clade of prokaryotes with ancient adaptations to life on land. *Mol Biol Evol* **26:** 335-343.

Borodina,I., Siebring,J., Zhang,J., Smith,C.P., van,K.G., Dijkhuizen,L., and Nielsen,J. (2008) Antibiotic overproduction in Streptomyces coelicolor A3 2 mediated by phosphofructokinase deletion. *J Biol Chem* **283:** 25186-25199.

Botella,E., Fogg,M., Jules,M., Piersma,S., Doherty,G., Hansen,A. *et al.* (2010) pBaSysBioII: an integrative plasmid generating gfp transcriptional fusions for high-throughput analysis of gene expression in Bacillus subtilis. *Microbiology* **156:** 1600-1608.

Brigulla,M., Hoffmann,T., Krisp,A., Volker,A., Bremer,E., and Volker,U. (2003) Chill induction of the SigB-dependent general stress response in Bacillus subtilis and its contribution to low-temperature adaptation. *J Bacteriol* **185:** 4305-4314.

Cherian,S., Reddy,M., and Ferreira,R. (2006) Transgenic plants with improved dehydration-stress tolerance: Progress and future prospects. *Biologia Plantarum* **50:** 481-495.

Cosgrove,K., Coutts,G., Jonsson,I.M., Tarkowski,A., Kokai-Kun,J.F., Mond,J.J., and Foster,S.J. (2007) Catalase (KatA) and alkyl hydroperoxide reductase (AhpC) have compensatory roles in peroxide stress resistance and are required for survival, persistence, and nasal colonization in Staphylococcus aureus. *J Bacteriol* **189:** 1025-1035.

Crowe,J.H., Crowe,L.M., and Chapman,D. (1984) Preservation of Membranes in Anhydrobiotic Organisms: The Role of Trehalose. *Science* **223:** 701-703.

de Goffau,M.C., Yang,X., van Dijl,J.M., and Harmsen,H.J. (2009) Bacterial pleomorphism and competition in a relative humidity gradient. *Environ Microbiol* **11:** 809-822.

Doan,T., Servant,P., Tojo,S., Yamaguchi,H., Lerondel,G., Yoshida,K. *et al.* (2003) The Bacillus subtilis ywkA gene encodes a malic enzyme and its transcription is activated by the YufL/YufM two-component system in response to malate. *Microbiology* **149:** 2331-2343.

Fredrickson,J.K., Li,S.M., Gaidamakova,E.K., Matrosova,V.Y., Zhai,M., Sulloway,H.M. *et al.* (2008) Protein oxidation: key to bacterial desiccation resistance? *ISME J* **2:** 393-403.

Gonzalez-Flecha,B. and Demple,B. (1995) Metabolic sources of hydrogen peroxide in aerobically growing Escherichia coli. *J Biol Chem* **270:** 13681-13687.

Greenspan,L. (1976) Humidity Fixed Points of Binary Saturated Aqueous Solutions. *Journal of Research of the National Bureau of Standards* **81A:** 89-96.

Gyan,S., Shiohira,Y., Sato,I., Takeuchi,M., and Sato,T. (2006) Regulatory loop between redox sensing of the NADH/NAD(+) ratio by Rex (YdiH) and oxidation of NADH by NADH dehydrogenase Ndh in Bacillus subtilis. *J Bacteriol* **188:** 7062-7071.

Haldenwang,W.G. (1995) The sigma factors of Bacillus subtilis. *Microbiol Rev* **59:** 1-30.

Ishikawa,T., Mizunoe,Y., Kawabata,S., Takade,A., Harada,M., Wai,S.N., and Yoshida,S. (2003) The iron-binding protein Dps confers hydrogen peroxide stress resistance to Campylobacter jejuni. *J Bacteriol* **185:** 1010-1017.

Lazarevic,V., Soldo,B., Medico,N., Pooley,H., Bron,S., and Karamata,D. (2005) Bacillus subtilis alpha-phosphoglucomutase is required for normal cell morphology and biofilm formation. *Appl Environ Microbiol* **71:** 39-45.

Lewis,K. (2000) Programmed death in bacteria. *Microbiol Mol Biol Rev* **64:** 503-514.

Marshall,B.J., Ohye,D.F., and Christian,J.H. (1971) Tolerance of bacteria to high concentrations of NaCL and glycerol in the growth medium. *Appl Microbiol* **21:** 363-364.

McLennan,N. and Masters,M. (1998) GroE is vital for cell-wall synthesis. *Nature* **392:** 139.

O'Brien,E.M. (1948) The Control of Humidity by Saturated Salt Solutions. Journal of Scientific Instruments 25[3], 73.

Petersohn,A., Antelmann,H., Gerth,U., and Hecker,M. (1999) Identification and transcriptional analysis of new members of the sigmaB regulon in Bacillus subtilis. *Microbiology* **145 (Pt 4):** 869-880.

Scott,W.J. (1953) Water relations of Staphylococcus aureus at 30 degrees C. *Aust J Biol Sci* **6:** 549-564.

Singh,R., Mailloux,R.J., Puiseux-Dao,S., and Appanna,V.D. (2007) Oxidative stress evokes a metabolic adaptation that favors increased NADPH synthesis and decreased NADH production in Pseudomonas fluorescens. *J Bacteriol* **189:** 6665-6675.

Stacy,R.A. and Aalen,R.B. (1998) Identification of sequence homology between the internal hydrophilic repeated motifs of group 1 late-embryogenesis-abundant proteins in plants and hydrophilic repeats of the general stress protein GsiB of Bacillus subtilis. *Planta* **206:** 476-478.

Varon,D., Brody,M.S., and Price,C.W. (1996) Bacillus subtilis operon under the dual control of the general stress transcription factor sigma B and the sporulation transcription factor sigma H. *Mol Microbiol* **20:** 339-350.

Volker,U., Engelmann,S., Maul,B., Riethdorf,S., Volker,A., Schmid,R. *et al.* (1994) Analysis of the induction of general stress proteins of Bacillus subtilis. *Microbiology* **140:** 741-752.

Wehrl,W., Niederweis,M., and Schumann,W. (2000) The FtsH protein accumulates at the septum of Bacillus subtilis during cell division and sporulation. *J Bacteriol* **182:** 3870-3873.

Winston,P.W. and Bates,D.H. (1960) Saturated Solutions For the Control of Humidity in Biological Research. *Ecology* **41:** 232-237.

Wolfe,A.J. (2005) The acetate switch. *Microbiol Mol Biol Rev* **69:** 12-50.

Xu,H., Sakakibara,S., Morifuji,M., Salamatulla,Q., and Aoyama,Y. (2003) Excess dietary histidine decreases the liver copper level and serum alanine aminotransferase activity in Long-Evans Cinnamon rats. *Br J Nutr* **90:** 573-579.

Yankovskaya,V., Horsefield,R., Tornroth,S., Luna-Chavez,C., Miyoshi,H., Leger,C. *et al.* (2003) Architecture of succinate dehydrogenase and reactive oxygen species generation. *Science* **299:** 700-704.

Supplementary Data

Table S1. Ratio between the levels of proteins from cells grown at a a_w 0.926 or 1 that were found to be significantly altered. Positive values denote that a protein was present at a higher concentration at a a_w value of 0.926.

Protein	Ratio	Function/Similarity
YusJ[b]	55.8	Acyl-CoA dehydrogenases (*fadE*)
RocA	20.1	1-Pyrroline-5-carboxylate dehydrogenase
OhrB[a,c]	17.8	Organic peroxide-resistance protein
YflT[a]	17.1	General stress protein 17M (ethanol stress)
YfkM[a]	12.5	General stress protein 18M (salt and ethanol stress)
ThrS	12.4	Threonyl-tRNA synthetase (major)
KatE[a,c]	12.4	Catalase 2, detoxification of hydrogen peroxide
YdaP[a,b]	11.0	Pyruvate oxidase (H_2O_2 production)
YjlD[b]	10.7[*]	NADH dehydrogenase; respiration (Menaquinone 7, no proton)
PfkA	10.6	6-Phosphofructokinase; glucose starvation induced
GsaB	9.8	(S)-4-amino-5-oxopentanoate → 5-aminolevulinate
PyrG	9.6	CTP synthetase, the final step of the pyrimidine nucleotide biosynthetic pathway
PycA	9.4	Pyruvate carboxylase; ATP + pyruvate + HCO_3^-→ ADP + phosphate + oxaloacetate.
YhdF[a,b]	8.2	Member of the short-chain dehydrogenases/reductases (SDR) family
YwkA	7.1	Upregulated by malate; NAD-dependent malic enzyme, makes pyruvate from malate.
YbaL	7.0	Also called SalA, mrp, rec233, ybxI; Upregulated by salt; Negatively regulates AprE (subtilisin), which is needed for sporulation
AcsA	6.9	Acetyl-coenzyme A (CoA) synthetase
YvyD[a]	6.9	Induced by σ^B, upregulation causes downregulation of the σ^L regulon (low temperature stress)
YvrE[a]	6.8	Unknown; similar to RNA polymerase (salt stress)
YcdF[a,b]	6.6	Similar to glucose 1-dehydrogenase (salt and cold stress)
YdaD[a,b]	6.4	Short chain dehydrogenase, similar to alcohol dehydrogenase
YdbD[a,c]	6.2	Unknown; similar to manganese-containing catalase
RsbW[a]	5.4	σ^B Inhibitor

Table S1 continued

RpsB	5.2[*]	Ribosomal protein S2
YdaG[a]	5.2	ABC-type multidrug transporter
GsiB[a]	5.0	Part of the ABC transporter complex gsiABCD involved in glutathione import
YdaE[a]	4.9	Unknown; homology with (lyxA) encoding D-lyxose (L-ribose) isomerase
DapA	4.7	Dihydrodipicolinate synthase, involved in cell wall peptidoglycan production and amino acid synthesis
YocK[a]	4.7	General Stress protein 16M (zinc finger) (ethanol stress)
CtC[a]	4.6	General stress protein, similar to ribosomal protein L25
Zwf[b]	4.4	Glucose-6-phosphate 1-dehydrogenase
Pgm	4.3	Phosphoglucomutase
YoxD[b]	4.2	Unknown; similar to 3-oxoacyl-acyl carrier protein reductase
PlsX	4.2	Acyl-acyl carrier protein (ACP):phosphate acyltransferase
CcpA	4.1	Transcriptional regulator (LacI family); mediates carbon catabolite repression (CCR)
MetS	4.0	ATP + L-methionine + tRNA(Met) → AMP + diphosphate + L-methionyl-tRNA(Met).
YvdF	4.0	Glucan 1,4-alpha-maltohydrolase
YxbG[a,b]	3.8	YcdF paralog (glucose-1-dehydrogenase)
YkcA	3.5	Hydroquinone-specific dioxygenase
Ipi	3.5	Intracellular proteinase inhibitor; important during sporulation
GlyS	3.4	Glycyl-tRNA synthetase beta subunit
GuaB[b]	3.4	Inosine 5'-phosphate + NAD^+ + H_2O → xanthosine 5'-phosphate + NADH
Dps[a,c]	3.3	Mini-ferritin; iron storage; DNA protection during oxidative stress
OhrA[c]	3.3	Organic peroxide-resistance protein
NhaX[a]	3.1	Induction by phosphate starvation, via the alternative sigma factor σ^B
ClpC[a]	3.1	ATPase subunit of the ClpC-ClpP protease
YqkC	3.1	Unknown
YqkF	3.0	Aldo/keto reductase
YvcT[b]	3.0	D-gluconate + $NADP^+$ → 2-dehydro-D-gluconate + NADPH + H^+

Table S1 continued

SerA[b]	3.0	D-3-phosphoglycerate dehydrogenase
GcvT	3.0	Aminomethyltransferase; the glycine cleavage system catalyzes the degradation of glycine
YwjH	2.9	Sedoheptulose 7-phosphate + D-glyceraldehyde 3-phosphate → D-erythrose 4-phosphate + D-fructose 6-phosphate
YsnA[a]	2.8	Unspecific diphosphate phosphohydrolase
CitG	2.7	Fumarate hydratase class II; (S)-malate → fumarate + H_2O.
GtaB[a]	2.7	UDP-glucose pyrophosphorylase
ProS	2.7	ATP + L-proline + tRNA(Pro) → AMP + diphosphate + L-prolyl-tRNA(Pro)
SdhA[b]	2.6	Succinate + acceptor → fumarate + reduced acceptor
YocB[a]	2.5	General stress protein
SecA	2.5	Part of the Sec protein translocase complex.
YsnF[a]	2.1	General stress protein; induced by phosphate starvation, via the alternative sigma factor σ^B.
YraA[a]	2.1	Cysteine proteinase; degradation of damaged thiol-containing proteins
GudB[b]	2.0	L-glutamate + H_2O + NAD^+ → 2-oxoglutarate + NH_3 + NADH

[a]Genes activated by σ^B
[b]Dehydrogenase
[c]Oxidative protection associated proteins
[*]Negative values are found in addition to positive values for these proteins. The negative values are due to low molecular mass degradation products of the respective proteins in the a_w = 1.0 sample.

Table S2. Ratio between the levels of proteins from cells grown at a a_w 0.926 or 1 that were found to be significantly altered. Negative values denote that a protein was present at a higher concentration at a a_w value of 1.

Protein	Ratio	Function/Similarity
GlyA	-71.4	Serine hydroxymethyltransferase
OdhA	-28.6	2-Oxoglutarate Dehydrogenase
PdhC	-27.8	Part pyruvate dehydrogenase multienzyme complex
FtsH	-27.0	ATP-dependent metalloprotease; cell-division protein
RpoB	-18.9	RNA polymerase B subunit gene
SucD	-18.2	TCA cycle; Step 7: ATP + succinate + CoA → ADP + phosphate + succinyl-CoA
FabI	-18.2	Enoyl-ACP reductase III
RpoC	-11.9	DNA-directed RNA polymerase subunit beta
CitZ	-12.8	TCA cycle; Step 1: acetyl-CoA + H2O + oxaloacetate → citrate + CoA
GlnA	-11.8	L-glutamine synthetase
MntA	-11.6	Part of an ATP-driven ABC transport system for manganese
AcoC	-10.5	Dihydrolipoyllysine-residue acetyltransferase
YtdI	-10.5	ppnK inorganic polyphosphate/ATP-NAD kinase
YdjL	-10.4*	Acetoine/butanediol dehydrogenase, fermentation (*BdhA*)
YcgN	-9.7	1-Pyrroline-5-carboxylate dehydrogenase
YjbG	-8.9	Oligopeptidase, protein degradation (*pepF*)
OdhB	-8.8	Dihydrolipoamide Transsuccinylase
RpsB	-8.7*	Ribosomal protein S2
YkrZ	-8.5	Acireductone dioxygenase
YugI	-8.0	Glucose-6-phosphate isomerase,
Icd	-7.9	Isocitrate dehydrogenase, TCA cycle
YurP	-7.6	Fructosamine 6-phosphate glycosidase
AtpA	-6.8	ATPase subunit alpha
DhaS	-6.4	Aldehyde dehydrogenase
CitB	-6.1	TCA cycle; Step 2/3: aconitate hydratase: citrate → isocitrate
OppD	-5.7	Isocitrate dehydrogenase
YjlD	-5.5	NADH dehydrogenase, respiration (Menaquinone 7)
Pgk	-5.5	Phosphoglycerate kinase
AtpD	-5.1	ATPase subunit delta
HutI	-5.1	Imidazolone-5-propionate hydrolase

Table S2 continued

RecA	-4.4	Pyruvate dehydrogenase multienzymecomplex
YwjH	-4.2	Transaldolase
YkrS	-3.7	Methylthioribose-1-phosphate isomerase
HutU	-3.6	Urocanase
YvbY	-3.0	Lactate catabolic enzyme (*LutC*)
HutG	-2.8	Formiminoglutamate hydrolase
Hom	-2.7	Homoserine dehydrogenase (NADPH); biosynthesis of methionine and threonine
TasA	-2.4	Major component biofilm matrix; biofilm formation
YvfW	-2.4	Lactate oxidase (*LutB*)
Mdh	-2.4	TCA cycle; Step 10: malate + NAD^+ → oxaloacetate + NADH + H^+
RibH	-2.1	Riboflavin synthase beta chain
GbsA	-2.1	Betaine aldehyde dehydrogenase
RocF	-2.0	L-arginine + H2O → L-ornithine + urea

*Negative values are found in addition to positive values for these proteins. The negative values are due to low molecular mass degradation products of the respective proteins in the a_w = 1.0 sample.

Chapter 4

Intracellular water activity limit, a turning point in microbial physiology

Marcus C. de Goffau, Jan Maarten van Dijl and Hermie J. M. Harmsen

Submitted for publication

Abstract

The availability of water, which can be expressed in terms of water activity (a_w), is one of the most important determinants for microbial homeostasis and growth. Microorganisms can adapt to low a_w values by accumulating high concentrations of compatible solutes but other mechanisms of adaptation, such as changes in cell morphology and cell wall composition, as well as the underlying physical principles, have hardly been addressed thus far.

By using an environmental control chamber containing a precisely controlled temperature/a_w gradient in combination with a mathematical approach, we demonstrate with *S. epidermidis* and *B. subtilis* that microorganisms not only have an environmental a_w growth limit, but also have an intracellular a_w limit. This internal a_w limit represents the point at which cells can no longer lower their internal a_w further without interfering with essential intracellular processes. To grow at a_w values below this limit they need to generate more water metabolically than that they lose to their environment. This limit can be calculated by measuring the a_w growth limit of an organism at different water vapor diffusivities using barometric pressure as a variable.

The intracellular a_w limit of an organism is furthermore shown to represent a turning point in its physiology. Microscopic examination, flow cytometry and other experiments show that adaptations in cellular differentiation and morphogenesis, hydrophilicity and cell wall composition all revolve around this critical parameter. It is hypothesized that as a result of a reduction in turgor that cells need to increase the mechanical stress on their cell wall bonds, as autolysins will not be able to remodel the cell wall sufficiently otherwise. *Staphylococcus epidermidis* and *Bacillus subtilis* can do so by either using specific morphological tricks or by generating less cross-linked cell walls.

Introduction

Water availability is one of the most important factors for microbial growth in many different ecological settings (Hansen, 1999). Its availability can be expressed in several ways but the two most useful ones are water potential (Ψ) and water activity (a_w). The Ψ and a_w values of deionized water are equal to 0 and 1 respectively, and if solutes are added both values become lower. Ψ and a_w can be used interchangeably according to Formula {1}:

$$\Psi = RT/V * \ln(a_w) \qquad \{1\}$$

where R is the universal gas constant, T is the temperature in Kelvin and V is the partial molal volume of water (Wiebe, 1981). On surface to air interfaces, the relative humidity (RH) can be directly linked to both Ψ and a_w, because the a_w value of a surface will be equal to the RH/100 of the air surrounding it under equilibrium conditions:

$$a_w = RH_e/100 \qquad \{2\}$$

RH_e values of at least 70% are needed to allow for the growth of certain molds, and they need to be even higher to allow for the growth of yeasts, Gram-positive bacteria and finally Gram-negative bacteria (80-95%) (Rahman, 2007). Microorganisms are capable of obtaining water from their environment as long as their internal a_w is lower than the external $RH_e/100$. As the accumulation of water is essential for cell growth, it would seem logical that the a_w growth limit of a microorganism should be at the point where its internal water potential is no longer lower than that of its external environment (Chirife *et al.*, 1981). Microorganisms will start losing water to their environment once the external water potential is lower than their internal water potential.

However, here we hypothesize that microorganisms can still grow slightly below their internal a_w limit as long as they can compensate for the loss of water to their

external environment by metabolically generating sufficient amounts of water. This view is, for example, supported by the finding that more than half of the intracellular water in exponentially growing *Escherichia coli* cells is generated metabolically, while in stationary-phase cells it is still almost one quarter (Kreuzer-Martin *et al.*, 2006).

Clearly, an organisms internal a_w limit needs to be measured in order to be sure that it differs from its a_w growth limit. One way of calculating the internal a_w value of a microorganism is by determining the intracellular pool of K^+, Na^+, Cl^-, amino acids, Mg^{2+}, phosphate and organic acid anions and then applying the proper mathematical equations (Chirife *et al.*, 1981). However, all methods to estimate the cellular internal a_w values that have been published so far are difficult to perform or suffer from inaccuracy (Koch, 2001).

An entirely different and more mathematical approach has been developed and applied in the present studies, where the internal a_w limit is calculated by measuring the a_w growth limit of a microorganism in an advanced relative humidity gradient system using barometric pressure as an additional variable. Importantly, barometric pressure influences the rate of water vapor diffusion, which is one of the prime reasons why vegetation tends to become more xeromorphic with increasing elevation (Smith and Geller, 1979). The predicted implication for microorganisms is that they will lose water at higher rates to their environment at lower barometric pressure values once $RH_e/100$ values become lower than their internal a_w limit. As such, lower barometric pressure values are expected to lead to higher a_w growth limits.

Even though hypoxia might seem to become a concern at low barometric pressure, a low partial oxygen pressure, or low pressures of other gasses in general, is counterbalanced by a similarly increased diffusion rate. For example, it has been reported that the CO_2 uptake rate in plants is sufficiently counterbalanced by the increased diffusion rate in experiments where the hypobaric pressure is at about or above 0.5 bar (Paul and Ferl, 2006).

In the present studies, we applied a pressure chamber containing a precisely controlled temperature/a_w gradient in combination with a mathematical approach

to calculate the internal a_w limits of the Gram-positive bacteria *Staphylococcus epidermidis* and *Bacillus subtilis*. This was achieved by measuring the a_w growth limits of these organisms at different water diffusion rates using barometric pressure as a variable. The results show that the intracellular a_w limits of *S. epidermidis* and *B. subtilis* are turning points in their physiology. Major adaptations in cellular differentiation and morphogenesis, hydrophilicity and cell wall composition can be related to this important biological parameter.

Results and Discussion

Mathematical equations

To understand how the internal a_w (a_w(I)) limit of a cell can be calculated by measuring the a_w growth limit of an organism (a_w(L)) at different atmospheric pressure values, it is important to first describe the principles of RH in greater detail. The RH of a volume of air is determined by only two parameters, the actual vapor pressure (e), and the air temperature which determines the saturation vapor pressure (e_s):

$$RH = 100 * e/e_s \qquad \{3\}$$

The saturation vapor pressure can be calculated using the following expression, which is commonly known as the Magnus formula:

$$e_s = C * \exp((A * T)/(B + T)) \qquad \{4\}$$

where the T is the temperature in Kelvin and the values of the coefficients A, B and C are 17.625, 243.04 K and 6.1094 mbar, respectively (Eskridge, 1996). The advanced relative humidity gradient system as shown in Fig. 1 consists of a closed system in which the average air temperature is regulated with a heating element, and the average RH at this temperature is modulated with a saturated salt solution.

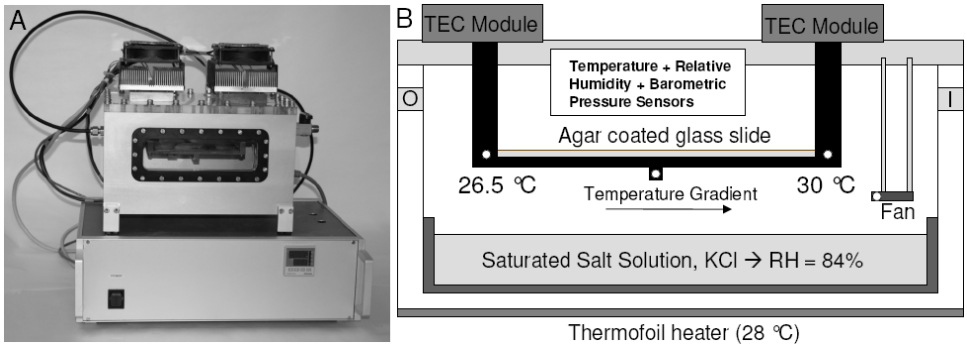

Figure 1. Environmental control chamber for creating a RH_e gradient. (**A**) Photograph of both the chamber (top) and its controlling unit (bottom). (**B**) Schematic representation of the control chamber. Thermo electric cooling (TEC) modules (top) are connected to a copper bridge (black) to create a local temperature gradient which, in turn, creates a RH gradient. Sensors inside the chamber (marked as small round white circles) are used for monitoring and controlling the average temperature in the chamber and the temperature gradient. The average RH inside the chamber is determined by a saturated salt solution in a receptacle at the bottom of the chamber. A vacuum pump is connected to "O" (left) and an air inlet is located at "I" (right). Sensors right under the lid register the average temperature, RH and pressure within the system.

Modulation of the RH with saturated salts is possible, because the a_w of a saturated salt solution, has a constant value as long as the solution remains saturated. Furthermore, the precise a_w value of a saturated salt solution depends on the particular salt that is used and the temperature (Greenspan, 1976). The RH of the air inside the closed system will become equivalent to the a_w value of the saturated salt solution once equilibrium conditions are reached (Formula {2}).

The most important part of the system depicted in Fig. 1 is that it contains an adjustable temperature gradient, which translates into a RH gradient as well. This is achieved by the coupling of two thermo-electric cooling modules with a connecting copper bridge in between. The average temperature, together with the chosen saturated salt solution, determines the actual vapor pressure (e) present within the whole system, while the local saturation vapor pressure (e_s) is determined solely by the local temperature. The saturation vapor pressure is thus

equal everywhere within the system except at the copper temperature gradient where the e_s is lower at the 'cold side' and higher at the 'hot side'. Consequently, the RH is relatively high at the cold side of the gradient and low at the hot side (see Formula {3}). On top of this copper bridge/temperature gradient agar coated slides can be placed that have been inoculated with the microorganism(s) of choice. By setting the average temperature and RH of the whole system, one can calculate the local RH_e at each position of the temperature gradient.

In general, it is easier for microorganisms to grow at the cold side of this gradient because the RH_e values are higher here than at the hot side. The a_w(L) of a microorganism can thus be calculated by simply determining at which position/temperature it can no longer grow in such a gradient. To grow at low a_w values, a microorganism needs to generate a low a_w(I) value. It can do so by accumulating high concentrations of intracellular compatible solutes, either by synthesizing them biochemically or by importing them, if available, from the external environment. There is however a lower limit to the a_w(I) of a particular microorganism as even higher concentrations of compatible solutes would start to interfere with essential intracellular processes. Microorganisms capable of tolerating or even requiring high concentrations of compatible solutes can thus achieve low a_w(I) limits.

In order for a particular microorganism to grow at a_w values below this a_w(I) limit, it needs to compensate for water losses to its environment by metabolically generating water. By limiting the amount of water it loses to its environment or possibly by increasing its catabolic rate, the a_w(L) of a microorganism can be lowered even further. The rate at which water is lost to the environment is a function of the water potential difference between the inside and the outside of a cell:

$$\Delta\Psi = RT/V * \ln(a_w(I)/(RH_e/100)) \qquad \{5\}$$

In plants the transpirational flux from leaves is quantified using Fick's first law for diffusion or Ohm's law analogy for electrical circuits (Nobel, 1974).

The same formula was adapted here to quantify the rate at which water is lost or gained when working with microorganisms:

$$F = D * \Delta\Psi/R \qquad \{6\}$$

where F is the rate of water loss (flux), D is the diffusion coefficient for water vapor in air and R is the physical resistance to water vapor diffusion through the cell wall. The diffusion coefficient for water vapor in air (D) is, in turn, dependent on the local temperature, and more importantly, the barometric pressure:

$$D = D(0) * (P(0)/P) * (T/T(0))\text{^}w \qquad \{7\}$$

where D(0) is the diffusion coefficient at T(0) equal to 273.15 K and P(0) equal to 1.01325 bar, w equals 1.75 for water vapor in air, T is the local air temperature and P is the barometric pressure (Boynton and Brattain, 1929; Smith and Geller, 1979). At the a_w(L) of an organism it can now be assumed that the rate of water loss to its environment (F) has become equal to the maximum amount of water that it can generate metabolically (G_m), thus at the a_w(L) it can be said that:

$$G_m = D * \Delta\Psi/R \qquad \{8\}$$

Assuming that G_m and R are constants at the a_w(L) of an organism, the coefficients D and $\Delta\Psi$ have become inversely proportional. By adjusting the barometric pressure the value of D can be varied rather efficiently {7}. It is now possible to calculate the value of the a_w(I) limit of an organism if one measures the a_w(L) at two different values of D, for example at 1 bar and at 0.5 bar:

$$G_m = (D/1) * \Delta\Psi(1\text{ bar})/R = (D/0.5) * \Delta\Psi(0.5\text{ bar})/R \qquad \{9\}$$

At the a_w growth limit, the difference between the internal water potential Ψ(I) and the external water potential Ψ(L) is thus twice as small at 0.5 bar than at 1 bar:

$$\Psi(I) - \Psi(L, 1\ bar) = 2 * (\Psi(I) - \Psi(L, 0.5\ bar))$$
$$\Psi(I) = 2 * \Psi(L, 0.5\ bar) - \Psi(L, 1\ bar) \qquad \{10\}$$

The values of Ψ(L, 1 bar) and Ψ(L, 0.5 bar) can be calculated by placing the measured a_w(L) values of an organism in Formula {1} and, in reverse, Ψ(I) can be used in the same formula to calculate its a_w(I) limit.

Calculating the a_w(I) limit of *S. epidermidis*

S. epidermidis ATCC 35984 was inoculated onto a glass slide coated with dried TSA, and incubated for 5 days on top of a RH gradient ranging from 95.0 to 77.7% RH at barometric pressure values of 0.5 and 1 bar. This gradient was created by using an average temperature of 28 ^{o}C and KCl as the saturated salt of choice (e = 32.8 mbar) combined with a temperature gradient going from 26.5 to 30.0 ^{o}C (Fig. 1). After the 5-day incubation period it was clearly visible that the a_w growth limits of the samples grown at either 0.5 or 1.0 were different (Fig. 2).

The a_w growth limits a_w(L, 1 bar) and a_w(L, 0.5 bar) as determined by microscopy were found to occur at locations on the gradient that had temperatures of 29.3 and 28.9 ^{o}C respectively. Notably, growing cells of *S. epidermidis* can be readily distinguished from non-growing cells at low RH values due to the fact that *S. epidermidis* cells show a very clear adaptive behavior near their a_w(L): the growing cells become significantly larger in size than cells grown at high RH values (de Goffau *et al.*, 2009).

The temperature values of 29.3 and 28.9 ^{o}C translate into local RH values of 80.6 and 82.7% RH, respectively (Figs. 2 and 3; Formulas {3} and {4}) and thus the values of Ψ(L, 1 bar) and Ψ(L, 0.5 bar) were calculated to be -30.1 and -26.5 J/cm^3, respectively (Formulas {1} and {2}).

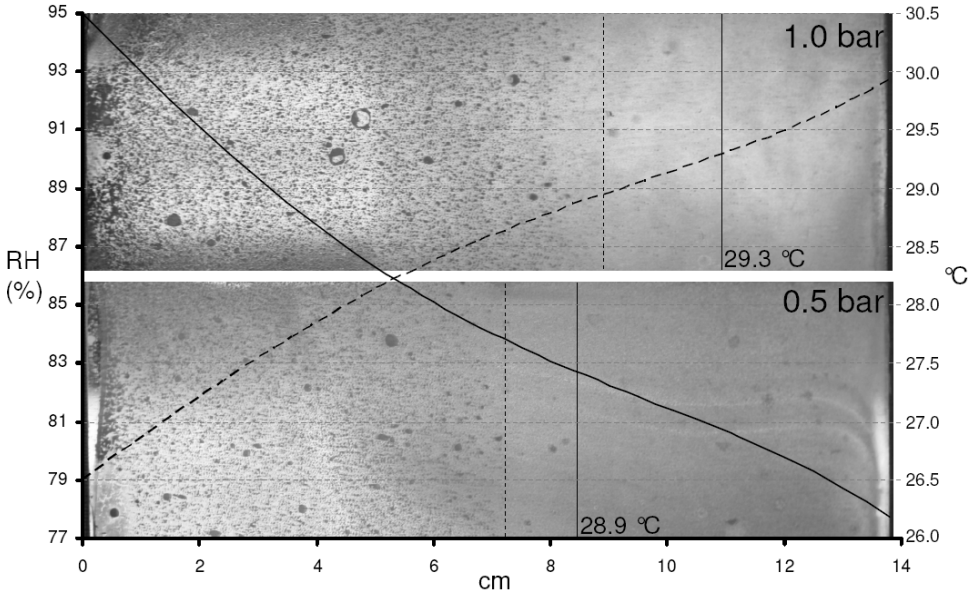

Figure 2. *S. epidermidis* ATCC 35984 grown in a RH gradient at 1.0 and 0.5 bar. *S. epidermidis* ATCC 35984 was grown at 1.0 bar (top) or 0.5 bar (bottom) on an agar-coated 13.8 cm long glass slide placed on top of the 14 cm long copper bridge (x-bar) of the control chamber. The temperature distribution along the x-bar is depicted by the upwards going dashed line. Temperatures are indicated on the right y-axis. The local RH_e is depicted by the downwards going solid line. RH_e values are indicated on the left y-axis. Visually apparent RH_e growth limits are depicted by vertical dashed lines but the actual growth limits were determined microscopically and are depicted by vertical solid lines.

In order to calculate the Ψ(I), Formula {10} now needs to be adjusted, because the ratio between the water diffusivity values at the a_w growth limits is not exactly equal to 2, but to 2.04. This relates to the fact that the temperatures at Ψ(L, 1 bar) and Ψ(L, 0.5 bar) differ 0.4 ^oC and the actual measured barometric pressure values during the experiments were equal to 1.013 and 0.495 bar (Formula {7}). The value of the Ψ(I) limit is calculated to be -23.1 J/cm^3, which translates into a a_w(I) limit of 0.847 for *S. epidermidis* 35984 when this bacterium is grown under the conditions tested.

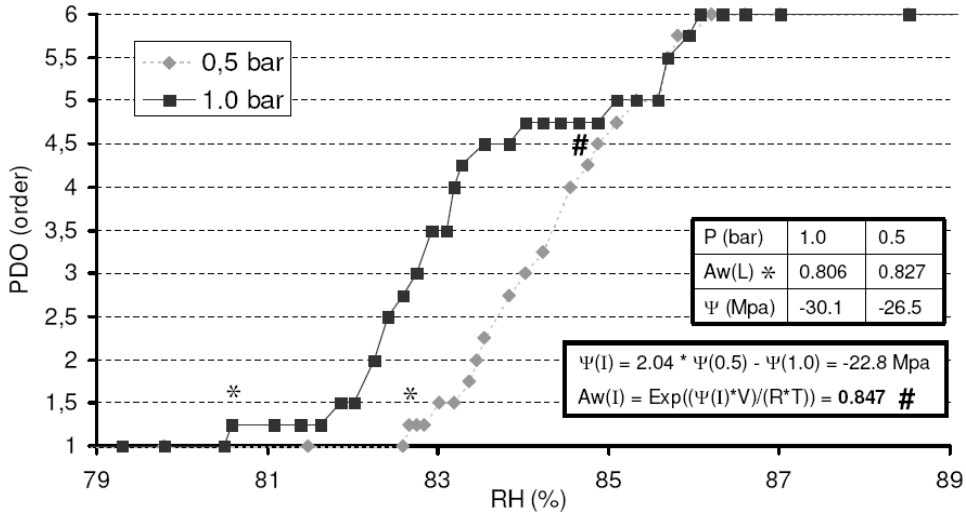

Figure 3. Population density order of *S. epidermidis* grown at 1.0 or 0.5 bar. *S. epidermidis* ATCC 35984 was grown at 1.0 or 0.5 bar as described for Fig. 2. A_w(L) growth limits (indicated by *) were used for calculating the external water potential value (Ψ) at these limits. These values of Ψ were used to calculate the internal water potential limit of *S. epidermidis* ATCC 35984, which was then used to calculate its a_w(I) limit, indicated by (#). The PDO scale reads as follows: **1.** No growth; **2.** One or two cell division per cell; **3.** Small clusters of cells; **4.** large clusters of cells; **5.** droplets of cells have grown confluent; **6.** droplets of cells have grown into large confluent layers.

During the microscopic inspection for determining a_w growth limits, the population density and cellular morphology were analyzed as well. Using the population density order system as described previously by de Goffau *et al.* (2009), it is observed that the population densities of the 1.0 and 0.5 bar experiments start to diverge from each other once the internal water activity limit of *S. epidermidis* is reached (Fig. 3). This seems quite logical as the accumulation of water, which is required for growth, takes place more slowly at 0.5 bar at $RH_e/100$ values below its a_w(I) since the loss of water is twice as large from this point onwards.

With respect to cell morphology, it was furthermore remarkable to see that *S. epidermidis* cells were at their largest at the external $RH_e/100 \leq a_w$(I) limit, compatible with the results of de Goffau *et al.* (2009). We have previously

observed that the walls of *S. epidermidis* cells grown at 1 bar are at their thickest below RH values of ~84% (de Goffau *et al.*, 2009). Thus it seems that *S. epidermidis* cells minimize their surface to volume ratio in order to reduce the rate at which water is lost to the environment as soon as they reach their a_w(I) limit. The previously observed increase in cell wall thickness upon reaching the a_w(I) limit could furthermore increase their physical resistance to water vapor diffusion through the wall.

Hydrophilicity of *S. epidermidis* in a RH gradient

To further investigate whether the a_w(I) limit of *S. epidermidis* ATCC 35984 could be a turning point for other relevant physiological features as well, the hydrophilicity of *S. epidermidis* cells grown in a RH gradient at 1 bar was investigated. It was expected that, as the external $RH_e/100$ becomes lower (but not yet as low as the a_w(I) limit), the rate of diffusion of water into the cell should become slower, because the differences between the internal and external Ψ values would become smaller. In order to attract water more easily from their environment *S. epidermidis* cells might therefore become more hydrophilic when the external RH_e becomes lower. This increase in hydrophilicity is expected to stop once the $RH_e/100 \leq a_w$(I) since a net loss of water occurs in such conditions.

To study cell hydrophilicity, the agar-coated glass slides were inoculated with a high starting density to cover the agar surface completely with *S. epidermidis* cells. After 5 days of incubation, the diameter of 5 µl water droplets placed on the resulting lawns of bacteria was used as a measure of hydrophilicity. Indeed, the hydrophilicity of the cells increased steadily upon decreasing RH (Fig. 4).

Remarkably, however, the increase in hydrophilicity did not only stagnate once the external $RH_e/100$ had reached the a_w(I) limit but, in fact, it started to decline again. This suggests that the cells benefit from a reduced hydrophilicity once the $RH_e/100$ has passed the a_w(I), possibly because this helps to reduce the loss of water, or that they simply try to simply conserve energy by not becoming more hydrophilic.

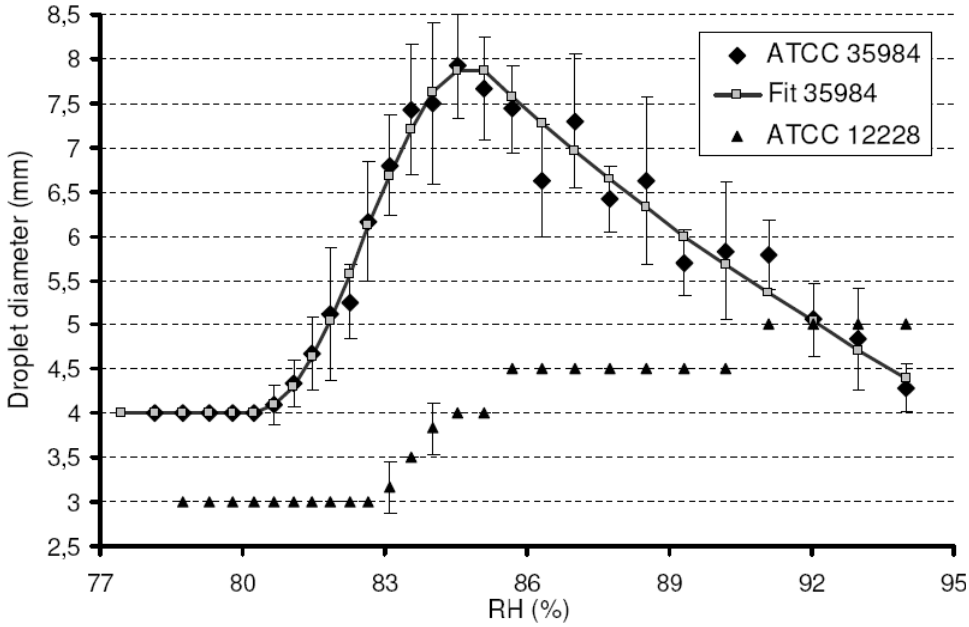

Figure 4. Hydrophilicity assay of *S. epidermidis*. A confluent layer of *S. epidermidis* ATCC 35984 or 12228 cells was grown on a RH gradient. Their hydrophilicity was tested after 5 days by pipetting 5 µl water droplets on top of the confluent layer as described in the Experimental Procedures.

As *S. epidermidis* ATCC 35984 is a well known biofilm former, it was tested whether biofilm formation might play a role in this phenomenon. To this end, the *S. epidermidis* strain ATCC 12228 was used, which is deficient in biofilm formation due to the absence of the *ica* genes. Interestingly, the hydrophilicity of the *S. epidermidis* ATCC 12228 strain was slightly higher than that of the 35984 strain at high RH values (droplet diameter ≈ 5 mm), but it slowly declined at declining RH values and it remained at a constant base level once the a_w(L) was reached at around 0.833. Though biofilm formation is thought to help protect microorganisms against desiccation (Ophir and Gutnick, 1994), it now seems that there might be an additional and perhaps even more important advantage of biofilm formation, namely the ability to attract water in response to low water availability.

A_w(I) limit of *Bacillus subtilis* in relation to its morphological changes

B. subtilis was grown in a setup similar to the *S. epidermidis* experiments except that a RH gradient was created from 97.1 to 88.9%, using an average temperature of 25 ^oC, and water instead of a saturated salt solution (e = 31.6 mbar), combined with a temperature gradient ranging from 25.5 to 27 ^oC. The a_w growth limits at 1 and 0.5 bar also differed for this species, and they were found to occur at 26.5 and 26.2 ^oC, respectively. This corresponds to local RH values of 91.6 and 92.9% RH. Using the same calculations as above, the Ψ(I) limit for *B. subtilis* was calculated to be -8.2 J/cm^3, which corresponds to an internal a_w limit of 0.942.

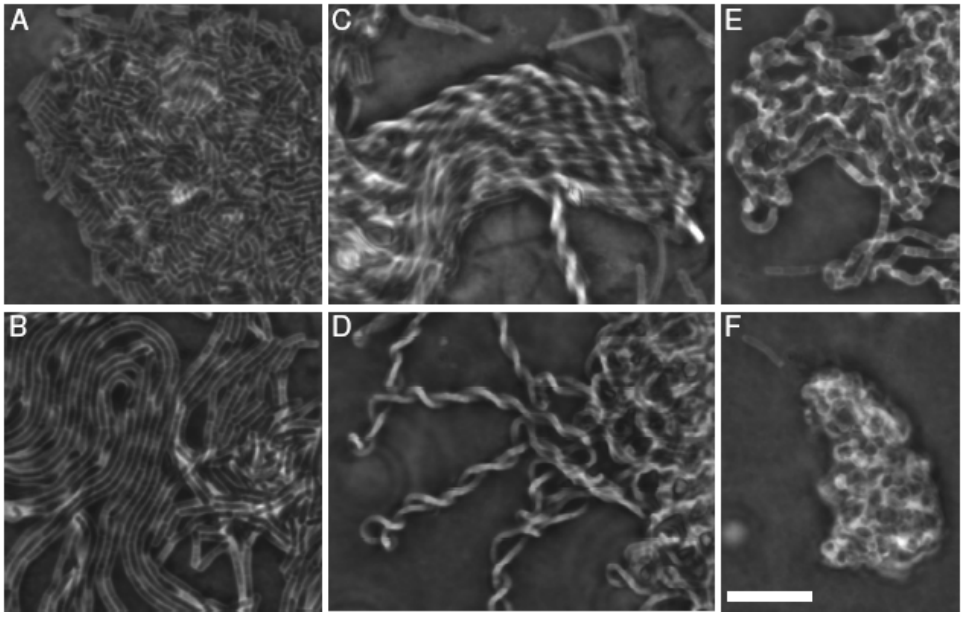

Figure 5. Morphological adaptations of *B. subtilis* 168 in a RH gradient. (**A**-**B**) Cells grow "normally" and eventually filamentously at a_w values between 1 and 0.95. (**C**-**D**) Cells can be found to differentiate into coils or coiled superstructures at a_w values between 0.95 and 0.936. (**E**-**F**) Globular cell shapes occur at a_w values between 0.936 and 0.916. The white bar indicates 10 μm.

Distinct morphological changes occurred concomitantly with the lowering of the RH (Figs. 5 & S1). The two most eye-catching morphological changes of *B. subtilis* in response to reduced water availability levels were that the cells started to differentiate into coiled superstructures weaving loose filaments into rope-like bundles at RH_e/100 values around the a_w(I) (0.95-0.936), and that the cells exchanged their rod-like shape for a more globular shape as the external RH came closer to the organisms a_w(L). The latter morphological change has been reported before (de Goffau *et al.*, 2009), but the coiled structures of wild-type *B. subtilis* cells are reported here for the first time. The detection of the coils was facilitated by the use of a less steep RH gradient, which was previously not possible due to unavailability of the environmental control chamber that was developed for the present studies.

Both observed morphological changes in response to limited water availability seem to help *B. subtilis* to minimize its surface to volume ratio, but this may actually not be the main function of these adaptations because they can also be related to turgor reduction.

Turgor reduction as a cause of morphological change

B. subtilis mutants exhibiting coiling behaviour have been described in the past. Such mutants were, for example, found to be deficient in autolysin activity (Mendelson, 1976). To explain the formation of helices by mutant *B. subtilis* cells, Mendelson proposed that the insertion of new material into the cell wall occurs along a helical path and that the peptidoglycan strands might themselves be arranged in a helical fashion. This view was supported by the finding that peptidoglycan strands are inserted and retained in the wall along a helical path with an average pitch of about 12 degrees (Daniel and Errington, 2003; Hayhurst *et al.*, 2008; Jones *et al.*, 2001). Insertion of new cell wall material and subsequent stretching of the pre-existing peptidoglycan layer during growth consequently generates a rotational torque in the direction in which the helix is unwound. In filamentously growing cells, this torque is expected to cause growth in a coiled fashion (Daniel and Errington, 2003).

Autolysins such as LytE (Carballido-Lopez *et al.*, 2006) can however relieve the cell wall of its tension by hydrolyzing peptidoglycan bonds. The total amount of stress that a bond bears is dependent both on torque and turgor. Importantly, the energy required for the hydrolysis of a peptidoglycan bond is inversely related to how much stress it bears (Koch, 1988). As such, a higher build-up of rotational torque is expected to occur at lower turgor values resulting in the coiling behaviour of *B. subtilis* (Figs. 5 & S1) near its a_w(I).

In fact, the build-up of rotational torque might be a way for *B. subtilis* to compensate for the loss of turgor and concomitantly for the loss of autolytic activity, which is required for the growth and division of cells via cell wall remodelling. As the simplest alternative for increasing the amount of stress per peptidoglycan bond is to reduce the total number of bonds in the cell wall, it can be hypothesized that it might be possible for *B. subtilis* to maintain a higher structural integrity by growing in a coiled fashion. Once the rotational torque can no longer sufficiently compensate for the loss of turgor, a lesser degree of cross-linking of *e.g.* pentapeptide chains of the peptidoglycan could serve to maintain a sufficient level of autolytic activity as the remaining turgor pressure would be imposed on a smaller number of bonds. Eventually such a decrease of cross-linking would lead to a loss of structural integrity causing *B. subtilis* to lose its rod-like shape and to adopt a more spherical shape.

The basic reasoning behind these ideas is that turgor causes rods to experience a circumferential stress on the cylindrical part of their cell wall that is twice as large as the axial stress on this part. In a cylindrical pressure vessel the circumferential stress is equal to the turgor pressure times the cell radius (*Pr*), while the axial stress is equal to *Pr/2* (Koch, 1988). At the poles of a rod-like cell, or in a spherical cell, the circumferential stress on the cell wall is equal to the axial stress *(Pr/2)*. Assuming that, concomitantly with a decrease in turgor, the weakening of the cell wall more or less decreases its axial and circumferential stress-bearing capacity to similar extents, the circumferential stress in the cylindrical part of a rod will eventually become too much for the cell wall to bear. A solution to this problem for a rod-like cell, while maintaining a similar volume, would be to become either coccoid or elongated and thin.

The latter solution however seems quite inefficient and impractical when one considers the increased surface area and how much extra cell wall material would be needed per cell. The coccoid-like shape, along with the fact that it still grows filamentously and thus clustered, would furthermore help the cell to minimize its surface to volume ratio.

In a similar manner a loss of turgor can also account for the morphological changes observed in *S. epidermidis*. As an alternative for generating rotational torque, *S. epidermidis* cells become larger when they reach their a_w(I) limit in a RH gradient. Any internal pressure that is still left will cause a greater stress on its cell wall bonds due to its increased radius (*Pr/2*), slightly elevating autolytic activity. However, the overall decrease in autolytic activity most likely causes a reduction of the turnover rate of cell wall material, which might explain why staphylococci get such thickened cell walls when grown near or below their a_w(I).

In addition, a decreased amount of cross-linking of the pentapeptide side chains can further increase the stress on the remaining cell wall bonds. The mechanism for achieving a reduced amount of cross-linking might either relate to a decreased activity of penicillin-binding proteins or to an increased incorporation rate of non-amidated murein monomers (Hanaki *et al.*, 1998). Such a decrease, in combination with a thickened cell wall, would furthermore explain the increased vancomycin resistance of *S. epidermidis* when grown near its a_w(I) limit (de Goffau *et al.*, 2009).

Turgor as a determinant for cell wall strength

As argued in the previous section, microbial cells may adapt to a loss of turgor by generating weaker, less cross-linked cells walls. Cross-linking of the glycan strands is catalyzed by transpeptidases, which connect the peptide side chains of adjacent glycan strands. The glycopeptide antibiotic vancomycin binds specifically to the terminal D-Ala-D-Ala end of peptide side chains, which have not yet been cross-linked. Therefore, vancomycin labeled with fluorescein was used as a marker to determine the relative amounts of uncrosslinked pentapeptides present within the peptidoglycan of cells growing in a RH gradient.

Both *S. epidermidis* and *B. subtilis* were grown in RH gradient setups as described above. The intensity with which vancomycin stained their cell walls after the 5 day incubation period was ascertained both by fluorescence microscopy and flow cytometry (Figs. 6, 7 and 8). Individual cells of *S. epidermidis* growing at high RH values could not be readily recognized microscopically. At the lower RH values, individual *S. epidermidis* cells stained with vancomycin-FL showed the highest fluorescence at RH values that were slightly lower than its a_w(I) limit. At RH values beyond the a_w growth limit, the fluorescence decreased again. These findings were confirmed by flow cytometry. The highest level of fluorescence was again measured at RH_e values slightly below the a_w(I) limit of *S. epidermidis*. The drop in the fluorescence intensity level when cells are grown below 82% RH can be explained by the fact that not all inoculated cells below this RH start to grow (Fig. 3).

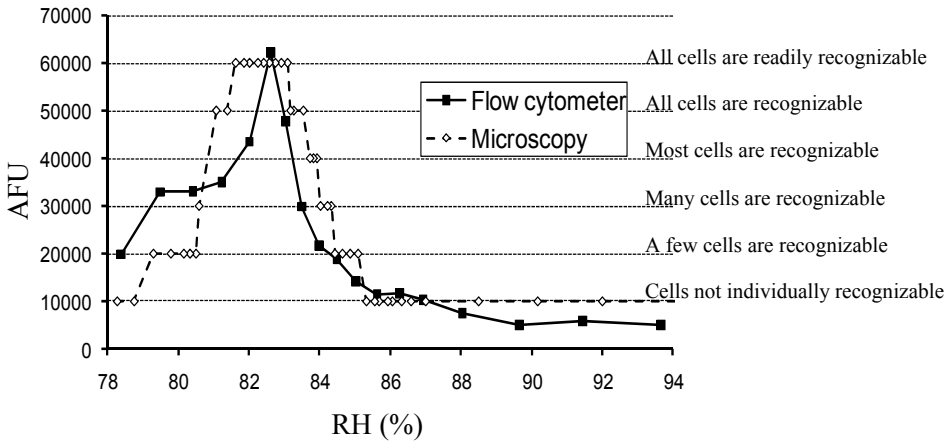

Figure 6. Vancomycin-FL fluorescence staining of *S. epidermidis* 35984. Vancomycin staining of *S. epidermidis* 35984 grown in a RH_e gradient was both observed microscopically (gray line, right axis) and with a flow cytometer (black line, left axis) as described in the Experimental Procedures.

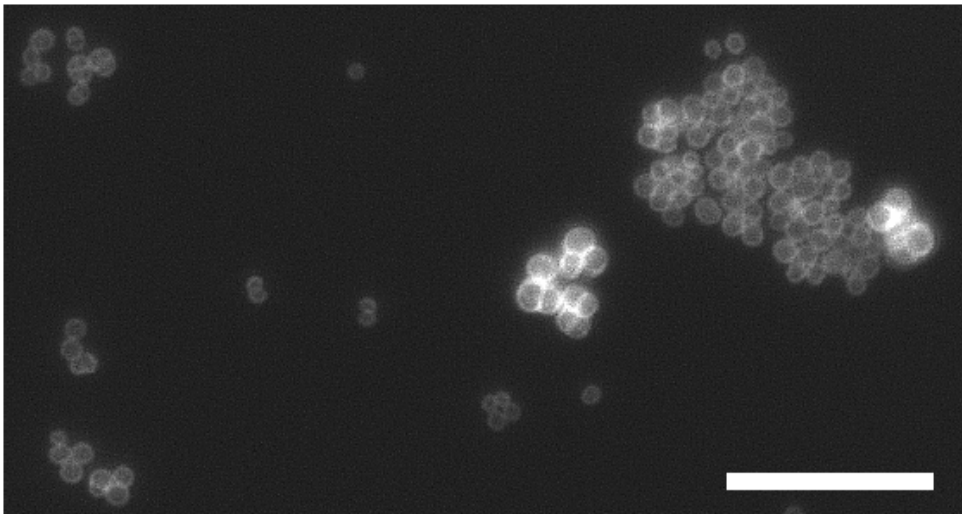

Figure 7. Vancomycin-FL fluorescence *S. epidermidis*. Example picture showing the fluorescence staining of *S. epidermidis* 35984 cells grown at 81.5% RH_e with vancomycin-FL. The largest cells with the thickest cell walls show the greatest level of fluorescence. The white bar indicates 10 µm.

The changes in the fluorescence levels upon vancomycin-FL staining were found to be lower and more complex in *B. subtilis* than in *S. epidermidis*. The low fluorescence levels made microscopic examination impossible. As shown by flow cytometry, the fluorescence of vancomycin-FL stained cells initially increased as the RH_e decreased, but it decreased again as the RH_e reached the a_w(I) limit of *B. subtilis* (94.2%; Fig. 8). Importantly, the first coiling behavior was observed as soon as this decrease commenced (95%). A second increase in fluorescence intensity occurred once cells stopped growing in coils and started their transformation from a rod-like to a globular shape (93.6-91.5%). The final fluorescence intensity below the a_w(L) of *B. subtilis* is thought to be the result of a last but futile effort of *B. subtilis* to adapt its cell wall to a dry environment.

The decrease in fluorescence at 95% RH_e can be explained at least partially by an increase in rotational torque as the coiling behavior commences at this point. The second increase in fluorescence coincides with absence of coiling and the onset

of the transition from a rod-like to a more globular cell shape. Possibly, rotational torque does not provide enough stress anymore at this point. The results shown in Fig. 8 suggest that *B. subtilis* employs a special mechanism of generating a structurally weaker and thus more stressed cell wall. The curved, bent and finally globular phenotype displayed by *B. subtilis* cells at a_w values below where it grows in a coiled fashion (~0.936) is similar to the phenotype of mutants that have been depleted of teichoic acid (Bhavsar *et al.*, 2004).

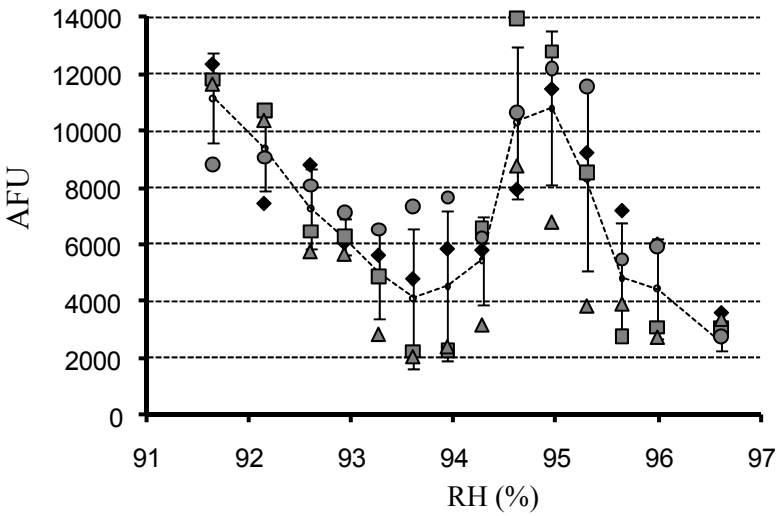

Figure 8. Vancomycin-FL fluorescence staining of *B. subtilis* 168. Vancomycin-FL fluorescence staining of *B. subtilis* 168 grown in a RH_e gradient was measured by flow cytometry as described in the Experimental Procedures. The dashed line represents the average of four independent measurements.

In *B. subtilis* approximately 62% of the cell wall is composed of teichoic acids (Boylen and Ensign, 1968) and, together with the peptidoglycan, teichoic acids provide cells with the tensile strength required to protect them from potentially detrimental effects of turgor pressure (Neuhaus and Baddiley, 2003). As such a significant reduction of the total amount of teichoic acid will lead to a reduction in the overall structural integrity of a cell, sufficiently stressing the remaining structural components.

Concluding Remarks

Reduced water availability has played a major role in the evolution of terrestrial prokaryotes and as such various mechanisms have evolved to address the many demands that this stress imposes on cells and especially their cell walls. Not only do cells need to become more avid in obtaining water from their environment, or more resistant against losing it, but they also need to find ways of increasing the mechanical stress on their cell walls in response to a decrease in turgor. The latter requirement cannot be simply solved by generating a thinner cell wall and the transformation into a protoplast-like L-form as this change would be in conflict with the requirement to prevent the loss of water and, possibly, the need for protection against mechanical insults.

Instead, our present results imply that these challenges are met by a combination of specific morphological changes, the accumulation of compatible solutes, biofilm formation and the reduction of cell wall cross-linking. Some of these mechanisms which allow staphylococci to adapt to the natural stress of reduced water availability, unfortunately, also seem to lie at the basis of their intrinsic ability to resist certain antibiotics (Hiramatsu, 2001), and their persistence and invasiveness as opportunistic pathogens (Li *et al.*, 2005). The internal a_w limit, which depends on the accumulation of compatible solutes, seems to be in the middle of the action where the most profound adaptations occur in response to the stress imposed by water limitation.

Research on sub-aerial biofilms, food spoilage, indoor microbial safety and various other topics related to microbial growth and water availability can benefit greatly from the environmental control chamber used in the present studies. This incubator allows for an unprecedented level of control over water availability, which is the most important, but also the experimentally most neglected parameter for microbial growth. In relation to this parameter, our results show that the intracellular a_w limit is an important turning point in microbial physiology.

Experimental Procedures

Bacterial strains and growth conditions

Bacillus subtilis 168, *Staphylococcus epidermidis* ATCC 35984 and 12228 were grown overnight in tryptic soy broth (TSB, Oxoid, England) at 37 ^{o}C before being used as an inoculant in a RH gradient assay.

Environmental control chamber

The environmental control chamber (Fig. 1) was custom made at the mechanical workplace of the University Medical Center Groningen. This airtight chamber consists of an anodized aluminium box with a polycarbonate lid. The lid is screwed on top of the box by a series of screws at the start of each experiment and is unscrewed again at the end. The combination of box and lid is made airtight by a rubber ring which, is placed into a milled groove on the top of the box top. The box is 30 cm long, 17 cm wide, 16 cm tall and has 1.5 cm thick walls. It furthermore contains a polycarbonate window on the side, a port on the back connected to a vacuum pump and a valve on the front to restore the barometric pressure to 1 bar at the end of an experiment in which the pump was utilized. The air pressure within the closed box is measured with a pressure sensor (SunX), which is connected to the control computer outside of the box, and to a Labjack U12 unit which in turn is connected to a personal computer running the Labview 8.2.1 software package. Using a Labview visual interface (VI) program, the desired barometric pressure can be selected, which causes the vacuum pump to be turned on via the Labjack U12 unit if the measured pressure is still higher than the desired pressure, and which turns the pump off when this is no longer the case.

A precisely controlled local temperature gradient is furthermore maintained inside of the box by coupling two thermo-electric coolers (TEC) (UT15-12-40-F2; Melcor) together by means of a copper bridge. The copper bridge consists of three slabs. Two of these slabs are connected through the lid to the TEC elements and are 2.7 cm thick. The third copper slab which is only 0.5 cm thick connects both thick copper slabs and forms the temperature gradient on

which agar coated glass slides can be mounted (see below). Temperature sensors (T67; Oven Industries) inside the bottom left and right of the copper bridge (Fig. 1) relay their information through the Labjack unit to the personal computer. The desired temperatures for the temperature gradient are chosen via Labview VI programs and, in combination with the temperature sensor input, they control the output of the TEC elements (via the Labjack unit) using thermoelectric module controllers (5C7-001; Oven Industries).

An additional temperature sensor (EL1034; Beckhoff), which also relays its information to the personal computer, is placed inside of a small fourth copper part that can be attached to various locations of the middle connecting part. This makes it possible to define the course of the temperature gradient more precisely as the gradient is almost, but not exactly linear due to the processes of radiation and convection. During an actual experiment this sensor is placed in the middle of the temperature gradient as a control.

A receptacle containing a saturated salt solution is placed at the bottom of the aluminium box to control the average relative humidity inside the box. The surface area of this saturated salt solution is enlarged by placing paper tissues inside the receptacle before adding a saturated salt solution to it. A thermofoil heater (Minco) is furthermore attached to the bottom of the box to regulate the average temperature inside the box.

The thermofoil heater is controlled by a GCS-300, a digital temperature indicating controller (Shinko), located within the control computer, which in turn is connected to a PT100 temperature sensor inside the box. This sensor is located next to the fan (Fig. 1) which is attached to the lid. The fan is an axial blower type 255H/2 (EBM Papst) and is in turn simply controlled by an on/off switch, which is always switched on during experiments in order to homogenize the temperature/humidity distribution of the air within the box.

A EI1050 digital temperature/humidity probe furthermore relays the average relative humidity and air temperature to the personal computer. The wiring for all of the sensors inside of the box goes through the lid in an airtight manner.

All information relayed to the personal computer is stored with another Labview VI program so that the measurements made within the environmental control chamber during an experiment can be checked retrospectively.

RH gradient assay

A glass slide of 13.8 cm long, 7.5 cm wide and 1 mm thick was coated with tryptic soy agar (TSA) by placing it in a plastic box (17x10 cm), and pouring 50 ml of TSA on top of it. When the TSA had solidified, the excess TSA on the sides of the glass slides was removed and the TSA layer on top of the glass slide was allowed to dry in a laminar flow cabinet for 2 days. Using an aerosolizer (de Goffau *et al.*, 2009), fine droplets of an overnight bacterial culture were inoculated onto the TSA agar coated glass slide, which was subsequently placed on top of the temperature gradient of the environmental control chamber.

At the start of each experiment the temperature on the left and the right side of the temperature gradient were chosen alongside with the average temperature and RH using the appropriate saturated salt solution to create the desired RH gradient. The glass slide was taken out of the chamber after 5 days and was inspected directly using phase contrast microscopy. Images were captured using a digital camera and software from SPOT, Diagnostic Instruments (Puchheim, Germany), coupled to an Olympus-BH2 fluorescence microscope (Zoeterwoude, The Netherlands).

Hydrophilicity assay

To measure the hydrophilicity of cells grown at different RH values, a high inoculation density was used to cover the agar surface with a confluent layer of cells at the start of the experiment. After 5 days of incubation, 5 µl water droplets were placed on top of the confluent cell layer. Multiple series of droplets were pipetted onto the glass surface. These series were subsequently grouped in cohorts of 0.5 cm (0.5-13.5). Each point in Fig. 4 is derived of almost 6 measurements on average for *S. epidermidis* 35984, and 3 measurements on average for *S. epidermidis* 12228.

Vancomycin-FL flow cytometer assay

These experiments were performed in exactly the same way as the RH gradient assays described above except that a dialysis membrane was deposited on top of the agar-coated glass slide before it was inoculated with bacteria. The dialysis membrane does not interfere with the uptake of nutrients by the growing bacteria, but it facilitates the collection of cells at the end of the experiment as it would be difficult otherwise to separate the cells from the agar and to divide the samples up in cohorts.

Cells were harvested after 5 days by cutting the dialysis membrane into ribbons and placing these ribbons into Eppendorf tubes. Each ribbon was 5 cm long and at most 0.5 cm wide. Ribbon width was increased to 1.0 cm in areas where cell growth was not expected to occur, or where it was expected to occur slowly. The ribbons were submerged in 1 ml Milli-Q water and approximately 40 mg 0.1 mm glass beads were subsequently added so that the cells could be removed from the ribbons by rapidly vortexing the samples for 1 minute.

The glass beads were spun down quickly by centrifugation, and the supernatant containing the cells was subsequently pipetted into new Eppendorf tubes and the samples were subsequently centrifuged for 2 minutes at 14k rpm to pellet the cells. After the removal of the supernatant each sample was resuspended in a 100 µl solution containing 1 µg/ml fluorescent vancomycin (BODIPY® FL vancomycin). Samples were subsequently incubated in the dark for 30 minutes at room temperature and the fluorescence of the cells in each sample was measured using an Accuri® C6 flow cytometer at 530 nm (GFP).

Acknowledgements

We wish to thank Wolter de Goede and Ben Vorenkamp for their support in the design and construction of the environmental control chamber.

Supplementary Figure

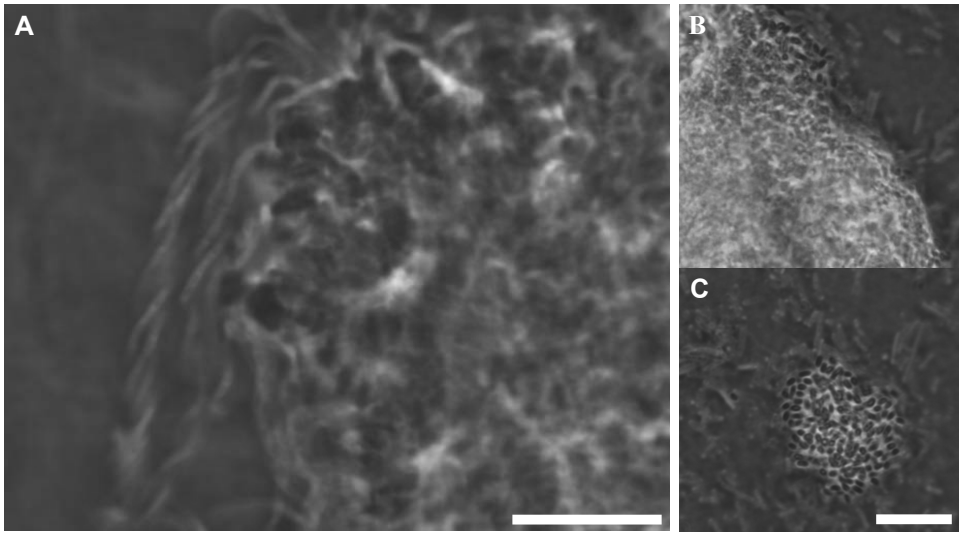

Figure S1. Morphological adaptations of *B. subtilis* 168 in a RH gradient. Cells differentiate into coils or coiled superstructures at a_w values between 0.95 and 0.936 and grow in more globular shapes below a_w values of 0.942. Sometimes both occur in close proximity (**A**). Close to the a_w growth limit only globular cell shapes occur (**B**) and clusters of cells start to sporulate (**C**). The white bars indicate 10 μm.

Reference List

Bhavsar,A.P., Erdman,L.K., Schertzer,J.W., and Brown,E.D. (2004) Teichoic acid is an essential polymer in Bacillus subtilis that is functionally distinct from teichuronic acid. *J Bacteriol* 186: 7865-7873.

Boylen,C.W. and Ensign,J.C. (1968) Ratio of teichoic acid and peptidoglycan in cell walls of Bacillus subtilis following spire germination and during vegetative growth. *J Bacteriol* 96: 421-427.

Boynton,W.P. and Brattain,W.H. (1929) Interdiffusion of gases and vapors. *International Critical Tables* 5: 62-64.

Carballido-Lopez,R., Formstone,A., Li,Y., Ehrlich,S.D., Noirot,P., and Errington,J. (2006) Actin homolog MreBH governs cell morphogenesis by localization of the cell wall hydrolase LytE. *Dev Cell* 11: 399-409.

Chirife,J., Ferro Fontan,C., and Scorza,O.C. (1981) The Intracellular Water Activity of Bacteria in Relation to the Water Activity of the Growth Medium. *Journal of Applied Microbiology* 50: 475-479.

Daniel,R.A. and Errington,J. (2003) Control of cell morphogenesis in bacteria: two distinct ways to make a rod-shaped cell. *Cell* 113: 767-776.

de Goffau,M.C., Yang,X., van Dijl,J.M., and Harmsen,H.J. (2009) Bacterial pleomorphism and competition in a relative humidity gradient. *Environ Microbiol* 11: 809-822.

Eskridge,R.E. (1996) Improved Magnus Form Approximation of Saturation Vapor Pressure. *Journal of Applied Meteorology* 35: 601-609.

Greenspan,L. (1976) Humidity fixed points of binary saturated aqueous solutions. *Journal of Research of the National Bureau of Standards* 81A: 89-96.

Hanaki,H., Labischinski,H., Inaba,Y., and Hiramatsu,K. (1998) Increase of non-amidated muropeptides in the cell wall of vancomycin-resistant Staphylococcus aureus (VRSA) strain Mu50. *Jpn J Antibiot* 51: 272-280.

Hansen,D.L. (1999) Microbial contamination. In *Indoor air quality issues*. London: Taylor & Francis, pp. 45-48.

Hayhurst,E.J., Kailas,L., Hobbs,J.K., and Foster,S.J. (2008) Cell wall peptidoglycan architecture in Bacillus subtilis. *Proc Natl Acad Sci U S A* 105: 14603-14608.

Hiramatsu,K. (2001) Vancomycin-resistant Staphylococcus aureus: a new model of antibiotic resistance. *Lancet Infect Dis* 1: 147-155.

Jones,L.J., Carballido-Lopez,R., and Errington,J. (2001) Control of cell shape in bacteria: helical, actin-like filaments in Bacillus subtilis. *Cell* 104: 913-922.

Koch,A.L. (1988) Biophysics of bacterial walls viewed as stress-bearing fabric. *Microbiol Rev* 52: 337-353.

Koch,A.L. (2001) Turgor pressure of bacterial cells. In *Bacterial growth and form*. Dordrecht, The Netherlands: Kluwer Academic Publishers, pp. 135-160.

Kreuzer-Martin,H.W., Lott,M.J., Ehleringer,J.R., and Hegg,E.L. (2006) Metabolic processes account for the majority of the intracellular water in log-phase Escherichia coli cells as revealed by hydrogen isotopes. *Biochemistry* 45: 13622-13630.

Li,H., Xu,L., Wang,J., Wen,Y., Vuong,C., Otto,M., and Gao,Q. (2005) Conversion of Staphylococcus epidermidis strains from commensal to invasive by expression of the ica locus encoding production of biofilm exopolysaccharide. *Infect Immun* 73: 3188-3191.

Mendelson,N.H. (1976) Helical growth of Bacillus subtilis: a new model of cell growth. *Proc Natl Acad Sci U S A* 73: 1740-1744.

Neuhaus,F.C. and Baddiley,J. (2003) A continuum of anionic charge: structures and functions of D-alanyl-teichoic acids in gram-positive bacteria. *Microbiol Mol Biol Rev* 67: 686-723.

Nobel,P.S. (1974) *Introduction to biophysical plant physiology*. San Francisco: Freeman.

Ophir,T. and Gutnick,D.L. (1994) A Role for Exopolysaccharides in the Protection of Microorganisms from Desiccation. *Appl Environ Microbiol* 60: 740-745.

Paul,A.L. and Ferl,J. (2006) The biology of low atmospheric pressure-Implications for exploration mission design and advanced life support. *Gravitational and Space Biology* 19: 3-17.

Rahman,M.S. (2007) Water activity and food preservation. In *Handbook of food preservation*. Rahman,M.S. (ed). Boca Raton: Taylor & Francis, pp. 447-474.

Smith,W.K. and Geller,G.N. (1979) Plant transpiration at high elevations: Theory, field measurements, and comparisons with desert plants. *Oecologia* 41: 109-122.

Wiebe,H.H. (1981) Measuring Water Potential (Activity) from Free Water to Oven Dryness. *Plant Physiol* 68: 1218-1221.

Chapter 5

Cold spots in neonatal incubators are hotspots for microbial contamination

Marcus C. de Goffau, Klasien A. Bergman,
Hendrik J. de Vries, Nico E. L. Meessen, John E. Degener,
Jan Maarten van Dijl and Hermie J. M. Harmsen
Submitted for publication

Abstract

Purpose: Thermal stability is essential for the survival of preterm neonates, which is achieved in incubators by raising the ambient temperature and humidity to sufficiently high levels. Microorganisms can however potentially thrive in such warm and humid environments. In this study, we investigated whether the level of microbial contamination within an incubator can be predicted solely on the basis of the local temperature distribution within an incubator, its average temperature, and humidity settings.

Methods: The temperature distribution within a Caleo® incubator was mapped with an infrared thermometer. Swab samples were taken from the warmest and coldest spots and these were plated out to determine the number of colony forming units at these locations.

Results: The data show that the level of microbial contamination increased significantly in areas of the incubator where the local temperature was lower than the average temperature of the air inside the incubator. This relates to the fact that the local equilibrium relative humidity is elevated sufficiently in these areas to sustain microbial growth. Especially the abundance of staphylococci, which are currently the main causative agents of sepsis in preterm neonates, was found to be elevated significantly in the cold areas.

Conclusions: The identification of local cold spots as hotspots for microbial contamination in neonatal incubators indicates that the incidence of sepsis in preterm neonates could be reduced by simple hygienic measures. In addition, our results call for an improved design of incubators lacking relatively cold spots which would preclude potentially hazardous growth.

Introduction

To increase the survival chances of premature infants, incubators have been developed in the past two centuries, which provide a thermoneutral environment. This environment must be defined in terms of temperature, humidity, convection and surrounding radiant heat sources.

Humidification of the incubators has helped in this respect as the greatest heat loss by preterm neonates is due to evaporative trans-epidermal water loss. Increased relative humidity (RH) reduces the rate of evaporation and, as a consequence, not only reduces evaporative heat loss (Charles, 1939), but also helps to maintain the electrolyte and fluid balance (Ducker and Marshall, 1995). These conditions which are required to maintain a thermoneutral environment unfortunately also increase the risk of microbial infection as the moist and warm habitat created within an incubator is intrinsically ideal for microbial growth.

As such, a fine balance is sought nowadays between the thermal requirements of a newborn and the level of humidification and heating of the incubator (Antonucci *et al.*, 2009). The highest levels of humidification and heating are used for the most immature infants with the lowest birth weights as they have the most trouble with maintaining their thermal stability (Heuchan *et al.*, 2009). The humidification and heating levels are lowered slowly in the course of the first days and weeks as the neonates' weight and the maturity of their skin barrier increases. The less immature neonates and the ones that have already spent some time in the incubator do not require such high temperature and humidity levels. It is shown in the present studies that the thermal requirements of the most fragile newborns are associated with the highest risk levels from a microbial point of view.

The availability of water is one of the most important factors for determining whether microorganisms can grow within any environment. This availability is determined on surface to air interfaces by the local equilibrium relative humidity (RH_e). Molds require RH_e values of at least 70% and RH_e values need to be even higher to allow for the growth of yeasts, Gram-positive and finally Gram-

negative bacteria (80-95%) (Rahman, 2007). The local RH_e on any location within an incubator can be calculated using only three variables, which are the local temperature on that particular location, the average air temperature of the incubator, and the average RH inside the incubator (Alduchov and Eskridge, 1996).

Both the average air temperature and RH are controlled and monitored within a modern incubator, such as the Caleo® incubator which was used in the present research, and these parameters are set to provide the child with the required thermal comfort. The local temperature on the walls inside the incubator is however not under direct control, but is instead dependent on the temperature difference between the inside and outside of the incubator and the airflow within the incubator. Condensation occurs on the walls of an incubator whenever the RH_e reaches 100%, which will be the case when the local temperature is equal or below the dew point temperature of the air inside the incubator. The greater the temperature difference is between the air inside the incubator and outside of it, the faster condensation will occur on local cold spots as larger temperature differences lead to relatively colder cold spots. The dew point temperature on such spots is also reached more quickly with increasing average RH values within the incubator. Microbial growth does however not require condensation (rain-out) as RH_e values not too far below 100% are also sufficient for this potential problem, depending on the microbial species (de Goffau *et al.*, 2009).

The present studies were performed at the Department of Neonatology of the Beatrix Children's Hospital, University Medical center Groningen (UMCG), The Netherlands, in a 24-bed level III NICU. The goal was to investigate whether the occurrence of microbial growth, or at least an increased level of microbial contamination, can be predicted by determining the local temperature distribution within an incubator in combination with its average temperature and RH settings. The first step was to map the temperature distribution within an incubator with an infrared thermometer to identify local cold and hot spots. Secondly, swabs were

taken from both cold and hot spots, and these were plated to compare the numbers of colony forming units (CFU) on these spots.

Another prediction was that no significant differences would be found between cold and hot spots in incubators which have relatively low levels of humidification and heating as the cold spots in these incubators would not be cold enough to create local RH_e values that are high enough for microbial growth. To test this, the sampled incubators were divided into two groups. Group 1 consisted of incubators with low average RH and temperature values ($RH \leq 60\%$, $T < 34$ °C). Group 2 consisted of incubators with high average RH and temperature values ($RH \geq 60\%$, $T \geq 34$ °C).

Finally, it was investigated whether the microorganisms isolated from the incubators could be correlated with actual infection rates, in particular when microbial species were found to be increased in frequency at the cold spots of Group 2.

Material and Methods

Thermal characterization of a Caleo incubator

A Fluke 62 Mini infrared thermometer (Conrad, Oldenzaal, The Netherlands) was used to measure the temperature distribution on the inside of a Caleo® incubator, which was set at an average RH of 70% and a temperature of 37 °C.

Sampling protocol

Neonates are routinely transferred into a freshly cleaned incubator every week and samples can thus be taken from the used incubator immediately after the switch without interfering with the care of the neonate. Sampling was performed with a cotton-tipped swab (Greiner-Bio-One, Alphen aan de Rijn, The Netherlands) moistened with 70µl physiological salt solution (0.85% NaCl). The swabs were rubbed vigorously against the identified cold and hot spots on the inner wall of the incubators.

Of the first seven incubators only 3 hot spots were swabbed per incubator and in between 4 to 7 colds spots. After that these numbers were standardized to taking 5 samples from fixed cold spots and 4 from fixed hot spots (Fig. 1). A few of these fixed spots were excluded from the analysis if remnants of bodily excretions, such as saliva, were noticed to be present on the locations that were to be sampled. In total, 11 incubators of Group 1 and 12 of Group 2 were sampled.

Cultivation

The swabs were immediately taken to the lab after sampling. The tips of cotton-tipped swabs were cut off and deposited in sterile tubes containing 1.6 ml physiological salt solution and three sterile glass beads (4 mm in diameter). These tubes were mixed for 30 seconds on a vortex mixer, incubated for 10 minutes at 4°C, and mixed again afterwards. Aliquots of 100 µl of the resulting suspensions were subsequently plated on both Blood Agar solid media and on Sabouraud solid media (Mediaproducts BV, Groningen, The Netherlands). The blood agar plates were incubated at 37°C, while the Sabouraud plates were incubated at room temperature. Microbial isolates were subsequently identified by colony morphology, microscopy (Gram staining, cell shape, clustering patterns, presence of spores) and by performing biochemical tests using API-20E.

Statistical analysis

The numbers of CFU recovered from the blood agar plates and the Sabouraud plates were summed up to determine the number of CFU per location. If a particular organism was found to be growing on both types of plates the above summation was adjusted such that only the highest number of CFU from either plate of this particular organism was used in the summation. As the numbers of CFU per location are not normally distributed, the non-parametric Mann-Whitney U test was used to assess whether the level of microbial contamination differed significantly between the different samples. A p-value <0.05 was considered significant.

Results

Temperature distribution of the Caleo incubator interior

The warm humidified air that is blown into the Caleo® incubator from the hot air vents does not reach all parts of the interior walls equally (Fig. 1).

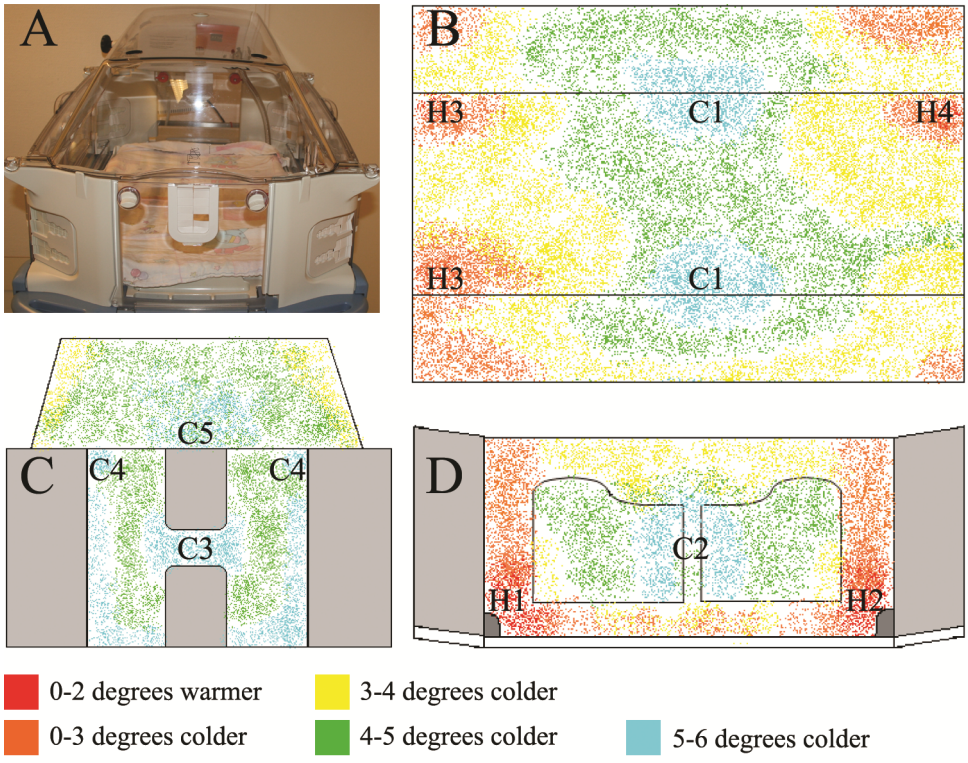

Figure 1. Temperature distribution within a Caleo neonatal incubator. (**A**) Example Caleo Incubator. (**B**) Top view. (**C**) Front view, which is very similar to the rear view. The part below C3 is optional. (**D**) Side-view, representing both sides. C1-C5 indicate cold sampling locations, H1-H4 indicate hot sampling locations. The same swab was used to sample locations in those cases where this location is indicated twice. Similarly, samples from H1, H2 and C2 also originate from two locations, namely the left and the right sides of the incubator. Samples were also taken from the rear side in case of C4 but not in case of C3 and C5 as the sampling surface of location C4 is comparatively small.

Various cold spots were found with temperatures up to 6 °C lower than the average air temperature (37 °C) and hot spots were up to 2 °C warmer. Cold spots were predominantly found at the front and backsides, and in the middle of the incubator on the doors and canopy. Hot spots mapped close to the hot air vents and on the canopy above the hot air vents. The temperature distribution was subsequently verified by looking at the different condensation profiles at decreased and elevated average RH values (55-85% RH).

Condensation profiles were found to be consistent with the measured temperature distribution apart from a few local exceptions. These exceptions were local cold spots where the low temperature values were not solely due to the airflow within the incubator but also due to the fact that the incubator is not airtight near these locations. This allows colder but dryer air from outside to influence the local RH_e. Such exceptions could be identified by condensation occurring at higher than expected average RH values at these specific locations. Only cold spots that were at least 5 °C colder than the average air temperature (37 °C) and where condensation occurred according to expectation were sampled. The hot spots were 0-2 °C warmer than the average air temperature.

Incubators with average air temperatures lower than 37 °C differed slightly in how much colder the cold spots were relative to the average air temperature. Smaller temperature differences between the inside and the outside of the incubator led to smaller temperature differences within an incubator. As incubators with lower average temperature values invariably also had lower average RH values, this led to an additive reduction in the local RH_e at the cold spots in such incubators. These findings were taken into account for defining the cut-off values used to divide the sampled incubators into two groups.

Group 1 represents the incubators in which the RH_e values of the cold spots were predicted not to exceed 80%. This RH_e of 80% was in turn chosen as it represents the growth limit of staphylococci, which are very xerotolerant human commensals (de Goffau *et al.*, 2009).

Microbial contamination of incubators

The number of colony forming units (CFU) obtained from each sampled location was taken as a measure for the level of microbial contamination (Fig. 2).

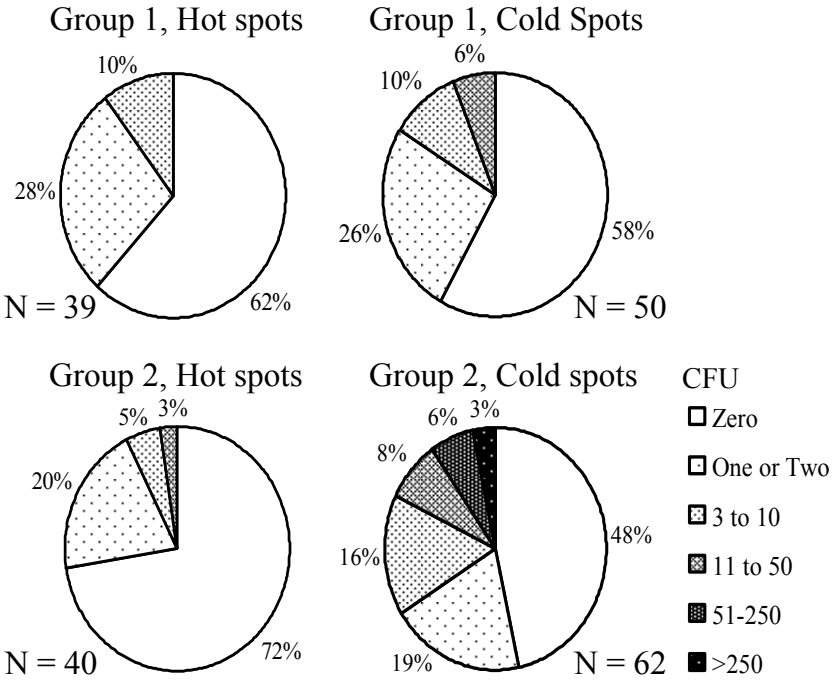

Figure 2. Microbial contamination on hot and cold spots in Group 1 and 2 incubators with low and high average RH values respectively. The numbers of colony forming units are indicated by different patterns. The numbers (N) of sampled spots and the relative frequencies (%) of colony forming units (CFU) are indicated.

No significant differences ($p = 0.336$) were found between the cold and hot spots from incubators that had RH values of 60% or lower in combination with average air temperatures lower than 34 °C (Group 1). Significant differences ($p = 0.004$) were however found between the cold and hot spots from the incubators that had RH values of 60% or higher in combination with average air temperatures higher than 34 °C (Group 2).

Even if the incubators were not divided into Groups 1 and 2, the differences in the CFUs at the hot and cold spots still remained significant but with higher a p-value (p = 0.013).

Interesting was the prevalence of certain microbial species found at the cold spots of Group 2 incubators compared to the hot and cold spots of Group 1 incubators and the hot spots of Group 2 incubators (Table 1). A direct comparison of the numbers of CFU found per species per location was however difficult as the distribution of the number of CFU per location is not normally distributed. To obtain the values shown in Table 1, the natural logarithm was therefore taken from the number of the CFU+1 of organisms from a particular type (e.g. staphylococci) per spot from a particular location type (Group 1 hot or cold spots or Group 2 hot or cold spots). The outcomes of all these spots were summed up and subsequently divided by the number of spots of that particular location type (39, 50, 40 & 62 respectively) and multiplied by 100.

Table 1. Prevalence of microbial groups at different locations in neonatal incubators.

$\frac{\sum(Ln(CFU+1))}{n.spots/100}$ (%)[#]	Group 1		Group 2	
	Hot spot	**Cold spot**	**Hot spot**	**Cold spot**
Staphylococci	8.1 (*10.3)*	18.4 *(14.0)*	9.7 *(12.5)*	**75.2** ***(35.5)***
Micrococci	16.6 *(17.9)*	15.9 *(16.0)*	16.7 *(10.0)*	11.6 *(12.9)*
Sporulating bacteria	1.8 *(2.6)*	1.4 *(2.0)*	6.2 *(7.5)*	6.2 *(4.8)*
Other Gram-positive bacteria	11.7 *(10.3)*	5.5 *(8.0)*	1.7 *(2.5)*	**26.7** ***(17.7)***
Gram-negative bacteria	5.3 *(7.7)*	1.4 *(2.0)*	9.0 *(7.5)*	22.2 *(9.7)*
Yeast	4.6 *(5.1)*	7.2 *(4.0)*	6.6 *(5.0)*	3.4 *(4.8)*
Molds	3.6 *(5.1)*	6.9 *(4.0)*	0.0 *(0.0)*	5.4 *(4.8)*

[#]Percentage of spots colonized with 1 or more CFU of the indicated microbial group.

Of particular interest is the very significant increase ($p < 0.0005$) in the numbers of CFU from staphylococcal species on the cold spots of Group 2 incubators. It was observed both within the UMCG (Table 2) and by others (Stoll *et al.*, 1996) that the vast majority of infections in preterm neonates are caused by coagulase-negative staphylococci and, at substantially lower rates, by the coagulase-positive *Staphylococcus aureus*.

Table 2. Pathogens associated with sepsis in neonates[#]

Organism	**No.**	**%**
Staphylococcus-coagulase negative	797	68.2
Staphylococcus aureus, non MRSA	113	9.7
Escherichia coli	67	5.7
Enterobacter cloacae	30	2.6
Streptococcus-group B	29	2.5
Streptococcus-alpha hemolytic	24	2.0
Klebsiella pneumoniae	22	1.9
Enterococcus faecalis	18	1.5
Klebsiella oxytoca	13	1.1
Candida albicans	12	1.0
Serratia marcescens	9	0.8
Pseudomonas aeruginosa	7	0.6
Enterococcus faecium	6	0.5
Haemophilus influenza	4	0.3
Acinetobacter baumannii	3	0.3
Methicillin resistant *S. aureus*	3	0.3
Others	12	1.0

[#]Number of cases and frequency are indicated at the UMCG in the years 2005-2009

The abundance of Gram-negative bacteria on cold spots of Group 2 incubators was also found to be slightly elevated, but was not statistically significant ($p = 0.252$). Of all the Gram-negative bacteria, a *Methylobacterium* species, which forms pink colonies on Sabouraud agar, stood out as it was several times found in high CFU numbers. *Micrococcus luteus* and other *Micrococcus* species were not found at increased frequency at the cold spots of Group 2 incubators. Nevertheless, these bacteria were often detected on blood agar plates in low CFU

numbers (1-4). Similarly, no noteworthy differences were observed for the numbers of Gram-positive sporulating bacteria, yeasts or molds. The number of Gram-positive bacteria not represented by the previously mentioned groups also increased significantly ($p = 0.019$) on the cold spots of Group 2 incubators. Amongst these 'other' Gram-positive bacteria, the enterococci are of particular interest as these bacteria were exclusively found on the cold spots of Group 2 incubators, sometimes at high CFU numbers.

Discussion

Significant differences in contamination levels were found between the cold and hot spots of neonatal incubators with relatively high average temperature and RH values (Group 2). In particular, the level of staphylococcal contamination was increased significantly. Staphylococci are known for their ability to grow at relatively low RH_e values and these bacteria are consequently one of the few organisms that can grow at cold spots which only reach RH_e values slightly above 80% (80-90%). They are furthermore very desiccation resistant (Beard-Pegler *et al.*, 1988) and ubiquitously present as part of the human microbiota. Consequently, there is a high probability to detect staphylococci at locations frequented by humans and, when the conditions permit, that these bacteria grow on such spots. Though staphylococci are mostly harmless commensals, some species are dangerous opportunistic pathogens, which can infect patients with a compromised immune system, such as preterm neonates.

Furthermore, the slightly increased numbers of Gram-negative bacteria at the cold sites of neonatal incubators with high humidity levels call for attention, because infections with Gram-negative bacteria, organisms which require especially high RH_e values, have the highest death rates (Stoll *et al.*, 1996). As the risk of infection increases for more premature neonates, our findings make it very well conceivable that this might at least be partially related to the environmental requirements in their incubators.

The slight increase in the number of methylobacteria, which are relatively non-pathogenic, and enterococci, which are important nosocomial pathogens, can likely be attributed to their ability to survive desiccation, and not so much their ability to grow at relatively low RH_e values. Methylobacteria are well known for their ability to survive high levels of radiation due to their efficient DNA repair systems (Romanovskaia *et al.*, 2002). This ability is equally relevant to survive DNA damage during desiccation due to oxidative processes (Fredrickson *et al.*, 2008). Enterococci, especially *E. faecium*, is a known producer of reactive oxygen species. This means that this organism also needs to be very efficient in dealing with oxidative stress as it would otherwise kill itself (Lammers, 2008). As such it is likely more capable of preventing oxidative processes from damaging its DNA during desiccation.

Temperature differences in incubators with relatively low average temperatures and RH values (Group 1) did not cause significant differences in microbial contamination between the colder and warmer areas inside of the incubator. The likely reason for this is that the local RH_e values on the cold sites of these incubators do not surpass 80%, which is needed for the growth of coagulase-negative staphylococci, such as *Staphylococcus epidermidis* (de Goffau *et al.*, 2009). Consistent with this notion, the Gram-negative bacteria that require even higher RH_e values in order to grow were found only in low quantities within incubators of Group 1. Even mold and yeast species, of which some can grow at RH_e values below 80%, were isolated too infrequently to be of any importance in the microbial contamination of these relatively 'dry' incubators.

Simple improvements in hygienic measures can readily be deduced from our present finding that the level of microbial contamination is the highest at the cold spots in incubators which have high average temperature and RH values. Especially, the occurrence of condensation on the interior of the incubator should be prevented as much as possible. When condensation does however occur, which often happens at high RH values, the condensate should be wiped away with a clean piece of disposable cloth. Clearly, this should not be done with a

reusable piece of cloth lying in the incubator. To minimize the spread of any microbial contamination throughout the incubator, the removal of condensate should only be done if a clear view is needed to handle the neonate. Also, after wiping away the condensate, the nurses hands should be disinfected before handling the neonate to prevent any bacterial transmission to the neonate. These simple hygienic measures are now common practice at the UMCG.

Furthermore, even in the absence of condensation, it might be advisable to change incubators more often than once a week for neonates lying in incubators with high temperature and RH values (Group 2). In addition, incubators from Group 2 could also be placed in wards with elevated room temperature values in order to prevent the formation of relatively cold spots, thus preventing microbial growth from occurring in the first place.

Ultimately, the most effective prevention of relatively cold spots can be achieved by improving the incubator design, for example by placing small heating elements at vital spots.

Conclusion

We have demonstrated that the level of microbial contamination is significantly elevated in incubators with high average air temperature and relative humidity values (RH $\geq$ 60%, T $\geq$ 34 °C), especially in the areas where the local temperature is lower than the average temperature of the air inside the incubator. Notably, the abundance of staphylococci, which are currently the main causative agents of sepsis in preterm neonates, was found to be elevated significantly in these cold areas. The identification of local cold spots as hotspots for microbial growth coupled with appropriate hygienic measures may therefore contribute significantly to a reduction of sepsis in neonates.

Acknowledgments

The authors thank the staff of the UMCG neonatology intensive care units, and in particular Thea Steenbergen, for their help in obtaining the Caleo® incubator samples. This work was supported by the Netherlands Institute for Space Research (SRON) grants MG-064 and MG-068 and served as a ground based model for predicting the occurrence of microbial contamination in closed environments, such as in spacecraft. Approval for this study was given by the head of the neonatology department, Prof. Dr. A.F Bos.

Reference List

Alduchov, O.A. and Eskridge, R.E. (1996) Improved Magnus Form Approximation of Saturation Vapor Pressure. *Journal of Applied Meteorology* **35:** 601-609.

Antonucci, R., Porcella, A., and Fanos, V. (2009) The infant incubator in the neonatal intensive care unit: unresolved issues and future developments. *J Perinat Med* **37:** 587-598.

Beard-Pegler, M.A., Stubbs, E., and Vickery, A.M. (1988) Observations on the resistance to drying of staphylococcal strains. *J Med Microbiol* **26:** 251-255.

Charles, C.C. (1939) A New Infant Incubator. *The American Journal of Nursing* **39:** 970-973.

de Goffau, M.C., Yang, X., van Dijl, J.M., and Harmsen, H.J. (2009) Bacterial pleomorphism and competition in a relative humidity gradient. *Environ Microbiol* **11:** 809-822.

Ducker, D.A. and Marshall, N. (1995) Humidification without risk of infection in the Dräger Incubator 8000. Lübeck, Germany, Drägerwerk.

Fredrickson, J.K., Li, S.M., Gaidamakova, E.K., Matrosova, V.Y., Zhai, M., Sulloway, H.M. *et al.* (2008) Protein oxidation: key to bacterial desiccation resistance? *ISME J* **2:** 393-403.

Heuchan, Williams, and Gonella . Humidity and Care of Humidification Systems in the Neonatal Department, reducing the risk of nosocomial infection. 2009. Glasgow, Scotland, Queen Mothers Hospital.

Lammers,M. Physiology of Enterococcus faecalis and faecium. 2008. University of Utrecht.

Rahman,M.S. (2007) Water activity and food preservation. In *Handbook of food preservation*. Rahman,M.S. (ed). Boca Raton: Taylor & Francis, pp. 447-474.

Romanovskaia,V.A., Rokitko,P.V., Mikheev,A.N., Gushcha,N.I., Malashenko,I., and Chernaia,N.A. (2002) The effect of gamma-radiation and desiccation on the viability of the soil bacteria isolated from the alienated zone around the Chernobyl Nuclear Power Plant. *Mikrobiologiia* **71:** 705-712.

Stoll,B.J., Gordon,T., Korones,S.B., Shankaran,S., Tyson,J.E., Bauer,C.R. *et al.* (1996) Late-onset sepsis in very low birth weight neonates: a report from the National Institute of Child Health and Human Development Neonatal Research Network. *J Pediatr* **129:** 63-71.

Chapter 6

Microbial growth in spacecraft in relation to water availability, microgravity and radiation

Marcus C. de Goffau, Jan Maarten van Dijl and Hermie J. M. Harmsen

Submitted for publication

Abstract

Various environmental factors influence the growth potential of microorganisms on surface to air interfaces, but the availability of water is usually the critical determinant for microbial growth and survival on a particular spot. In spacecraft this is no different. Microgravity and the increased levels of radiation however make spacecraft environments unique. Here, we review the correlation of these two parameters with the availability of water and as a consequence, increased microbial growth and/or survival.

Under microgravity conditions thermal convection does not occur and this influences the temperature distribution on board of spacecraft. In turn, this can enhance the local availability of water on surface to air interfaces. Furthermore, increased ionizing radiation will possibly select for microorganisms with enhanced desiccation resistance as both stressors share the same molecular resistance mechanisms.

Microgravity does not only affect the environment of the astronauts, but also the microbiological niches represented by the astronauts themselves. A shift in the nasal microbiota of astronauts is expected as a result of the cephalic fluid shift, since this phenomenon causes nasal congestion that will lead to a more humid/moist nasal environment.

Increased awareness of these relationships will allow a minimisation of the microbial risks imposed on astronauts, which is important because astronauts are likely to be temporarily immune-compromised due to microgravity and radiation.

Introduction

On earth, water availability is one of the most important prerequisites for microbial growth in all ecological settings. Consequently, the availability of water for microbial growth has a huge impact on human health and wellbeing. This view is underscored by the fact that the equilibrium relative humidity (RH_e) is a key parameter for the air quality in buildings. The RH_e is the most important determinant of indoor bio-aerosol levels; the main cause of building-related illnesses (Green *et al.* 2003). This is not surprising as the particular environmental needs and capabilities of different microorganisms vary enormously. In every building there are usually plenty of microbial species to be found whose general microbial requirements such as temperature, nutrients, oxygen or light can be met. The only thing that is often missing in the potential replicative lives of these organisms is the availability of enough water (Hansen 1999).

In spacecraft this is no different. Spacecraft hygiene is, however, not only important to prevent the growth of pathogenic microbes that threaten the health and wellbeing of potentially immunocompromised astronauts (Kaur *et al.* 2008), but also to prevent the growth of bio-fowling spacecraft-deteriorating microbes, the so called technophiles (van Tongeren *et al.* 2006). The main differences between buildings on earth and spacecraft are the factors of gravity and radiation. Here we review the correlation of these two parameters with the availability of water as well as the consequences for microbial growth and survival.

Relative humidity, temperature & microgravity

Relative humidity control is a critical part in preventing microbial growth as RH values of at least 70% are needed to allow for the growth of molds, and they need to be even higher to allow for the growth of yeasts, Gram-positive and finally Gram-negative bacteria (80–95%) (Rahman 2007). The Mir space station was

severely lacking such control since molds overgrew virtually all interior surfaces of this space station. Even the electrical wiring on board was covered with moulds, which actually caused several life-threatening incidents (Novikova 2004). A plethora of potentially pathogenic microorganisms (and a variety of other life forms) was furthermore found in samples of free floating condensate, which had accumulated behind panels on board the Mir.

The unwanted growth of microbes is more effectively prevented on board of the International Space Station (ISS) where the environmental control and life-support system (ECLSS) maintains the cabin atmosphere in between 25 and 75% RH. Although these numbers seem to indicate that the ISS is too dry for microbial growth, except for perhaps some of the hardiest moulds, the actual level of bacterial contamination within the ISS (Castro *et al.* 2004; Novikova *et al.* 2006; Novikova 2004) and an almost disastrous computer malfunction (Oberg 2007) seem to indicate otherwise. In this respect it is important to note that the ability of microorganisms to thrive at solid surface to air interfaces, which are seemingly too dry for microbial growth can be understood if one adds temperature into the equation, because the RH can be locally increased or decreased depending on local differences in temperature.

In any closed compartment, so also in the cabin of a space station, the availability of water is determined by the local equilibrium RH (RH_e). In turn, the RH_e is dependent on the actual water vapour pressure present within the cabin air and the saturation vapour pressure, which becomes higher with higher temperatures. The actual water vapour pressure (e) is the same everywhere within the cabin if there is sufficient ventilation, but the saturation vapour pressure (e_s) is dependent solely on the local temperature (Lawrence 2005). The RH_e is equal to $100*e/e_s$. This means that if there is a cold spot in a particular part of the cabin, the local RH_e near that spot will be higher than the average RH of that part of the cabin as the e_s at that spot will be lower than the average e_s (Lstiburek and Carmody 1996). A clear example of these principles is presented in Fig. 1, where a building is shown that suffers from spotted building syndrome.

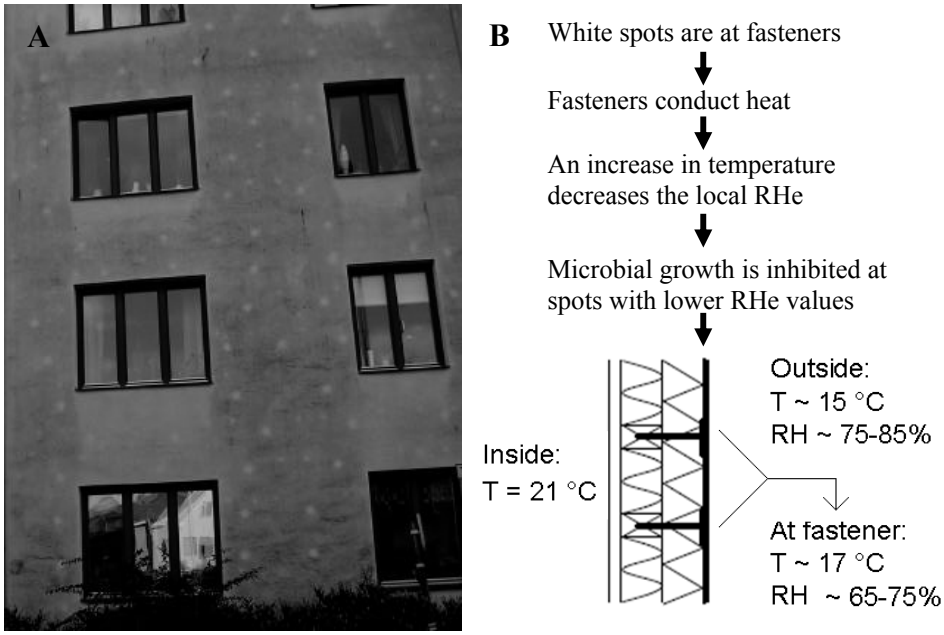

Figure 1. Spotted building syndrome. An example of the interplay between humidity and temperature differences that determine the possibility of microbial growth. (**A**) Microbial growth occurs everywhere on the wall of this building except at the white spots behind which fasteners have been mounted. (**B**) Schematic representation of the fasteners in the wall of a building with spotted building syndrome. The values given are merely illustrative. Pictures were kindly provided by Dr. Sanne Johansson.

The white spots on the wall of this building are a consequence of the use of metal fasteners, which conduct heat from the inside to the outside of the building. The fasteners thus create spots where the local temperature is elevated to such an extent that the RH_e becomes too low for microbial growth (Johanssen *et al.* 2005). Conversely, such metal fasteners can also cause local cold spots inside the building that could enable microbial growth.

Thus, although the ideal environment for microbial growth is both humid and warm, the actual locations where growth might be possible within a system are the locations that are colder than the average temperature. Temperature control is therefore a most critical aspect of relative humidity control. The more inhomogeneous the temperature distribution is within a compartment, such as the

cabin of a space station, the higher the probability will be that it contains niches where microbial growth can actually occur.

One of the distinguishing environmental conditions encountered on board of spacecraft, microgravity, is a complicating factor for relative humidity control as thermal convection does not occur in spacecraft cabins due to a lack of gravity. On earth air will start to circulate in a room where there is a cold spot (*e.g.* a window) on one side and a hot spot (*e.g.* a heater) on the other side of the room. Air circulation as a consequence of temperature differences does not occur under conditions of microgravity and, as such, the temperature distribution is more likely to be inhomogeneous in spacecraft (Fig. 2).

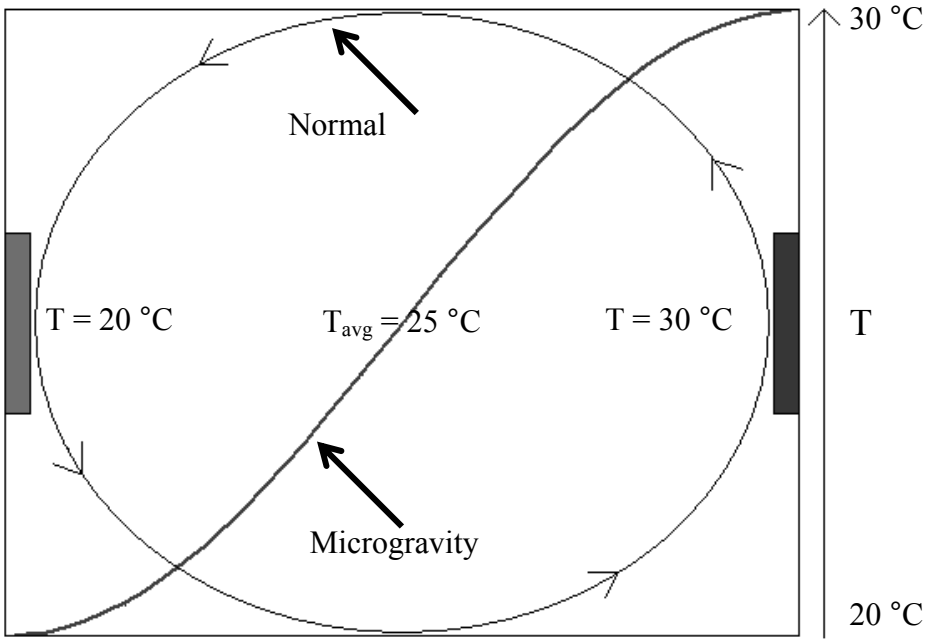

Figure 2. Effect of the presence or absence of gravity on the air flow or the temperature distribution in a closed compartment. The boxes on the left and right represent cold (20 °C) and warm (30 °C) elements in a compartment that has an average temperature of 25 °C. Arrows indicate the expected airflow under conditions of normal gravity, or the temperature distribution under conditions of microgravity.

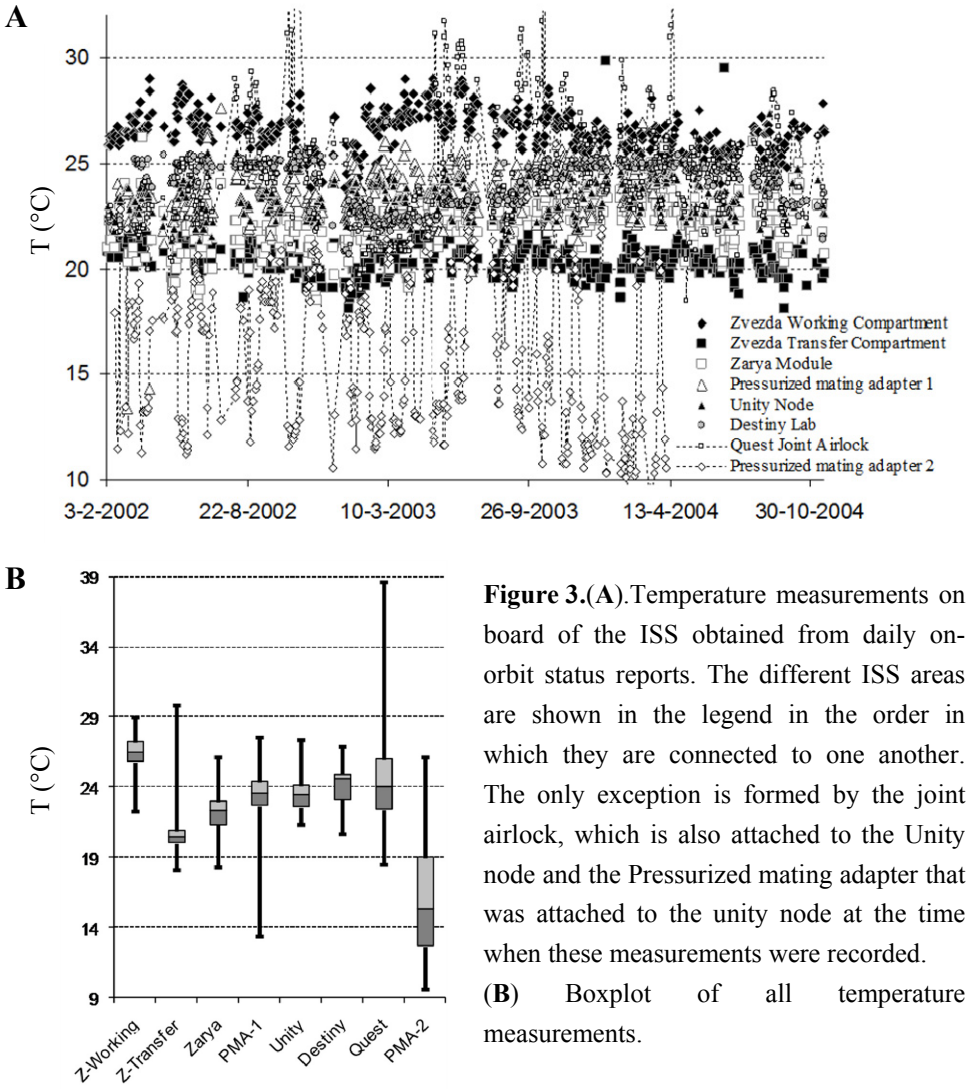

Figure 3.(**A**).Temperature measurements on board of the ISS obtained from daily on-orbit status reports. The different ISS areas are shown in the legend in the order in which they are connected to one another. The only exception is formed by the joint airlock, which is also attached to the Unity node and the Pressurized mating adapter that was attached to the unity node at the time when these measurements were recorded. (**B**) Boxplot of all temperature measurements.

The cabin air temperature within the ISS is said to range between 17 and 28 °C with dew point temperatures between 4.4 and 15.6 °C (ESA 2008). The temperature distribution in between the different ISS modules is, however, quite variable both in time and space according to the data mined from daily on-orbit status reports for the period between 2002 and 2004 (Fig. 3) (http://www.spaceref.com/news/statusreports.html).

There is for instance a temperature difference of about 7 °C between the working compartment of the Russian Zvezda module and its transfer compartment which couples the Zvezda module to the Zarya module. Also, temperatures within the U.S. joint airlock (Quest) and the pressurized mating adapter 2 (PMA-2) fluctuate heavily in time. Temperatures of the PMA-2 are furthermore often worrisomely low. Intermodular air flows might thus have the potential to temporarily cause local niches where the availability of water is high enough for microbial growth. For example, if the RH of the working compartment of the Zvezda module would be about 50% and if this air would be blown into its transfer compartment, then the local RH inside the transfer compartment would rise to 76%, which is high enough for the growth of various moulds.

Intramodular temperature differences are furthermore also expected to exist, because the air flow within modules cannot reach all spaces equally well, especially not behind panels. Local temperature fluctuations in time might furthermore cause the existence of niches, which are transiently conducive to microbial growth when temperatures are at their lowest. A selection for desiccation resistant microorganisms is likely to occur at such spots when the temperatures again rise.

Radiation and desiccation resistance

Radiation on board the ISS forms a potential health hazard for astronauts, as they are subjected up to 1 millisievert of radiation per day, which is about the same as someone would get from natural sources on Earth in a whole year (Samuel 2002; Shavers *et al.* 2004). Notably however, the radiation also has the potential to interact with the microbial ISS inhabitants in unexpected ways. Not only does an increased amount of radiation increase the mutational frequency, but it is also likely to indirectly select for an increased desiccation resistance in various microbes. It has been shown previously that it is possible to select indirectly for radiation resistant bacteria by selecting for desiccation resistance (Sanders and Maxcy 1979), and high radiation environments were shown to be enriched with

fungal and bacterial groups known for their desiccation resistance and/or their ability to grow at low RH values (Dadachova and Casadevall 2008; Fredrickson *et al.* 2004). The molecular mechanisms that both types of resistance seem to require to comparable extents are highly effective DNA repair and efficient responses to the insults caused by oxidative stress (Fredrickson *et al.* 2008). The accumulation of DNA damage during desiccation, which needs to be repaired once the environment inhabited by the microorganism becomes humid enough again for growth, has been attributed to the formation of reactive oxygen species. Heavy-ion radiation, a major component of absorbed cosmic radiation on board of the ISS, causes double stranded DNA breaks while X-ray and gamma-ray radiation cause oxidative stress and, consequently, oxidative DNA damage (Masumura *et al.* 2002).

On earth the selection for desiccation resistance occurs in just one single generation in every cycle in which microorganisms become dehydrated and hydrated again as no new generations are made during desiccation. The same is true on board the ISS with the exception perhaps that the cycles in which certain locations become dry and humid might be shorter.

Radiation represents a stressor that does not necessarily interfere with the growth of cells as long as water is available. However, radiation may be a selective factor for microbes that possess the molecular mechanisms that are needed for desiccation resistance. This double selection pressure on board the ISS might thus favor species, which are more desiccation tolerant, such as e.g. *Acinetobacter radioresistens*, *Methylobacterium* sp., *Bacillus* sp., *Staphylococcus sp.,* and several actinobacteria (Castro *et al.* 2004; Novikova *et al.* 2006; Novikova 2004), or together with the increased mutational frequency, it might actually make an impact at the intraspecies level.

The radiation levels on board of the ISS however seem unlikely to significantly influence the viability or growth speed of most microorganisms, except for perhaps the most radiation sensitive ones (Tallentire 1980; Qiu *et al.* 2004), as the radiation exposure dose, even when taken together cumulatively over longer time periods, should not even come close to becoming microbiostatic

or microbicidal. Nevertheless data on *Rhodospirillum rubrum* show that even a rather low dose of ionizing radiation of 2 mGy, to which this bacterium was exposed during a 10-day stay on board the ISS, induces a significant response on both the transcriptomic and proteomic levels (Mastroleo *et al.* 2009). Interestingly, this response entailed both an induction of a large number of genes related to oxidative stress and of several genes involved in DNA repair.

Microgravity and the cephalic fluid shift

Microgravity not only has an effect on the availability of water in the astronauts' environment, but also on the microbial niche that the astronauts represent themselves. Water makes up about two thirds of the weight of the human body and under normal gravity conditions much of this water would settle downwards in an upright standing individual if it were not for the strong pumping action of the human heart. In space however, the heart causes excessive pumping of fluids towards the head thereby causing the astronauts' faces to become puffed and furthermore giving them continuously a stuffy nose due to nasal congestion (Bungo *et al.* 1985). A continuous horizontal positioning of the human body on earth, a "poor mans" version of microgravity, causes the very same symptoms.

Normally, the main microbial components of the nasal cavity are coagulase negative staphylococci, such as *Staphylococcus epidermidis*, which can grow at RH_e values as low as 80% and, to a lesser degree, the coagulase positive *Staphylococcus aureus*, which needs RH_e values of 87% or higher. While microorganisms are often the cause of a nasal congestion (sinusitis) on earth, the microgravity-induced nasal congestion in space likely creates a more humid environment for microorganisms to grow, possibly influencing the composition of the nasal microbiota. Consistent with this view, the total number of viable *S. aureus* cells and the level of cross-contamination with this particular organism has been found to increase in space (Decelle and Taylor 1976; Taylor 1974). An increase of the amount of Gram-negative bacteria, such as *Proteus*, *Klebsiella*, *Enterobacter*, *Citrobacter*, and *Escherichia coli*, has also been noted

(Ilyin 2005). These organisms, which are all notorious agents of nosocomial infections, require even higher RH_e values for growth. The increased numbers of bacteria from these two groups in the anterior nares of astronauts is probably related to a competitive advantage that these organisms have over *S. epidermidis* in a more moist environment. This would fit with the observation that *S. epidermidis* is comparatively more fit than *S. aureus* and various Gram-negative bacteria at slightly lower humidity values (~80-90% RH_e) (de Goffau *et al.* 2009).

Whether it is actually the local humidity or the possibly increased wetness of the nose mucosal lining that drives the changes in microbial flora is a matter of discussion. Motility experiments for example performed with *B. subtilis* in our lab seem to indicate that microgravity conditions are likely to increase the frequency at which this Gram-positive bacterium displays its swarming behaviour.

During these experiments 5 µl droplets of a *B. subtilis* cell suspension were transferred to blood agar plates, which were closed airtight and incubated at room temperature either in various orientations or in a random positioning machine (RPM) (Huijser 2000). Colonies on plates that were placed in the RPM or incubated in an upside-down orientation with the lid at the bottom (another "poor mans" version of microgravity) displayed swarming behaviour in ~50% of the cases while colonies on plates with the lid on top displayed this behaviour in only ~30% of all cases ($n \geq 200$ each orientation) (Fig. 4). An explanation for these observations was found when blood agar plates were incubated vertically instead. Droplets of *B. subtilis* transferred to the bottom half of these plates almost always showed swarming behaviour while those on the top half did not (Fig. 4).

The cause of this particular difference is that moisture sags down to the bottom half of these plates thereby creating a less viscous and water-rich environment that enables swarming. Moisture is simply more abundant at the surface of the plates grown in the RPM or with the lid on the bottom, which is a situation that is probably comparable with the situation at the mucosal lining of the nose of astronauts in space.

Other processes important in interspecies competitions, such as quorum sensing, secretion of proteins, excretion of metabolites and uptake of nutrients are likely also influenced by this altered state of hydration.

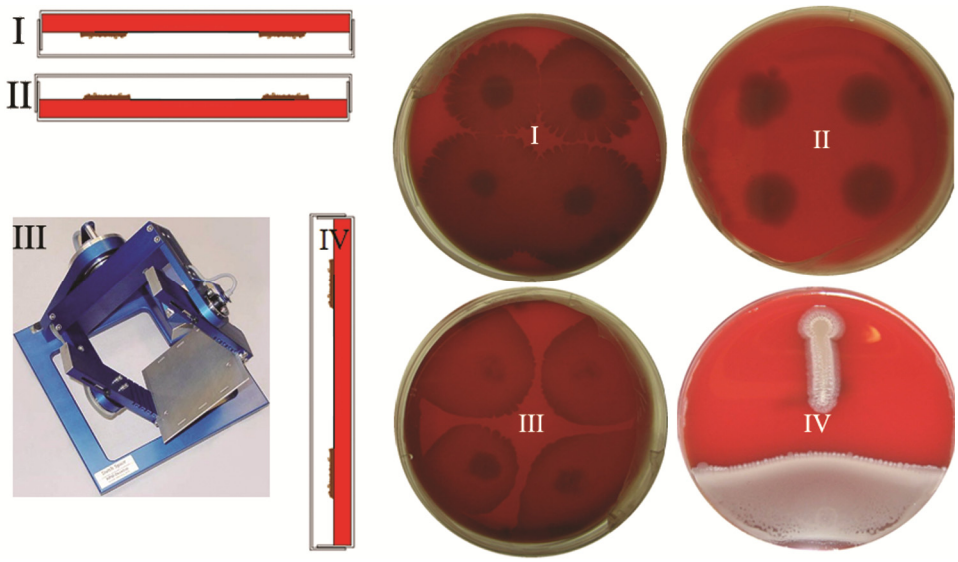

Figure 4. Effects of the orientation of agar plates on the swarming behavior of *Bacillus subtilis*. Droplets of a *B. subtilis* cell suspension (5 µl) were transferred to blood agar plates, which were incubated at room temperature in an upside down position (**I**), in a right side up position (**II**), in a random positioning machine (RPM, **III**), or in a vertical position (**IV**). The plated cells displayed swarming behavior in at least 50% of all such experiments on plates incubated upside down (**I**) and in the RPM (**III**). Swarming behavior was observed far less frequently (~30%) on plates incubated in the right side up position (**II**). When plates were incubated vertically, the *B. subtilis* droplets deposited on the bottom half almost always displayed swarming behavior while those deposited near the top did not (**IV**).

Discussion

The relationship of how the temperature distribution within a spacecraft directly determines the local RH_e should be kept in mind in the design of future spacecraft. As all parts of a spacecraft are intimately connected, any spot with high RH_e values will represent a potential microbial health hazard because it allows for the multiplication and potential dissemination of microorganisms. The identification of such microbial "hotspots" is in fact currently underway on a small scale in the Russian KPT-12/EXPERT experiment behind panels inside of the Zvezda service module (NASA 2010). Hygienic measures can be implemented more efficiently on the basis of a better understanding of the exact temperature distribution on board the ISS.

The impact of the correlation between radiation and desiccation resistance on board the ISS is currently largely unknown and definitely deserves further investigation. This correlation is likely to become even stronger on extended future space missions for example to Mars. However, on such extended missions the main focus concerning the protection from radiation should of course be on the crew, and how to improve the protective radiation shielding of such a spaceship.

Finally, the possible ecological shift caused by the cephalic fluid shift that increases the occurrence of opportunistic pathogens, such as *S. aureus*, within the nasal cavity could increase the incidence of infectious diseases, including the development of styes or boils (Taylor *et al.* 1977) during space missions. The same factors that are generally recognized as direct hazards for the health of astronauts, microgravity and radiation, thus also seem to increase the risk of infectious diseases indirectly by increasing the opportunities for microbial growth and/or survival and by possibly facilitating the selection for more pathogenic species.

Acknowledgments

The Random Positioning Machine was kindly provided by Jack J.W.A. van Loon of the Dutch Experiment Support Center (DESC) at the ACTA-VU-University, Amsterdam, and supported by the Netherlands Institute for Space Research (NWO-SRON).

Reference List

Bungo MW, Charles JB, Johnson PC, Jr. (1985) Cardiovascular deconditioning during space flight and the use of saline as a countermeasure to orthostatic intolerance. *Aviat.Space Environ.Med.* **56,** 985-990.

Castro VA, Thrasher AN, Healy M, Ott CM, Pierson DL (2004) Microbial characterization during the early habitation of the International Space Station. *Microb.Ecol.* **47,** 119-126.

Dadachova E, Casadevall A (2008) Ionizing radiation: how fungi cope, adapt, and exploit with the help of melanin. *Curr.Opin.Microbiol.* **11,** 525-531.

de Goffau MC, Yang X, van Dijl JM, Harmsen HJ (2009) Bacterial pleomorphism and competition in a relative humidity gradient. *Environ.Microbiol.* **11,** 809-822.

Decelle JG, Taylor GR (1976) Autoflora in the upper respiratory tract of Apollo astronauts. *Appl.Environ.Microbiol.* **32,** 659-665.

ESA (2008) 'European guide to low gravity platforms.'

Fredrickson JK, Zachara JM, Balkwill DL, Kennedy D, Li SM, Kostandarithes HM, Daly MJ, Romine MF, Brockman FJ (2004) Geomicrobiology of high-level nuclear waste-contaminated vadose sediments at the hanford site, washington state. *Appl.Environ.Microbiol.* **70,** 4230-4241.

Fredrickson JK, Li Sm, Gaidamakova EK, Matrosova VY, Zhai M, Sulloway HM, Scholten JC, Brown MG, Balkwill DL, Daly MJ (2008) Protein oxidation: key to bacterial desiccation resistance? *ISME J* **2,** 393-403.

Green CF, Scarpino PV, Gibbs SG (2003) Assessment and modeling of indoor fungal and bacterial bioaerosol concentrations. *Aerobiologia* **19,** 159-169.

Hansen DL (1999) Microbial contamination. In 'Indoor air quality issues'. pp. 45-48. Taylor & Francis: London

Huijser RH (2000) 'Desktop RPM: New small size microgravity simulator for the bioscience laboratory.'

Ilyin VK (2005) Microbiological status of cosmonauts during orbital spaceflights on Salyut and Mir orbital stations. *Acta Astronaut.* **56,** 839-850.

Johanssen S, Wadso L, and Sandin K. (2005) Microbial growth on buildings facades with thin rendering on thermal insulation. Royal Institute of Technology, Stockholm, Sweden.

Kaur I, Simons ER, Kapadia AS, Ott CM, Pierson DL (2008) Effect of spaceflight on ability of monocytes to respond to endotoxins of gram-negative bacteria. *Clin.Vaccine Immunol.* **15,** 1523-1528.

Lawrence MG (2005) The Relationship between Relative Humidity and the Dewpoint Temperature in Moist Air: A Simple Conversion and Applications. *Bulletin of the American Meteorological Society* **86,** 225-233.

Lstiburek J, Carmody J (1996) 'Moisture control handbook: Principles and practices for residential and small comercial buildings.' John Wiley & Sons: New York

Mastroleo F, Van HR, Leroy B, Benotmane MA, Janssen A, Mergeay M, Vanhavere F, Hendrickx L, Wattiez R, Leys N (2009) Experimental design and environmental parameters affect Rhodospirillum rubrum S1H response to space flight. *ISME.J.* **3,** 1402-1419.

Masumura K, Kuniya K, Kurobe T, Fukuoka M, Yatagai F, Nohmi T (2002) Heavy-ion-induced mutations in the gpt delta transgenic mouse: comparison of mutation spectra induced by heavy-ion, X-ray, and gamma-ray radiation. *Environ.Mol.Mutagen.* **40,** 207-215.

NASA. NASA ISS On-orbit Status Reports. 2010.

Novikova N, De BP, Poddubko S, Deshevaya E, Polikarpov N, Rakova N, Coninx I, Mergeay M (2006) Survey of environmental biocontamination on board the International Space Station. *Res.Microbiol.* **157,** 5-12.

Novikova ND (2004) Review of the knowledge of microbial contamination of the Russian manned spacecraft. *Microb.Ecol.* **47,** 127-132.

Oberg, J. Space Station: Internal NASA Reports Explain Origins of June Computer Crisis. IEEE Spectrum . 2007.

Qiu X, Sundin GW, Chai B, Tiedje JM (2004) Survival of Shewanella oneidensis MR-1 after UV radiation exposure. *Appl.Environ.Microbiol.* **70,** 6435-6443.

Rahman MS (2007) Water activity and food preservation. In 'Handbook of food preservation'. (Ed. MS Rahman) pp. 447-474. (Taylor & Francis: Boca Raton)

Samuel, E. Space station radiation shields 'disappointing'. New Scientist . 2002.

Sanders SW, Maxcy RB (1979) Isolation of radiation-resistant bacteria without exposure to irradiation. *Appl.Environ.Microbiol.* **38,** 436-439.

Shavers MR, Zapp N, Barber RE, Wilson JW, Qualls G, Toupes L, Ramsey S, Vinci V, Smith G, Cucinotta FA (2004) Implementation of ALARA radiation protection on the ISS through polyethylene shielding augmentation of the Service Module Crew Quarters. *Adv.Space Res.* **34,** 1333-1337.

Tallentire A (1980) The spectrum of microbial radiation sensitivity. *Radiation Physics and Chemistry (1977)* **15,** 83-89.

Taylor GR (1974) Recovery of medically important microorganisms from Apollo astronauts. *Aerosp.Med.* **45,** 824-828.

Taylor GR, Graves RC, Brockett RM, Ferguson K, Mieszkuc J (1977) Skylab environmental and crew microbiology studies. In 'Biomedical results from Skylab'. (Eds RS Johnston and LF Dietlein) (Scientific and Technical Information Office, National Aeronautics and Space Administration: Washington)

van Tongeren S, Raangs G, Welling G, Harmsen H, Krooneman J (2006) Microbial detection and monitoring in advanced life support systems like the international space station. *Microgravity Science and Technology* **18,** 219-222.

Chapter 7

Summary and general discussion

The availability of water, which can be best expressed in terms of equilibrium relative humidity (RH_e) or water activity (a_w), is one of the most critical parameters for microbial growth. Unlike in plants, the microbial mechanisms of adaptation to water-limited environments were poorly understood when the research described in this thesis was initiated. While it was known that microorganisms can adapt to low RH_e/a_w values by accumulating high concentrations of compatible solutes (Csonka, 1989), very little was known about other mechanisms of adaptation, such as changes in cell morphology and cell wall composition. Also, the underlying physical principles had hardly been addressed. This related to the difficulties in studying these parameters in controlled non-liquid environments, and to the fact that the mechanisms of microbial cell shape maintenance have only been elucidated in recent years.

A simple but efficient manner of creating a RH_e on a surface-to-air interface is described in *Chapter 2*. Using a selection of eight saturated salts in a 96-wells plate, a RH_e gradient was created with which the response of various microbial species to reduced water availability was studied. Not only were RH_e growth limits determined, which was the initial purpose of this setup, but distinct differences in morphology and growth patterns were observed as well. Gram-positive cocci increased in cell size as they approached humidity growth limits and staphylococcal species started growing in tetrad/cubical formations instead of their normal grape-like structures. Their cell walls were furthermore shown to

increase in thickness using transmission electron microscopy. Gram-negative rods displayed wave-like patterns, forming larger waves as they became increasingly filamentous at low humidity. At decreasing RH_e values, the Gram-positive rod *Bacillus subtilis* initially displayed the same patterns as Gram-negative rods and was even found to grow in filamentously coiled superstructures (illustrated in *Chapter 4*). At even lower RH_e values, *Bacillus subtilis* became shorter, curved, and eventually almost coccoid. Moreover, *B. subtilis* started to sporulate near its RH_e growth limit. In contrast, the formation of spores ceased in fungal species as they no longer formed asci near their RH_e growth limit. Comparable with various bacterial morphological changes, their hyphae were found to become rounder and much thicker near this limit.

The observed changes in morphology of *B. subtilis* were subsequently shown to be completely reversible using time-lapse microscopy (*Chapter 3*) showing that these changes are in fact most likely adaptations that allow this microorganism to grow optimally under conditions of reduced water availability. The proteomics analyses described in *Chapter 3* subsequently revealed a strong induction of many σ^B-regulated stress-responsive proteins.

Three groups of differentially regulated proteins were identified. One group is involved in regulating intracellular osmotic values through the accumulation of compatible solutes. The second group of regulated proteins modulates changes in cell wall composition, which is likely to be linked with the observed morphological adaptations. The last and largest group of differentially regulated proteins however is involved in combating the detrimental effects of oxidative stress. Deletion mutants lacking the *sigB* gene or the σ^B-regulated catalase *katE* gene were severely impaired in the adaptation to low RH_e values, indicating a need for *B. subtilis* to protect itself against self-inflicted oxidative stress under water-limited growth conditions.

A common theme in the observed morphological adaptations to limited water availability seems to be the need to reduce the cells' surface to volume ratio. A single cell can achieve this by becoming larger, thicker and rounder, and a group of cells by clumping together. This would help to minimise the rate of water loss

via evaporation at low RH_e values. The observed increases in cell wall thickness in staphylococci furthermore add credence to this view (*Chapter 2*). The fact that cells need to be able to remodel their cell walls in order to grow and divide places yet another set of constraints on the cell wall. Autolysins play a major role in the remodeling process of cell walls as they can digest cell-wall peptidoglycan.

Peptidoglycan is a polymer of amino sugars cross-linked by short peptides, which forms a covalent matrix that surrounds the cytoplasmic membrane and constitutes the major skeletal component of the cell wall. It is critical in maintaining cell shape and in preventing osmotic lysis under hypotonic conditions (Smith *et al.*, 2000). The cleavage of peptidoglycan bonds is facilitated by any kind of physical tension on the bonds of the cell wall, such as turgor, as the energy required for hydrolysis of a peptidoglycan bond is inversely related to how much stress it bears (Koch, 1988). A hypotonic or a high RH_e environment thus facilitates the tasks of autolysins in cellular processes, such as cell growth, cell-wall turnover, peptidoglycan maturation and cell division. Low RH_e values however represent a 'hypertonic environment' as water is less easily acquired or even lost instead of gained in such a 'dry' environment.

The difference between the external and internal osmotic pressure, or more precisely the water potential difference ($\Delta\Psi$), which can be calculated directly from the external RH_e and internal a_w respectively (*Chapter 4*), directly determines the amount of turgor and thus the amount of physical stress on the bonds of a cell wall (Fig. 1). The only way in which some measure of turgor is maintained in an environment where the external water potential is lower than the internal water potential, indicated by (-) in Fig. 1, is by generating more water metabolically than the rate in which it is lost to its environment. Growth no longer occurs once the rate of water loss exceeds the rate in which it can be produced metabolically (RH_e growth limit). The turgor at this point has finally become equal to zero.

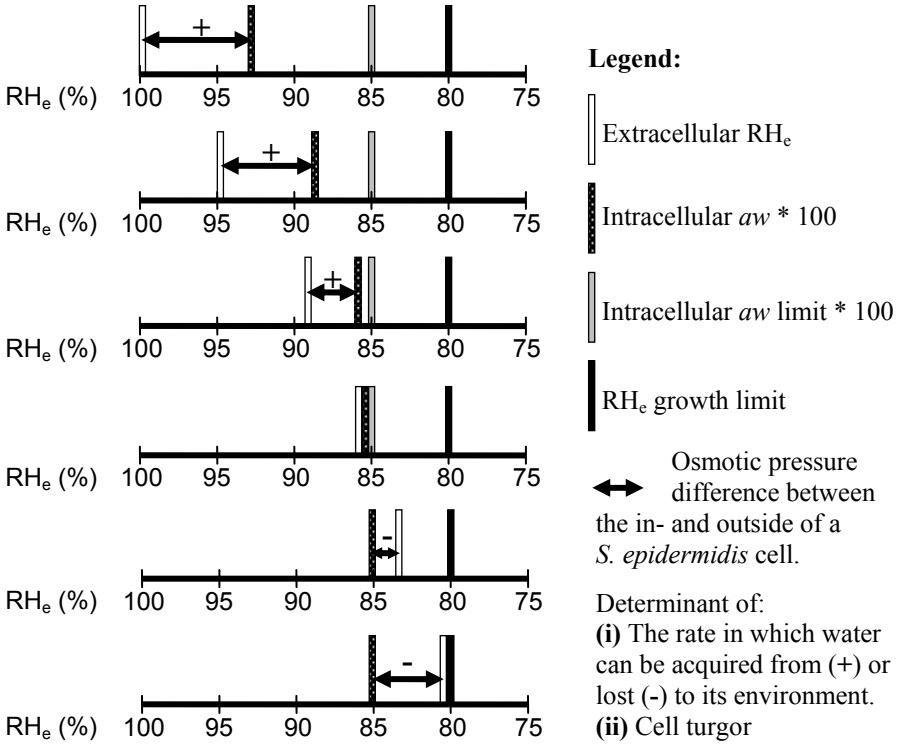

Figure 1. Example of the internal a_w development of *S. epidermidis* grown in a RH_e gradient in relation to the osmotic pressure difference between the inside and outside of a cell. The extracellular RH_e is controlled directly in a RH_e gradient and the RH_e growth limit can be measured by microscopic inspection of cell growth. Exact values of the intracellular a_w are unknown unless they become equal to the intracellular a_w limit of an organism.

The growth rate-limiting factor of a microorganism at low RH_e values is the rate in which it can accumulate water. This rate is, in turn, dependent upon the rate in which a microorganism can produce water by metabolizing carbohydrates, and by how well it can minimise the rate of water loss via evaporation. It thus makes sense for a microorganism to uncouple the catabolic and anabolic rates at low RH_e values as water production instead of energy production is becoming an increasingly important goal of catabolism. Thus, the apparently increased level of self-inflicted oxidative stress in *B. subtilis* cells growing at low RH_e could very

well be due to this disequilibrium between anabolism and catabolism since an increased transfer of electrons to oxygen is likely to give rise not only to water but also to detrimental reactive oxygen species (Ballesteros *et al.*, 2001). The oxidative damage of proteins and other important cellular compounds continues or even increases when the cells start to 'burn up' carbohydrates in order to produce water, whereas the anabolic rate (synthesis of e.g. new proteins) and the growth rate in general are slowed down to a crawl at low RH_e values.

Notably, cellular processes such as cell growth, cell-wall turnover, peptidoglycan maturation and cell division are increasingly more difficult to perform by autolysins in a RH_e gradient as the turgor decreases concomitantly with the RH_e. Cells thus need to find ways of increasing the mechanical stress on their cell wall bonds in order for autolysins to productively cleave the peptidoglycan. A solution to this problem is to divide the remaining turgor over a smaller number of bonds within the peptidoglycan cytoskeleton. In other words, to create a weaker, less cross-linked cell wall. It is shown in *Chapter 4*, using fluorescently labelled vancomycin, that both *S. epidermidis* and *B. subtilis* do indeed generate less cross-linked cell walls, by leaving a higher fraction of the peptidoglycan pentapeptide side chains unconnected. In addition it is shown that both species employ specific morphological tricks to increase the stress on their cell wall bonds even further. *S. epidermidis* does so by becoming larger, as the stress borne per individual bond is directly proportional to the product of the radius of a cell and its turgor pressure (Koch, 1988). Fig. 2 summarizes the changes in physiology of *S. epidermidis* in response to low RH_e values.

B. subtilis increases the stress on its cell wall using an even more ingenious method. By twisting and turning and growing in coiled superstructures, this bacterium creates a rotational torque (Daniel and Errington, 2003), which adds yet another source of physical stress on the bonds of the cell wall. The generation of rotational torque might be a way for *B. subtilis* to compensate for the loss of turgor and concomitantly for the loss of autolytic activity, which is required for the growth and division of cells via cell wall remodeling.

Eventually, the rotational torque will no longer provide enough additional stress. Once this point is reached in a RH_e gradient, *B. subtilis* will again start weakening its cell wall, which will cause its structural integrity to become insufficient for maintaining its rod-like (optimal) shape. The consequence of this is that cells will assume a more globular shape as was observed in the different studies described in this thesis.

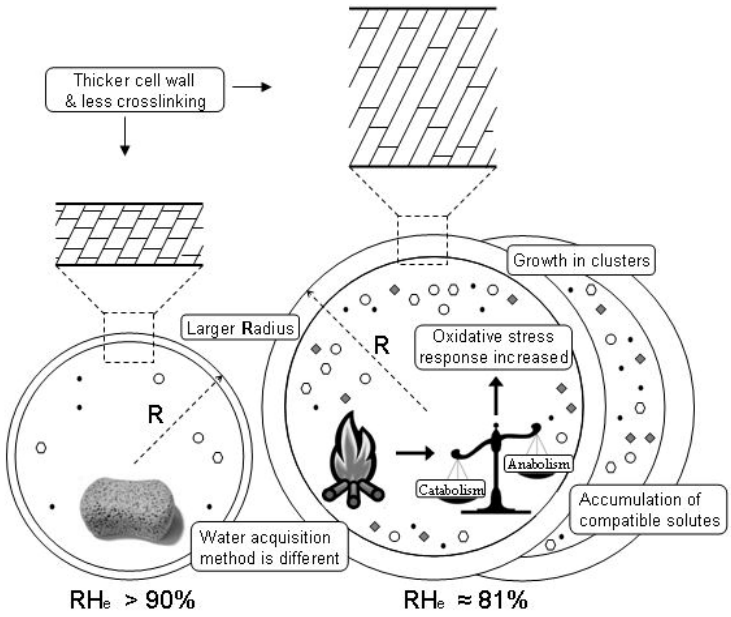

Figure 2. Physiological differences between *Staphylococcus epidermidis* ATCC 35984 grown at high and at low RH_e values. Staphylococcal cells reduce their surface to volume ratio by becoming larger, by growing in clusters and by having a thicker cell wall at lower RH_e values in order to minimize the rate of water loss via evaporation. Even though water is being lost at RH_e values slightly above the RH_e growth limit, a low turgor level is maintained by generating water metabolically. The remaining level of stress on the cell wall is amplified by creating a less cross-linked cell wall, and an increased cell radius also helps in this respect. At the RH_e growth limit, the accumulation of compatible solutes is not sufficient anymore to lower the internal water potential below the external water potential. Consequently, the required water is generated metabolically, thereby causing an imbalance between catabolism and anabolism that leads to elevated levels of oxidative stress.

The temperature/RH_e (T/RH_e) gradient technique based on the use of an environmental control chamber as described in *Chapter 4* is far more complex and has more controllable variables than the 96-well's RH_e gradient of *Chapter 2*. In this setup, a temperature gradient in combination with a controlled average temperature and relative humidity within a closed compartment creates a precisely controlled RH_e gradient on top of the temperature gradient. The advantage of the 96-well's RH_e gradient over the environmental control chamber is that it has a much higher throughput since 96-well's plates are not hard to come by. The simplicity and low cost furthermore make the 96-well's RH_e gradient a very suitable tool for educational purposes. On the other hand, the T/RH_e gradient technique is superior in its RH_e control/precision and in creating any kind of desired RH_e gradient as it is not limited by a limited selection of saturated salts.

The first objective of the T/RH_e gradient technique was to mimic the way in which RH_e gradients occur on surface-to-air interfaces in closed systems, such as neonatal incubators (*Chapter 5*) or on the cabin of the International Space Station (ISS) (*Chapter 6*). The second objective was to calculate the intracellular water activity limit (Fig. 1) of species by measuring their RH_e growth limits at different water diffusivity values. This can be efficiently achieved in this system by using different barometric pressure values as the diffusivity of water is inversely related to the barometric pressure (Smith and Geller, 1979). A higher diffusivity of water (low pressure) leads to a less low RH_e growth limit as it causes increased rates of evaporation while the maximum production of metabolically produced water remains the same. The mathematics needed for these calculations are described in detail in *Chapter 4*.

Demonstrating the existence of the intracellular water activity limit was a crucial part of the explanations for the changes in morphology, cell wall composition and oxidative stress, but was also shown to be a physiological turning point for other important factors. As the RH_e decreases and approaches the intracellular a_w limit of a cell, the rate of absorption of water from the air will become lower. To counteract this, it is shown in *S. epidermidis* 35984 (*ica* +) that its cells become more hydrophilic as the RH_e approaches the intracellular a_w

limit, and that this increase subsides again when the RH_e has passed this limit (*Chapter 4*). A higher level of hydrophilicity is likely useful to attract water at a faster rate as long as the internal water potential (Ψ) is lower than the external Ψ, but this will most likely become useless when the reverse is true. Biofilm formation was furthermore correlated with hydrophilicity as these patterns were not observed in *S. epidermidis* 12228 (*ica* -), a non-biofilm forming strain.

Another more directly clinical relevant factor was the increase in vancomycin resistance in staphylococci (*Chapter 2*). This antibiotic normally binds to the uncross-linked pentapeptide side chains of peptidoglycan, which are normally cross-linked by penicillin-binding proteins, where and when this is needed (Hiramatsu, 2001). At low RH_e values the cell wall is becoming much thicker and less cross-linked, providing many more potential sites for vancomycin to bind to before its saturation of the peptidoglycan becomes so high that further cell growth is precluded.

Importantly, the physiological characteristics of microorganisms growing at low humidity are in many cases more ecologically relevant, and sometimes even more clinically relevant than their textbook appearance at high humidity as their natural habitats are often drier than the standard environments they usually encounter in the lab. The most clinically relevant aspect of a microorganism in relation to the availability of water however remains its RH_e growth limit as this factor can be used to predict its ability to grow on a specific surface.

The ecological theory that was behind the RH_e gradient described in *Chapter 4*, namely that microbial growth occurs only on surfaces where the temperature is low enough in comparison to the rest of the environment so that the local RH_e is high enough to permit growth, was verified in *Chapter 5* by investigating the sites of microbial contamination in neonatal incubators. Apart from having a very high clinical relevance, this study demonstrated the importance of this ecological theory in predicting the occurrence of microbial growth in an actual ecological setting. The temperature distribution of the interior of a neonatal incubator was mapped with an infrared thermometer to identify local cold spots on which the local RH_e might be elevated enough for the

occurrence of microbial growth. A large difference in the amount of microbial contamination was indeed found between the samples taken from such cold sites (with RH_e values > 80%) and samples taken from relatively warmer sites (RH_e << 80%). Especially staphylococci were found to take advantage of local cold spots. This is not surprising as species such as *S. epidermidis*, one of the most xerotolerant human skin commensals (Otto, 2009), requires RH_e values above 80% in order to grow. It can grow thus grow at the 80-91% RH_e range where many other bacteria are incapable of growing and likely has a competitive advantage over most other bacteria below 94% *(Chapter 2)*.

Coagulase-negative staphylococci, such as *S. epidermidis*, are the main cause of sepsis in neonates (Stoll *et al.*, 1996) and as such this finding is potentially of major clinical relevance. The most premature and vulnerable neonates lie in incubators with the highest average temperature and RH values. These incubators have the highest numbers of niches with RH_e values above 80% and, according to the theory, they represent the highest risk for the development of neonatal sepsis. In view of the potential health hazard for neonates it will be important to investigate this correlation in more detail in future studies. In the meantime it is preferable to use the identification of local cold spots as hotspots for microbial contamination to improve certain basic hygienic measures, and to improve the design of neonatal incubators in such a way that the number of cold spots is minimized.

Finally, *Chapter 6* builds on several of the concepts developed in the previous chapters to review the possible importance of microgravity and increased levels of radiation in relation to the availability of water and the occurrence of microbial growth in spacecraft. Thermally induced convection does not occur under microgravity conditions and, consequently, larger temperature differences between surfaces are expected to occur in spacecraft. This will lead to a potential increase in the number of niches where the RH_e is high enough for microbial growth to take place. In other words, microgravity will cause an increased heterogeneity of the temperature on board, which will lead to higher risks for microbial contamination.

In addition, increased radiation levels possibly select for microorganisms with enhanced desiccation resistance (Dadachova and Casadevall, 2008; Fredrickson *et al.*, 2004) as both stressors share the same molecular resistance mechanisms; a robust DNA repair capability and a strong oxidative stress response (Fredrickson *et al.*, 2008).

It should be noted that microgravity does not only affect the environment of the spacecraft crew, but also the microbiological niches represented by the crew members themselves, especially their noses. While the pumping action of the human heart causes sufficient amounts of fluids to be pumped up towards the brain on earth, this upward pumping of fluid becomes excessive in micro-gravity conditions thereby causing a puffed up face and a continually stuffy nose. The nose is thus turned into a more humid/moist micro-environment, possibly facilitating the selection of more pathogenic species which require higher RH_e values. Because of this, *Staphylococcus aureus*, with a RH_e growth limit of 87%, for example might be favoured over *S. epidermidis* (81%) (Decelle and Taylor, 1976; Taylor, 1974). Increased awareness of these possible relationships will allow a minimization of the microbial risks imposed on astronauts, which is important because astronauts are likely to be temporarily immunocompromised due to the direct effects of microgravity and radiation.

Notably, the cephalic fluid shift that affects astronauts might be equally important in patients who are bedridden for lengthy periods of time as they experience the same symptoms. Several studies suggest that bedridden patients are at a higher risk of developing aspiration pneumonia and that this is associated with a higher prevalence of *Staphylococcus aureus*, *Pseudomonas aeruginosa* and several other Gram negative bacteria (Michishige *et al.*, 1999; The committee for The Japanese Respiratory Society guidelines in management of respiratory infections, 2004). It should therefore perhaps be investigated whether it is recommendable for patients to be in an upright sitting position more frequently during long hospital stays, and whether this would indeed reduce the incidence of pathogenic species within the oral and nasal cavities.

In conclusion microorganisms are not simply rod- or sphere-like objects with fixed characteristics, but they are dynamic entities with a highly adaptable and flexible physiology. This flexibility is dearly needed as it is rare for a microorganism to inhabit an environment with constant optimal conditions. Something is always lacking and in closed environments this something is usually water. On a macroscopic scale the availability of water determines whether and what kind of microbial growth is possible, but it is also a determinant of microbial physiology on a cellular level. A mathematical/physical approach as employed in this thesis has led to exciting new ideas and concepts and has identified critical environmental parameters, which can now be used in clinically relevant environments, such as neonatal incubators for the improvement of basic hygienic measures. For example, in order to predict where microbial growth is most likely to occur within a given environment, one must look out for the cold spots and not for hot spots. These very same concepts also explain why molds are so often found to decorate the walls of bathrooms and why certain attics or basements have a rich musty smell. Improper insulation and or ventilation in combination with sufficiently high humidity levels and large enough temperature differences are usually to blame. The observed changes in the physiology of microorganisms on a cellular level are furthermore not only visually fascinating, but they also represent a real challenge in terms of the underlying mathematical/physical principles. The adaptations to low RH_e values as documented in this thesis sometimes create the most beautiful microbial landscapes, but the real art lies in understanding these changes.

Reference List

Ballesteros,M., Fredriksson,A., Henriksson,J., and Nystrom,T. (2001) Bacterial senescence: protein oxidation in non-proliferating cells is dictated by the accuracy of the ribosomes. *EMBO J* **20:** 5280-5289.

Csonka,L.N. (1989) Physiological and genetic responses of bacteria to osmotic stress. *Microbiol Rev* **53:** 121-147.

Dadachova,E. and Casadevall,A. (2008) Ionizing radiation: how fungi cope, adapt, and exploit with the help of melanin. *Curr Opin Microbiol* **11:** 525-531.

Daniel,R.A. and Errington,J. (2003) Control of Cell Morphogenesis in Bacteria: Two Distinct Ways to Make a Rod-Shaped Cell. *Cell* **113:** 767-776.

Decelle,J.G. and Taylor,G.R. (1976) Autoflora in the upper respiratory tract of Apollo astronauts. *Appl Environ Microbiol* **32:** 659-665.

Fredrickson,J.K., Zachara,J.M., Balkwill,D.L., Kennedy,D., Li,S.M., Kostandarithes,H.M. *et al.* (2004) Geomicrobiology of high-level nuclear waste-contaminated vadose sediments at the hanford site, washington state. *Appl Environ Microbiol* **70:** 4230-4241.

Fredrickson,J.K., Li,S.m., Gaidamakova,E.K., Matrosova,V.Y., Zhai,M., Sulloway,H.M. *et al.* (2008) Protein oxidation: key to bacterial desiccation resistance? *ISME J* **2:** 393-403.

Hiramatsu,K. (2001) Vancomycin-resistant Staphylococcus aureus: a new model of antibiotic resistance. *Lancet Infect Dis* **1:** 147-155.

Koch,A.L. (1988) Biophysics of bacterial walls viewed as stress-bearing fabric. *Microbiol Rev* **52:** 337-353.

Michishige,F., Yoshinaga,S., Harada,E., Hirota,K., Miyake,Y., Matsuo,T., and Yasuoka,S. (1999) Relationships between activity of daily living, and oral cavity care and the number of oral cavity microorganisms in patients with cerebrovascular diseases. *J Med Invest* **46:** 79-85.

Otto,M. (2009) Staphylococcus epidermidis--the 'accidental' pathogen. *Nat Rev Microbiol* **7:** 555-567.

Smith,T.J., Blackman,S.A., and Foster,S.J. (2000) Autolysins of Bacillus subtilis: multiple enzymes with multiple functions. *Microbiology* **146 (Pt 2):** 249-262.

Smith,W.K. and Geller,G.N. (1979) Plant transpiration at high elevations: Theory, field measurements, and comparisons with desert plants. *Oecologia* **41:** 109-122.

Stoll,B.J., Gordon,T., Korones,S.B., Shankaran,S., Tyson,J.E., Bauer,C.R. *et al.* (1996) Late-onset sepsis in very low birth weight neonates: a report from the National Institute of Child Health and Human Development Neonatal Research Network. *J Pediatr* **129:** 63-71.

Taylor,G.R. (1974) Recovery of medically important microorganisms from Apollo astronauts. *Aerosp Med* **45:** 824-828.

The committee for The Japanese Respiratory Society guidelines in management of respiratory infections (2004) Aspiration pneumonia. *Respirology* **9:** 35-37.

Nederlandse samenvatting

Op aarde is de beschikbaarbheid van water één van een van de meest cruciale factoren voor microbiele groei. Deze parameter is daarom uitermate relevant als het gaat om zaken zoals hygiëne of de houdbaarheid van voedsel. Aan boord van een permanent bewoond ruimtestation, zoals het International Space Station (ISS), is een goede controle van de waterbeschikbaarheid voor microbiële groei wellicht nog belangrijker voor de hygiëne dan op aarde, aangezien potentieel pathogene bacterien niet alleen de gezondheid van astronauten kunnen bedreigen maar ook omdat microbiële groei het ruimtestation zelf kan aantasten. Hierdoor zijn in het verleden ook al gevaarlijke situaties ontstaan, vooral in het russische ruimtestation MIR. Daar komt nog bij dat het immuunsysteem van astronauten bij langdurig verblijf in de ruimte zwakker wordt. Het doel van dit proefschrift was om factoren te identificeren, waarmee voorspeld kan worden welke microben op welke plekken kunnen groeien in afgesloten compartimenten waarin mensen zich voor langere tijd bevinden. Dit is in detail onderzocht voor het ruimtestation ISS en voor couveuses die gebruikt worden voor de zorg aan premature neonaten in het Universitair Medisch Centrum Groningen.

De relatieve luchtvochtigheid (RH) of de water activiteit van een object (a_w) zijn zeer geschikte termen om de beschikbaarheid van water voor microbiele groei in uit te drukkken. Als men in een gesloten systeem (een doos) de RH constant houdt op 50% en daarin een blokje hout plaatst, dan zal de a_w aan het oppervlak van dit blokje hout uiteindelijk gelijk worden aan de RH gedeeld door honderd (= 0,5). Aan de hand van de a_w van een object kan men vervolgens voorspellingen doen welke microorganismen op of in een dergelijk object zouden kunnen groeien. Schimmels hebben bijvoorbeeld meestal a_w waardes van boven de 0,7 nodig, bij Gram-positieve bacteriën is 0,8 of meer vereist en Gram-negatieve bacteriën hebben minstens a_w waardes van 0,9 nodig (meestal zelfs hoger). Aan de hand van het vochtgehalte van een object (g/m^3) valt dit niet te voorspellen aangezien het type materiaal bepaalt hoe stevig het water

"gebonden" is, waardoor het water in meer of mindere mate vrij beschikbaar is om opgenomen te worden door microorganismen.

De relatieve luchtvochtigheid (RH) van een gesloten ruimte kan ook beïnvloed worden door hier een object in te plaatsen, dat een bepaalde wateractiviteit (a_w) heeft. Als het object maar groot genoeg is ten opzichte van de ruimte waarin het geplaatst wordt, dan zal de RH uiteindelijk gelijk worden aan de a_w keer honderd. Voor het onderzoek dat in dit proefschrift beschreven wordt is gebruik gemaakt van verzadigde zoutoplossingen om de RH te beïnvloeden. Het idee hierachter is dat puur water een a_w heeft van 1 (en dus zou zorgen voor een RH van 100% in een gesloten systeem). Als men hieraan zouten toevoegt, dan zullen de zout-ionen de polaire watermoleculen in meer of mindere mate binden, waardoor ze minder vrij kunnen bewegen (minder beschikbaar zijn). Dit heeft als gevolg dat de a_w van een zoutoplossing lager wordt dan 1. Als men een verzadigde zoutoplossing maakt van een bepaald zout, dan bevat deze oplossing bij een constante temperatuur een constante concentratie aan zout-ionen. De rest van het onopgeloste zout blijft in dit geval over in een gekristalliseerde vorm. Als water uit deze oplossing verdampt zullen er zout-ionen uitkristalliseren en als er water wordt toegevoegd aan de oplossing lossen er juist weer zoutkristallen op. Hierdoor blijft de zoutconcentratie van een verzadigde zoutoplossing altijd gelijk en blijft de a_w van een verzadigde zoutoplossing altijd constant. Door het juiste zout te kiezen kan iedere gewenste relatieve luchtvochtigheid boven de desbetreffende geconcentreerde zoutoplossing gecreëerd worden.

In hoofdstuk 2 van dit proefschrift wordt een techniek beschreven waarbij een relatieve luchtvochtigheidsgradient ingesteld wordt door 8 verschillende verzadigde zoutoplossingen te pipetteren in de verschillende rijen van een 96-wells plaat. Het deksel van deze 96-wells plaat, dat gecoat is met een agar voedingsbodem, wordt hier bovenop geplaatst zodat de RH per welletje met zoutoplossing vervolgens de a_w van de agar recht boven zich bepaald. Op de hierdoor ontstane a_w gradiënt kan men vervolgens de invloed testen van de beperkte beschikbaarheid van water op afzonderlijke micro-organismen door deze van te voren te inoculeren op de agar voedingsbodem. In hoofdstuk 2 staan

diverse morfologische veranderingen van verschillende bacteriesoorten beschreven, welke er grotendeels op neerkomen dat micro-organismen de neiging hebben hun oppervlakte/volume ratio te minimaliseren bij lage RH/a_w. Dit kan bijvoorbeeld bereikt worden door rondere vormen aan te nemen, door grotere individuele cellen te vormen of door geclusterd te groeien. Bovendien passen bacteriën zich aan om zo goed mogelijk water vast te kunnen houden door bijvoorbeeld dikkere celwanden aan te leggen. Dit laatste heeft als indirect effect dat de bacteriën ook meer resistent worden tegen bepaalde antibiotica.

In hoofdstuk 3 van dit proefschrift wordt dieper in gegaan op de aanpassingen van bacteriële cellen aan een lage relatieve luchtvochtigheid. Voor deze studie is *Bacillus subtilis* gebruikt, een staafvormige Gram-positieve sporulerende bacterie, waarover al zeer veel bekend is. Dit laatste maakt het mogelijk om analyses te doen op het niveau van de eiwitten die onder verschillende condities door de bacteriën gesynthetiseerd worden (proteomics). In de onderhavige studies is onderzocht welke eiwitten *B. subtilis* in meer of mindere mate aanmaakt bij een lage RH. Drie verschillende types van veranderingen vielen hierbij op.

Ten eerste produceert *B. subtilis* bij lage RH meer eiwitten die belangrijk zijn bij het produceren van sterk polaire/geladen stofjes welke enkel als doel hebben om de interne osmotische waarde van *B. subtilis* te verhogen. Hierdoor kan een *B. subtilis* cel bij lage RH waarden alsnog water aantrekken of is deze in ieder geval beter in staat om water vast te houden. Ofwel, *B. subtilis* brengt zijn interne a_w waarde omlaag als de RH/a_w van zijn omgeving ook omlaag gaat. Het tweede type verandering had te maken met eiwitten die betrokken zijn bij de synthese van celwandmateriaal. Dit valt goed te rijmen met de waargenomen morfologische veranderingen van *B. subtilis* onder deze omstandigheden, zowel qua vorm als qua celwand samenstelling. De laatste waargenomen verandering was dat *B. subtilis* bij lage RH enorm lijkt te lijden onder oxidatieve stress. *B. subtilis* probeert dit zo goed mogelijk tegen te gaan door enzymen te produceren die deze stress kunnen wegnemen, zoals bijvoorbeeld de katalases die waterstofperoxide kunnen omzetten in water en zuurstof. Dat de oxidatieve stress

onder deze condities potentieel dodelijk is werd aangetoond met bepaalde *B. subtilis* mutanten zonder een bepaalde katalase (KatE). Deze mutanten bleken niet meer in staat te zijn om te groeien bij RH-waarden waarbij wildtype cellen nog wel konden groeien. De oorzaak van deze oxidatieve stress valt mogelijk te zoeken in een veranderd metabolisme bij lage RH. Normaal gesproken kan een bacterie aan water komen door dit aan zijn omgeving te onttrekken. Wanneer echter de RH/100 of de a_w van zijn omgeving lager wordt dan zijn eigen interne a_w waarde kan hij alleen nog maar water verliezen. Mogelijk kan een bacterie dit verlies aan water alsnog compenseren door het metabool d.m.v. verbranding zelf te produceren. Zolang de cel maar meer water produceert dan hij verliest zou hij moeten kunnen groeien.

Onder condities waarbij voldoende water beschikbaar is dient verbranding van voedingsstoffen door een bacterie voornamelijk om de energie te produceren die benodigd is voor groei en celdeling. Bij lage luchtvochtigheid lijkt deze geproduceerde energie slechts groei mogelijk te maken bij de gratie van het bijproduct water, dat onder die condities essentieel is voor die groei van een cel. Er ontstaat hierdoor een onbalans tussen katabolisme en anabolisme. Deze onbalans is wellicht de oorzaak van de verhoogde oxidatieve stress die de cellen ondervinden bij een lage RH.

In hoofdstuk 4 wordt dieper ingegaan op het thema dat cellen mogelijk nog kunnen groeien in een omgeving waar de externe RH/100 of a_w lager is dan hun interne a_w zolang ze maar genoeg water kunnen produceren. Dit wordt in hoofdstuk 4 aangetoond in experimenten met *B. subtilis* en *Staphylococcus epidermidis*, een Gram-positieve kokken soort. Voor dit onderzoek werden deze bacteriën gekweekt in een geavanceerd RH–gradiëntsysteem, waarin de barometrische druk verlaagd kan worden naar 0,5 atmosfeer. Het idee hierachter is dat de verdampingssnelheid van water omgekeerd evenredig is met de luchtdruk. Bij een half atmosfeer zal water dus 2 keer zo snel uit cellen kunnen verdampen wanneer de externe RH/100 lager is dan de interne a_w van de cel. Gesteld dat een cel zijn interne a_w kan verlagen naar 0,85 en kan doorgroeien tot een externe a_w van 0,80 (80% RH), dan verliest deze cel bij externe a_w waarden

lager dan 0,80 meer water dan hij kan produceren waardoor hij niet verder kan groeien. Bij een a_w van 0,81 verliest zo'n cel ook water aan zijn omgeving, maar hij kan dan nog net genoeg water produceren waardoor hij nog net kan groeien, zij het zeer langzaam. Als nu echter de druk verlaagd wordt naar 0,5 atmosfeer dan verliest de cel bij een externe a_w van 0,81 twee keer zo snel water als bij 1 atmosfeer. Het gevolg hiervan is dat de cel bij een externe a_w van 0,81 bij 0,5 atmosfeer niet meer kan groeien. Bij 0,5 atmosfeer zal de externe a_w groeilimiet van deze cel dus omhoog gaan naar ongeveer 0,825 (+/- tussen 0,80 en 0,85 in).

Een ander aspect dat beschreven wordt in hoofdstuk 4 is hoe de druk op een bacteriële celwand van binnenuit (de turgor) de samenstelling van de celwand bepaalt. Normaal gesproken is de druk die op een celwand staat evenredig met het verschil betreffende de beschikbaarheid van water tussen de binnenkant en de buitenkant van een cel. Als de externe RH gelijk is aan 100% en de interne a_w van een cel gelijk is aan 0,95, dan zal de turgor van een cel ongeveer gelijk zijn aan de turgor van een cel met een interne a_w van 0,90 die zich in een omgeving bevindt met een RH gelijk aan 95%. Een cel die echter in een omgeving geplaatst wordt met een RH van 87% zal minder turgor hebben dan de voorgaande voorbeelden indien hij zijn interne a_w bijvoorbeeld niet lager kan krijgen dan 0,85. Bij een RH van 82% zal de turgor helemaal zeer klein zijn aangezien de enige vorm van druk die dan nog op de celwand staat gelijk is aan het verschil tussen de hoeveelheid water die een cel metabool kan generen en de hoeveelheid water die een cel verliest aan zijn omgeving. Cellen hebben de turgor-druk op hun celwand echter nodig om zich goed te kunnen delen. Hoe meer druk er op de verbindingen in hun celwand staat, hoe makkelijker deze verbindingen tijdelijk verbroken kunnen worden, zodat de cel zich wat kan uitrekken.

Als de druk op de celwand (turgor) dus wegvalt dan kunnen cellen zich moeilijker kunnen delen. Een mogelijke oplossing hiervoor is om, wanneer de turgor laag is, een celwand te creëren waarin minder verbindingen zitten. Hierdoor verdeelt de resterende turgor zich over een kleiner aantal verbindingen, waardoor de stress per verbinding weer toeneemt en deze gemakkelijker tijdelijk verbroken kan worden voor de celgroei. De celwand zelf bestaat onder andere uit

een groot peptidoglycaan polymeer dat in meer of mindere mate met zichzelf verbonden is met zijbruggen, zoals de mazen in een net. Wanneer zo'n zijbrug ongebonden is kan men hieraan een fluorescente probe binden. Experimenteel is er in *S. epidermidis* vastgesteld dat deze zijn celwand daadwerkelijk "zwakker" lijkt te maken bij lage luchtvochtigheid door meer van dit soort zijbruggen ongebonden te laten, zodat de mazen van het 'celwandnet' groter worden.

De geavanceerde relatieve luchtvochtigheidgradiënt-techniek beschreven in hoofdstuk 4 is tevens ook ontwikkeld als een ecologisch model systeem voor zowel het ISS als voor couveuses (hoofdstukken 5 & 6). Dit systeem bestaat uit een luchtdicht kastje, waarin een relatieve luchtvochtigheidgradiënt wordt gecreëerd door het aanleggen van een temperatuurgradiënt. Deze temperatuur-gradiënt wordt gegenereerd met behulp van twee peltier elementen (thermo-electrische koel/verwarmingselementen), die met elkaar verbonden zijn door middel van een koperen plaat. Door de stroomrichting in een peltier element in te stellen kan men deze laten koelen of verwarmen. Op die manier kan iedere gewenste temperatuurgradiënt ingesteld worden.

De gemiddelde temperatuur van het gehele systeem kan worden ingesteld met behulp van een verwarmingselement dat de gehele bodem van het systeem verwarmt. De gemiddelde relatieve luchtvochtigheid binnen dit systeem wordt ingesteld met behulp van een bak gevuld met een verzadigde zoutoplossing. De gemiddelde temperatuur en relatieve luchtvochtigheid bepalen samen wat de daadwerkelijke hoeveelheid water per liter lucht binnen dit systeem is. De lokale temperatuur bepaald echter hoeveel water er lokaal per liter lucht opgelost kan zitten. Hoe warmer de lucht, hoe meer water deze kan bevatten en hoe kouder hoe minder. Aangezien de daadwerkelijke hoeveelheid vocht overal gelijk is binnen dit systeem zal aan de koude kant van de temperatuurgradiënt de relatieve luchtvochtigheid het hoogst zijn en aan de warme kant het laagst. Condensatie zal optreden aan de koude kant wanneer hier de temperatuur zodanig laag gemaakt wordt, dat de maximale hoeveelheid vocht per liter die de lucht bij deze temperatuur kan bevatten gelijk is aan de daadwerkelijke hoeveelheid vocht per liter binnen dit afgesloten systeem (RH = 100%).

Door een glaasje te coaten met een agar-voedingsbodem en deze te inoculeren met bacteriën en bovenop deze temperatuur/RH-gradiënt in het koperen verbindingsstuk te leggen kan vervolgens gekeken worden naar de RH groeilimiet van de desbetreffende bacteriën. De belangrijkste conclusie die getrokken kan worden uit experimenten met dit RH-gradiënt systeem is dat microbiële groei juist makkelijker kan plaatsvinden op de wat koudere plekken binnen een gesloten systeem dan op de wat warmere plekken, omdat de lokale RH alleen op de koude plekken hoog genoeg is om groei te laten plaatsvinden.

Het principe dat microbiële groei juist makkelijker kan plaatsvinden op koude plekken en niet op warme plekken wordt in hoofdstuk 5 in een klinische setting op de proef gesteld door te kijken naar microbiële contaminatie in couveuses. In een couveuse worden zowel de temperatuur als de relatieve luchtvochtigheid op een constant hoog peil gehouden, zodat de baby voldoende warm blijft en niet uitdroogt (via transpiratie). De RH in een couveuse is meestal niet hoger dan 70% en zou derhalve niet of slechts nauwelijks voldoende zijn voor microbiële groei. De temperatuurverdeling in een couveuse is echter niet homogeen. Dit komt doordat warme vochtige lucht vanuit vier poorten de couveuse ingeblazen wordt, waarbij de ingestelde luchtcirculatie helaas niet alle plekken in de couveuse gelijkmatig bereikt. In de couveuse ligt de temperatuur meestal tussen de 30-37 °C terwijl dit buiten de couveuse 21 °C is (kamertemperatuur). Hierdoor is de temperatuur op de binnenwand van de couveuse lager op de plekken waar de lucht minder goed langs circuleert dan op plekken waar de warme lucht wel voldoende langs gaat. De koudere plekken kunnen wel 6-7 °C kouder zijn dan de gemiddelde temperatuur van de lucht in de couveuse, waardoor de lokale RH op dergelijke plekken wel 30% hoger kan zijn. Hierdoor treedt in sommige gevallen zelfs condensatie op. In ieder geval is de lokale RH op de koude plekken hoog genoeg om microbiële groei in principe mogelijk te maken, terwijl dit op de wat warmere plekken aan de binnenwand van de couveuse niet het geval zou moeten zijn. Door couveuses te bemonsteren en de verkregen monsters met behulp van kweekmethoden te analyseren is inderdaad

gebleken dat de microbiële contaminatie aanzienlijk hoger is op de koude plekken aan de binnenwand dan op de warme plekken.

Tenslotte gaat hoofdstuk 6 specifiek over het gesloten systeem waarop het promotieonderzoek in principe gericht was, namelijk de microbiële groei aan boord van het ISS. Het belangrijkste verschil t.o.v. gesloten systemen op aarde is dat de zwaartekracht verwaarloosbaar is aan boord van het ISS. dit heeft onder andere twee belangrijke gevolgen met betrekking tot de beschikbaarheid van water. Ten eerste is er geen thermale convectie wanneer er geen zwaartekracht is. Dit betekent dat warme lucht niet opstijgt en koude lucht niet daalt. Op aarde zou bijvoorbeeld in een kamer in de buurt van een raam de lucht kunnen afkoelen (omdat het buiten kouder is dan binnen) en in de buurt van een verwarming zou de lucht weer opwarmen. Dit zou dan als gevolg hebben dat de lucht in deze kamer gaat circuleren. Aan boord van het ISS is dit niet het geval door de afwezigheid van zwaartekracht met als gevolg dat temperatuursverschillen meer in stand gehouden worden.

Wanneer de temperatuursverschillen ergens binnen een gesloten systeem groter zijn is de kans ook groter dat er plekken zullen zijn binnen dit gesloten systeem waar de temperatuur laag genoeg is om een lokale RH te creëren, die hoog genoeg is voor microbiële groei. Uit temperatuursgegevens van het ISS blijkt dat er aan boord van het ISS inderdaad grote temperatuursverschillen zijn, zowel tussen de verschillende modules als binnen de modules. Deze niet-homogene temperatuursverdeling verhoogt de kans op microbiële groei en dientengevolge ook de kans dat één der bemanningsleden een infectie oploopt, of dat deze microbiële groei het ruimtestation zelf aantast.

Een ander gevolg van het ontbreken van zwaartekracht is dat er bij astronauten relatief te veel vocht richting het hoofd wordt gepompt. Op de aarde is het ten gevolge van de zwaartekracht juist noodzakelijk om bloed actief naar het hoofd te pompen. Het bloed dat naar het hoofd gepompt wordt zakt op aarde echter weer in voldoende mate naar beneden als men rechtop staat. In de ruimte is dit niet het geval zodat de astronauten ten gevolge van overtollig vocht onder meer een opgeblazen hoofd en een verstopte neus krijgen. Het kost meestal

redelijk wat tijd (weken) voordat het lichaam van een astronaut zich een beetje heeft aangepast aan de omstandigheden in de ruimte. De verstopte neus en de in algemenere zin vochtigere neusslijmvliezen zorgen er wellicht voor dat de neuzen van astronauten in de ruimte een vochtigere omgeving vormen dan op aarde. Hierdoor valt er mogelijk een verandering te verwachten in de soorten van micro-organismen, die in de neuzen van astronauten zullen domineren. De eerder genoemde *S. epidermidis*, die normaal gesproken dominant is doordat hij ook bij zeer lage luchtvochtigheid kan groeien, zou bijvoorbeeld ten opzichte van *Staphyloccos aureus* wel eens in het nadeel kunnen komen. De opportunistsch pathogene *S. aureus* bacterie heeft namelijk een vochtigere omgeving nodig dan zijn minder pathogene 'broertje' *S. epidermidis* (hoofdstuk 2). Men ziet dan ook dat de verspreidingssnelheid en prevalentie van *S. aureus* bij astronauten relatief hoog ligt.

Samenvattend kan uit het onderhavige onderzoek geconcludeerd worden dat het voornamelijk zaak is temperatuursverschillen zo veel mogelijk te voorkomen om microbiele groei in gesloten ruimtes tegen te gaan, zowel op aarde als in de ruimte. Dezelfde conclusie valt uiteraard eveneens te trekken voor woonhuizen, bijvoorbeeld in de badkamer, kelder of zolder. Isolatie en een goed ontworpen ventilatie systeem zijn hierin van cruciaal belang. Een lage RH alleen is echter niet altijd afdoende en kan zelfs averrechts werken aangezien een te lage RH weer andere gezondheidsproblemen met zich mee brengt.

Een belangrijk aspect dat wellicht nog meer onderzocht moet worden betreft de eigenschappen van microorganismen die groeien bij een niet optimale (lage) RH. Deze groei-omstandigheid lijkt namelijk voor verschillende micro-organismen meer op de normale natuurlijke omgeving waarin ze groeien en zich vermenigvuldigen bij een laag vochtigheidsgehalte. Door deze micro-organismen op hun eigenschappen te onderzoeken in een vochtige omgeving, wat de meestal normale procedure is in een laboratorium, ziet men wellicht belangrijke aspecten in de fysiologie van deze organismen over het hoofd.

Dankwoord

Er staan al 7 referentie lijsten in dit proefschrift, maar de belangrijkste en de meest gelezen is toch deze, de menselijke referentie lijst. Op de eerste plaats in dit dankwoord moet natuurlijk mijn vrouw Daphne komen. Samen hebben we een nieuw leven opgebouwd in Groningen, de laatste tijd zelfs erg letterlijk met als gevolg een rijk gezinsleven. Op het moment van dit schrijven heb ik al 1 jaar lang mogen genieten van mijn dochter Gabrielle en wanneer u dit leest zal ik ook trots mogen wezen op mijn 2^{e} wondertje. Ik hou van jullie.

Verder wil ik Hermie Harmsen bedanken, voor zijn rol als begeleider, als sparringpartner voor zowel goede als slechte ideeën maar vooral ook gewoon als vriend. Dit laatste is misschien ook wel een belangrijke reden dat hij de komende twee jaar nog niet van me af is. Hiervoor ook dank aan Gjalt Welling, welke ook al aanwezig was op mijn 1^{e} sollicitatiegesprek.

Vier jaar lang heb ik verder het geluk gehad om in de belangstelling te staan van Jan Maarten van Dijl, met wie de samenwerking zo goed & productief was dat hij uiteindelijk zelfs mijn promoter is geworden. Ik hoop dat deze samenwerking vooral door blijft gaan de komende tijd. Verder wil ik mijn andere promoter John Degener bedanken voor het vertrouwen in mij en voor zijn bijdrage aan klinisch relevante stukken. Tevens wil ik mijn leescomissie bedanken, dat ze mijn droge labwerk hebben willen beoordelen.

Ook mijn kamergenoten Jessica en Vivianne verdienen hier een plaatsje, niet zozeer omdat ze het zo lang met mij uitgehouden hebben (Jessica) of omdat ze zo goed waren om thee voor mij te zetten (Vivianne, mijn vrouwelijke paranimf) maar vooral voor de gezelligheid tijdens en buiten het werk (kraambezoek). Also May deserves special mention here. I enjoyed the time that you were here in which we worked together quite a lot (Dreamteam ;-)). I hope you and your son are doing well.

De onderzoeksgroep zelf heb ik ook altijd als erg prettig ervaren, evenals alle lab-uitjes naar Verweggistan (Friesland), sinterklaas feestjes, een volleybal toernooi en de tal van borrels met jullie. Bedankt ook verder voor jullie hulp/expertise tijdens mijn onderzoek (Sandra, Girbe, Emma & Sjouke).

Behalve dat ik veel geleerd heb tijdens mijn tijd hier heb ik ook hopelijk veel geleerd aan (en ook weer geleerd van) mijn studenten. Rienk voor zijn mooie werk met schimmels, Rik en Dirk voor hun couveuse werk en Indiomar voor de bacteriele overlevingsexperimenten.

Verder wil ik ook nog het ondersteunende personeel bedanken. De secretaresses welke altijd wel klaar stonden om mij te helpen of om over koetjes of kalfjes te praten. Bert in de keuken waar ik ook altijd terecht kon als ik iets nodig had of vies gemaakt had maar ook de mensen van de diagnostiek naast mij wiens ervaring ik vaak nuttig kon gebruiken en met wie het aangenaam toeven was in Ni Hao na de jaarlijkse labschoonmaakbeurt.

Voor het onderzoek in couveuses, welke een perfect model systeem vormden om mijn theorieën in praktijk te testen, wil ik Klazien Bergman en Nico Meessen bedanken voor hun hulp en inbreng. Verder, voor het werk dat ik gedaan heb betreffende de invloed van zwaartekracht op microbiële groei wil ik Jack van Loon bedanken voor zijn ideëen en het uitlenen van de random positioning machine. Ook de mensen van de werkplaats van het UMCG wil ik bedanken, met name Wolter de Goede en Ben Vorenkamp, voor het in elkaar zetten van mijn computer aangedreven klimaat controle kastje.

Buiten het werk om had ik gelukkig ook nog een leven vol met belangrijke mensen. Ik wil bijvoorbeed mijn DnD genoten bedanken voor de mogelijkheid om iedere vrijdag avond mezelf met creatieve onzin te kunnen vermaken. Verder mijn jaarclubgenoten uit Wageningen waarvan in het bijzonder Guido Voets, mijn mannelijke paranimf (nog zo'n DnD fanaat). Ook Gilead Wegen, welke ik al sinds de basisschool ken en welke mijn getuige was op mijn huwelijk mag hier niet ontbreken. Jammer dat Groningen zo ver in het noorden ligt anders zagen we elkaar wel wat vaker.

Afsluitend wil ik graag mijn familie (en schoonfamilie) bedanken voor hun gezelschap, steun in moeilijke tijden en en hun pogingen om mijn onderzoek te begrijpen. Hopelijk lukt dat nu nog beter met dit boekje. Helaas ben ik gedurende mijn AIO-schap mijn resterende 3 grootouders verloren, maar ik weet zeker dat ze nu apetrots op me zijn (en vooral waarschijnlijk op mijn kroost).